AN ABSTRACT OF THE DISSERTATION OF

Ratih E. Lusianti for the degree of Doctor in Philosophy in Chemical Engineering presented on March 4, 2014.

Title: Improving the Post-Thaw Processing of Cryopreserved Red Blood Cells Using a Combined Approach of Mathematical Modeling and Microfluidics.

Abstract approved: _____

Adam Z. Higgins

This study lays the groundwork on potential techniques that could be employed to improve the post-thaw wash processing of cryopreserved human red blood cells. Transfusion of red blood cells is one of the most commonly practiced procedures in clinical medicine. Millions of red blood cell units are transfused to patients every year. The current method of preservation of red blood cells only allows a short refrigerated shelf life of 6 weeks, which causes logistical issues and frequent shortages during the time when donor availability is decreased. Cryopreserving red blood cells in the presence of 40% w/v glycerol extends the stable shelf life of red blood cells to 10 years. The long stable shelf life allows stockpiling of transfusable RBC units. Although this preservation method is clinically approved and routinely performed, the use of cryopreservation in blood banking is limited to only autologous and rare units. One of the main reasons for this limitation is the time consuming post-thaw wash process required to remove the glycerol before the unit can be used for transfusion. The need to plan the amount of

washed units makes the use of cryopreserved red blood cells for unscheduled transfusion particularly challenging. In this work, we have attempted to improve the efficiency of the post-thaw removal process by using modern scientific approaches. Using the mathematical model for cell membrane transport, we have demonstrated that glycerol can be rapidly extracted from red blood cells without excessively damaging the cell membrane in a batch process. This rapid glycerol removal approach was then applied into a membrane based microfluidic platform for adaptation into an efficient continuous process. A mathematical model of the membrane based microfluidic device capable of predicting the transport of water and solutes was developed to assist in the design of an efficient deglycerolization process. Glycerol removal experiments using a prototype of the device validated model predictions and demonstrated successful partial continuous deglycerolization of cryopreserved red blood cells. Simulations generated using the mathematical model shows that it is possible to rapidly deglycerolize cryopreserved red blood cells in a continuous process to levels acceptable for transfusion. With the potential for efficient continuous post-thaw wash processing, it is hoped that cryopreserved red blood cells may become a more attractive option for use in clinical therapy.

Improving the Post-Thaw Processing of Cryopreserved Red Blood Cells Using a Combined Approach of Mathematical Modeling and Microfluidics

by

Ratih E. Lusianti

A DISSERTATION

Submitted to

Oregon State University

in partial fulfillment of
the requirements for the
degree of

Doctor of Philosophy

Presented March 4, 2014
Commencement June 2014

Doctor of Philosophy dissertation of Ratih E. Lusianti presented on March 4, 2014.

APPROVED:

Major Professor, representing Chemical Engineering

Head of the School of Chemical, Biological, and Environmental Engineering

---

Dean of the Graduate School

I understand that my dissertation will become part of the permanent collection of Oregon State University libraries. My signature below authorizes release of my dissertation to any reader upon request.

Ratih E. Lusianti, Author

ACKNOWLEDGEMENTS

To ensure that I acknowledge everyone that deserved acknowledging in helping me complete this dissertation and don't miss anyone, I shall start at the very beginning. I would like to express the deepest gratitude to my parents for giving me my life and for raising me to be the person that I am today (a good human being). I would like to thank my little sister, whose friendship I value greatly from the time we were kids until today. I would like to extend much gratitude to my advisor, Dr. Adam Higgins. Your vision, hands-on approach, attention to detail, wisdom, guidance, and unparalleled availability have gotten me through many technical roadblocks through the course of this program. I would also like to thank my committee members Dr. Joseph McGuire, Dr. Kendra Sharp, Dr. Joe Baio, and Dr. Adam Alani for the advice they have given in regards to this project. To all the members of the Higgins Laboratory at Oregon State University (past and present), thank you for supporting this work in various ways. Dr. Ally Davidson, thank you for showing me the ropes on how to become a proper graduate student back when I was a noob. John Lahmann, thank you for making the beautifully handcrafted acrylic housing. Without you I would still be using my old decrepitly made housing and life would undoubtedly be a lot harder. Thank you to the folks outside the lab that have helped me in this project. Andy Brickman, thank you for always being there to brainstorm and fix unexpected equipment breakdowns. Concomitant conversations about garage sales, fishing, and restaurants have helped lighten the mood as you expertly work to fix equipment malfunctions. Jack Rundel and Thomas Lindner at MBI, thank you for taking the time to personally train me on various techniques and equipments. Elisha

Brackett, Lea Clayton, and Charlie Williams, thank you for always helping me with the administrative aspects of this project. To Dr. Phil Harding, your interest and advice in my professional development has been greatly appreciated. To Dr. Skip Rochefort, thank you for allowing me to monopolize your TGA for many months. Without that lovely machine I would have never been able to be complete this work. Thank you to Oregon State University and the National Science Foundation for financially supporting this project. Leaving graduate school without a mountain of debt is truly amazing, and I am forever grateful. And last but not least, to my incredible husband, Dr. Kevin Caple, and my furry child, Layla. Thank you for getting me through many emotional breakdowns during the course of completing this degree. Without you in my life I would be lost (more cartons of ice cream would be consumed) and I cannot thank you enough for the support and love you have given me.

CONTRIBUTION OF AUTHORS

Chapter 3 was written with contributions from Dr. James Benson and Dr. Jason Acker as co-authors under the guidance of Dr. Adam Higgins. The mathematic algorithm of the optimized procedure in Chapter 3 was developed by Dr. James Benson. Dr. Mariia Zhurova was a main contributor to the experimental data collection and analysis of the fetal red blood cells in Chapter 4, along with co-authoring the manuscript under the guidance of Dr. Jason Acker and Dr. Adam Higgins. The manuscript of Chapter 5 was co-written with the advice and guidance of Dr. Adam Higgins.

TABLE OF CONTENTS

Page

TABLE OF CONTENTS (Continued)

Page

TABLE OF CONTENTS (Continued)

Page

LIST OF FIGURES

LIST OF FIGURES (Continued)

LIST OF FIGURES (Continued)

Figure Page

LIST OF TABLES

LIST OF APPENDICES

Improving the Post-Thaw Processing of Cryopreserved Red Blood Cells Using a Combined Approach of Mathematical Modeling and Microfluidics

Chapter 1: Introduction

1.1 OVERVIEW

Transfusion of red blood cells (RBCs) is one of the most commonly performed therapeutic procedures in clinical medicine. It is estimated that over 15 million units of RBCs are transfused to patients every year in the US alone [1]. Due to the high clinical demand, donated RBC units must be preserved using a method that allows for long storage life without the degradation of viability as well as cell function. Currently, blood banks and hospitals use refrigerated blood in their reserve almost exclusively. Depending on the type of hypothermic storage solution used, RBCs can be stored in a refrigerated state for up to 6 weeks [2-4]. Although blood banks and hospitals carefully manage their RBC inventory, seasonal shortages and outdating still prove to be significant issues [1, 5]. Recent published studies also indicate a higher incident for complications in patients receiving transfusion of older refrigerated RBC units [6-8], suggesting that the storage period for refrigerated RBCs to avoid these issues may be as short as two weeks [6, 9]. A reduction in the acceptable refrigeration period of RBCs would have a dramatic impact on the RBC supply chain.

RBCs have been successfully cryopreserved with excellent post-thaw viability since the 1950s. The use of frozen RBCs in blood banking has the potential to mitigate problems associated with refrigerated blood. Unlike refrigeration, storage in cryogenic

temperatures completely halts cellular metabolism, effectively preserving the quality of the cells even after an extended period of storage. In 1987, the FDA approved a storage shelf-life of ten years for cryopreserved RBCs; however, a study done to examine the quality of frozen RBCs conducted since the 70s reveal that RBCs can be frozen in the presence of 40% w/v glycerol at -80 °C for up to 37 years with an acceptable post-thaw in-vitro recovery [10]. The incredibly long storage shelf-life of cryopreserved RBCs would enable blood banks and hospitals to stockpile strategic reserves to mitigate seasonal shortages, improve availability during the events of a natural disaster, as well as for military application during the time of war. The increased usage of cryopreserved blood would provide overall stability to the RBC supply chain because an infinite amount of frozen units can be stored without product degradation for long periods of time.

Although cryopreservation of blood in the presence of 40% w/v glycerol is common practice, the types of RBCs that receive this treatment are currently limited to rare and autologous units only. The limitation is due to the time consuming post-thaw wash process that is required to remove the glycerol before the cells can be transfused into patients. This unaddressed disadvantage makes the short-notice use of frozen blood for any clinical purpose particularly challenging. Until a more efficient method of washing glycerol from frozen-thawed blood is discovered, the increased usage of frozen blood in clinical therapy is unlikely.

1.2 MOTIVATION

The main goal of this study is to promote and facilitate increased usage of frozen-thawed RBCs in clinical therapy by attempting to discover a more efficient method of deglycerolization. The two main questions this study seeks to answer are: (1) Can glycerol be removed rapidly from thawed cryopreserved RBCs without causing excessive irreversible membrane damage, and (2) Can the removal process be converted into a continuous process for increased efficiency rather than the batch centrifugal-based removal process currently used today. Being able to continuously remove glycerol from cryopreserved RBCs would eliminate the need to plan the number of RBC units to wash to accommodate the often unpredictable clinical demand. It would also eliminate the cost of additional refrigeration equipment needed to store washed RBC units as they can be kept frozen until needed. By introducing a continuous procedure capable of removing glycerol from the cells in transit, it is hoped that the usage of cryopreserved RBCs would increase and possibility extend to unscheduled allogeneic donation units in the future.

1.3 ORGANIZATION OF DISSERTATION

This dissertation is structured using the manuscript layout as an option made available by the Graduate School. An extensive literature review pertinent to this study is presented in Chapter 2. Chapters 3-5 are publication manuscripts written throughout the last three and a half years and submitted to various peer-reviewed journals. Each manuscript is preceded by a header page which contains information on the manuscript title, author names, journal name, as well as submission dates.

In Chapter 3, the possibility of rapidly removing glycerol from cryopreserved blood is explored. Based on published biophysical data and the cell transport model, it is possible to remove glycerol from cryopreserved RBCs while maintaining cell volume to within the known safe osmotic tolerance limits in an optimized time of 32 seconds. In this chapter, the optimized deglycerolization procedure as well as various systematic rapid deglycerolization procedures were modeled and then tested experimentally to obtain a washing protocol that yields at least 80% cell recovery in the shortest amount of time.

Chapter 4 presents the work that was done to ascertain the osmotic tolerance limits of cryopreserved RBCs. The knowledge of the osmotic tolerance limit of cryopreserved RBCs is critical in designing an effective washing procedure that would not cause excessive osmotic damage to the cells. However, osmotic tolerance limit information available in existing in literature are limited to RBCs in their natural state or equilibrated in various glycerol concentrations. Cryopreserved RBCs have endured the glycerolization, freezing, and thawing process, all of which are known to have a detrimental effect on the cell membrane. Hence, it is possible for cryopreserved RBCs to have osmotic tolerance limits that are much more conservative compared to less processed RBCs. The results from fetal RBCs receiving the same treatment done by our collaborator from the University of Alberta were also presented in this manuscript.

Chapter 5 presents our attempt at continuously removing glycerol using a single channel microfluidic membrane device. A theoretical model that predicts the transport of solutes was developed and used to guide the design of single pass experiments in the device. The results presented in this chapter demonstrate that it is possible to achieve

complete continuous removal of glycerol from cryopreserved RBCs by linking multiple devices in series. The model can be used as a tool to select the proper operating condition in each device to achieve the desired mass transfer while avoiding excessive osmotic effects in a reasonable amount of time.

Chapter 6 contain the lessons that were learned throughout the duration of this project and the future direction of this study. The main purpose of this chapter is to lay out pertinent information regarding the deglycerolization of RBCs learned thus far, so that in the future the process can be optimized. This chapter also contains experimental work relevant to the continuous deglycerolization of RBCs that has yet to be incorporated into the system. Concluding remarks are also made in this chapter to complete this dissertation.

Chapter 2: Literature Review

2.1 CRYOPRESERVATION OF RED BLOOD CELLS

Cell based therapy can be defined as a form of medical treatment that aims to replace, repair, or enhance the biological function of damaged tissue or organs by transplanting or transfusing isolated living cells into the body [11]. Transfusion of RBCs is classic example of successful cell based therapy that is practiced every day. With the advancement of modern medicine, the popularity of cell based therapy is projected to increase into the future, subsequently increasing the demand for cell based products. One of the main obstacles in providing cell based products to the public is the issue of preservation and storage of living biomaterials. In order to maintain steady supply for the unpredictable demand, a preservation method that maintains viability and full function of the cells for an extended period of time is crucial. Cryopreservation is a plausible option for the mass production of cell based products because it significantly extends the shelf life of biomaterials without loss of viability.

Cryopreservation is a technique of maintaining the viability of biological samples at cryogenic temperatures, between -80°C to -196°C. At these temperatures, any chemical, biological, and physical activity is dramatically slowed at a cellular level, enabling long-term storage of the product without the degradation of viability of function. The challenge of cryopreservation is in maintaining cell viability during the cooling and warming stage of the process when the cells are transitioning between physiological and stable storage temperatures. At this transitional stage, the cells are exposed to many harsh

phenomena such as exposure to intracellular and extracellular ice as well as cell dehydration, all of which could significantly damage the cell. To maintain viability during the cooling process, cryoprotectants (CPAs) are commonly added to the media.

CPAs commonly used in cryopreservation are divided into two groups depending on their mechanism of action: permeating and non-permeating [12, 13]. Non permeating CPAs like sugars, sugar alcohol, and hydroxyethyl starch are commonly used in low concentrations in conjunction with a rapid cooling procedure. The protective mechanism of non-permeating CPA is thought to be through dehydrating the cells at sub-freezing temperature to reduce the incidence of intracellular ice formation [14]. Permeating CPAs like glycerol and dimethyl sulfoxide (DMSO) can be used in rapid or slow cooling cryopreservation procedures. High permeating CPA concentrations are commonly used with a rapid cooling procedure for vitrification. In the vitrification cooling process, when temperatures are sufficiently low, the high concentrations of CPA in the media become so viscous that they solidify into a vitreous glassy state, effectively avoiding the formation of ice [15]. For slow cooling procedures, permeating CPAs may protect the cells by several mechanisms, including prevention of excessive cell volume reduction, and avoiding lethal concentrations of electrolytes [12, 13, 16]. Additionally, permeating CPA may also protect the cells by lowering the chemical potential of water, effectively reducing the incidence of ice formation at any given temperature [17, 18].

Glycerol's cryoprotective properties were discovered in 1949 when Polge, Smith, and Parkes successfully revived various types of spermatozoa that had been frozen and thawed in a media containing glycerol [19]. The following year Smith discovered that by

adding glycerol to a suspension of RBCs, normal cell morphology could be maintained after freezing and thawing, thus avoiding hemolysis [20]. In 1951, Mollison and Sloviter discovered that good in vivo cell recovery of frozen-thawed RBCs can be achieved if the glycerol is removed prior to transfusion [21]. This finding marked the realization that the storage of blood products can be extended from mere weeks to months or even years. What remained to be the main obstacle to clinical application of frozen blood was the lack of a standardized methodology to add and remove the glycerol.

In 1972, Meryman empirically developed a glycerolization, storage, and deglycerolization protocol that reliably produced very good cell recovery post-wash [22]. In this method, fresh RBCs are glycerolized to approximately 40% w/v in two steps and then placed in a metal canister to be frozen in a -80ºC mechanical freezer. Thawing is simply done by immersing the frozen bag in a 37°C water bath for several minutes. The deglycerolization process involves several washing steps carried out in a centrifugal cell washer. The cells are initially washed with 12% saline, followed by an intermediate wash using 1.6% saline, and then a final wash with isotonic saline until less than 1% of the initial glycerol remains in the suspension [23], producing an average washed cell recovery of about 95% [24]. Because of its reliability, Meryman's high glycerol method has been made one of the approved RBC cryopreservation methods by the AABB. A method using precise rapid cooling, lower glycerol concentration (20% w/v), and storage in the vapor phase of liquid nitrogen (-196°C) originally developed by Rowe is the other cryopreservation method approved by AABB [25]. The low glycerol method is more commonly carried out in Europe, whereas in North America, the majority of RBC units

are cryopreserved using the high glycerol method [2]. Although it reliably produces high washed cell recovery, the centrifugal cell washers employed to carry out Meryman's deglycerolization process have historically been open or non-sterile systems. Thawed cryopreserved RBCs washed using an open centrifugal cell washer must be used within 24 hours to avoid problems with bacterial contamination. The short post-wash storage time leads to logistical issues as well as wasted units. Additionally, centrifugal systems for use in conjunction with Meryman's deglycerolization process need to be manually operated, making it labor intensive.

More recently, Valeri has developed a new functionally closed centrifugal cell washer – the Haemonetics ACP 215 Automated Cell Processor [26, 27]. This device is capable of glycerolizing (to the high glycerol concentration) as well as washing RBCs post-thaw in a closed system. Valeri's deglycerolization method involves the use of only 12% saline and isotonic saline, simplifying and economizing the procedure by eliminating the need for an intermediate wash [28]. Thawed blood using this method has an average cell recovery that is slightly lower than Meryman's method at approximately 87%, but can be stored at 4°C for 14 days without bacterial contamination, afforded by processing in a closed system [27]. The ACP 215 can also be used to wash RBCs cryopreserved using the low-glycerol method, although the resulting cell recovery is slightly lower than that for the high-glycerol method [29]. Valeri's glycerol addition and removal method for use with the ACP 215 Cell Processor is now also approved by the AABB and is currently considered the state-of-the-art procedure for washing cryopreserved RBCs [23].

Although the introduction of the ACP 215 Cell Processor has simplified a previously labor intensive procedure and improved the storage period for washed cells, the total washing process time still stands at approximately one hour [28]. Additionally, RBC units still need to be washed one at a time, making it necessary to plan ahead as to how many units need to be washed to meet the often unpredictable clinical need of transfusable RBCs. Hence, increased use of cryopreserved RBCs will remain unlikely until glycerol can be removed continuously.

2.2 RED BLOOD CELL MEMBRANE TRANSPORT AND PROPERTIES

Historically, CPA addition and removal procedures have mainly focused on the avoidance of osmotic damage. This usually entails a multi-step procedure where the cells are exposed to solutions that would induce CPA transport in an incremental manner to avoid excessive cell volume changes. For example, Meryman's addition of glycerol is carried out in three steps: the first step is a slow addition of a small aliquot of 6.2 M glycerol solution with gentle agitation, the second step involves leaving the cells undisturbed for 5 to 30 minutes to allow full equilibration with the extracellular solution, and finally in the third step a larger aliquot of 6.2 M glycerol solution is added slowly to reach a glycerol concentration of approximately 40% w/v [30]. The deglycerolization in the ACP 215 is also carried out using a step-wise approach by adding different volumes of saline solutions to facilitate slow permeation of glycerol out of the cells. The thawed blood is deglycerolized in three phases: (1) first the RBCs are diluted in three steps using 50 ml of 12% saline, 340 mL and 400 mL of 0.9% saline 0.2% glucose solution, (2) the

diluted RBCs are then washed in five steps with 60 mL, 70 mL, 100 mL, 150 mL, and 300 mL of 0.9% saline 0.2% glucose solution, centrifuging after each step to remove the supernatant which contain the permeated glycerol, and finally (3) the washed cells are resuspended in 240 mL of AS-3 for a total process time of 57 minutes per unit RBC [28]. Both the glycerolization and deglycerolization procedure was empirically developed using the rationale that slow gradual changes in solution composition would enable the avoidance of osmotic damage. Although it produces good cell recovery, conventional method of CPA removal and addition to RBCs can be very time intensive. The time required to remove glycerol stands as the main obstacle in more widespread use of cryopreserved blood.

Efficient protocols to remove glycerol from RBCs can be designed using modern approaches like mass transfer modeling. Cell membrane transport models like the Kedem-Katchalsky (KK) or two-parameter (2P) formulation can be used to model the movement of water and solute across cell membranes, resulting in predictions of cell volume changes [31, 32]. Cell membrane mass transfer modeling can be used to design a protocol that varies the extracellular concentration with time to maximize the driving force of CPA transport while maintaining cell volume to within the known osmotic tolerance limits to avoid membrane damage. By maximizing the driving force of CPA transport, the process time can potentially be significantly reduced when compared to the conventional step-wise approach. The success of a modeling approach to determine an optimized CPA removal procedure relies on the accuracy of the measured cell membrane properties such as permeability values and osmotic tolerance limits.

The human RBC has been a widely studied model for cell membrane transport for over 50 years. Existing literature on measuring various cell membrane properties with varying methods and physiological interpretations are expansive. The variations in the results of such studies make is particularly challenging to select the most accurate membrane property value for use with the cell membrane transport model. The membrane permeability values directly used in the cell membrane transport model to predict mass transfer during CPA removal are the hydraulic conductivity (L_p) and the solute (in this case glycerol) diffusive permeability (P_s).

The hydraulic conductivity is a cell property that quantifies the transport of water through the cell membrane. Human RBCs are much more permeable to water when compared to most other cell types [33]. Because water moves through the membrane at a rapid speed, it is difficult to obtain accurate measurements of hydraulic conductivity. Numerous studies have attempted to measure and observe the effects of certain variables on the hydraulic conductivity of human RBCs with varying results. Experiments conducted by Terwilliger and Solomon as well as Sha'afi and Gary Bobo indicate that hydraulic conductivity is either invariant with changes in solute concentration or decreases with increasing concentration [34, 35]. Results from other studies seem to indicate that the presence of permeating solutes such as glycerol [36, 37], ethylene glycol [36], and dimethyl sulfoxide (DMSO) [37] in the medium depresses the value of the hydraulic conductivity. Based on the results of these studies, Mazur hypothesized that the hydraulic conductivity is independent of the concentration of non-permeating solutes, but dependent on the concentration of permeating solutes in unfrozen solutions [38].

McGrath summarized all the values reported from available literature and found that the hydraulic conductivity of human RBC ranges between $7.6 \cdot 10^{-13}$ to $2 \cdot 10^{-12} \frac{m}{Pa \cdot s}$ [33].

The human RBC cell membrane allows the passage of water more readily than it does permeating solutes like glycerol. For this reason, the glycerol diffusive permeability is expected to be the rate limiting factor that controls the excursions of cell volume after the initial rapid transport of water. Consequently, the success of a modeling approach to predict cell volume changes relies most heavily on an accurate value for glycerol diffusive permeability. Unfortunately, reported values of glycerol diffusive permeability of human RBCs in literature are as variable as values for hydraulic conductivity. Carlsen and Wieth measured glycerol diffusive permeability using radioactive labeled glycerol and found that the value was lower at acidic pH and decreases with increasing glycerol concentration [39]. Experiments using a photometric method to measure the cell volume change employed by Stein and Danielli also found a decrease of glycerol diffusive permeability with increasing glycerol concentration [40]. Du and colleagues used electron paramagnetic resonance to monitor the aqueous cell volume change versus time during glycerol permeation [41]. The results obtained using this method was found to be slightly higher than those reported by Carlsen and Wieth and Stein and Danielli. Mazur and Miller used the time to lysis and osmotic stress method to measure diffusive permeability [42], resulting in values that are comparable to those reported by Du et al. Saari and Beck as well as Jay and Rowlands used a modified time to lysis method to measure the glycerol diffusive permeability [43, 44]. The values reported from these studies were found to be much lower than the general trend. The variability in the

reported glycerol diffusive permeability values for human RBCs is illustrated in Figure 2.1.

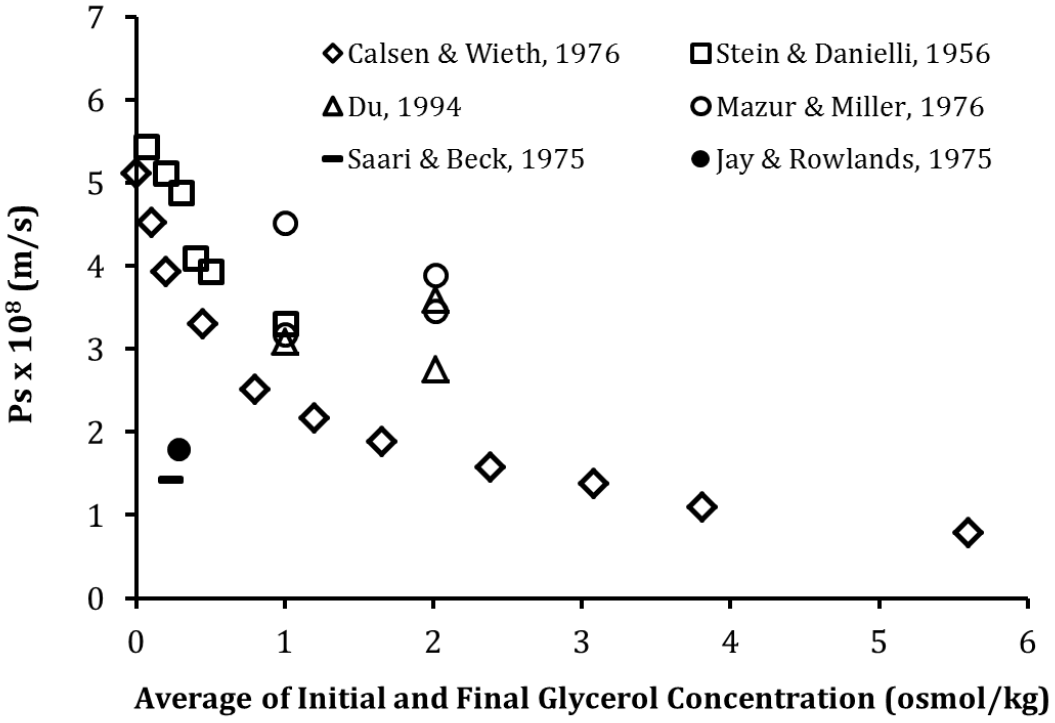

Figure 2.1. Summary of glycerol diffusive permeability values for human RBCs as reported in literature.

The final membrane property that must be considered when designing a successful CPA removal protocol is the osmotic tolerance limits. During the removal process, cells are subjected to potentially damaging osmotic stresses. The osmotic tolerance limits are defined as the extent of volume excursions the cell can withstand before incurring irreversible membrane damage [45]. Many studies have examined the osmotic fragility of fresh human RBCs in the presence of saline. The hypotonic osmotic fragility of human RBCs is examined by exposing the cells to various hypotonic saline solutions. Typically, the results of such experiments are quantified in terms of the saline

concentration required to induce approximately 50% hemolysis. The saline concentration to induce 50% hemolysis was found to range between 130 to 160 mOsm/kg H2O for human RBCs [46-51]. These saline concentrations correspond to a relative osmotically active cell volume $(V_c - V_b)/W_{iso}$ of 2.31 and 1.89, respectively, where V_c is the swollen total cell volume, V_b is the osmotically inactive cell volume, and W_{iso} is the osmotically active cell volume at isotonic conditions, assuming an isotonic total cell volume of 94 μm^3 and an osmotically inactive fraction of 0.287. In terms of total relative cell volume $V_c/V_{c,iso}$ these saline concentrations correspond to values of 1.93 and 1.62, respectively where $V_{c,iso}$ is the total cell volume at isotonic conditions.

Several studies have also determined the osmotic fragility of human RBCs in hypertonic environments by exposing them to saline solutions up to 0.8 M [52, 53]. Meryman observed that a minimum cell volume was reached when cells were exposed to saline concentrations 4.5 times the isotonic. This saline concentration corresponds to an osmotically active relative cell volume of 0.22 or a relative cell volume of 0.44 [52]. Lovelock obtained a minimal osmotically active cell volume of 0.19 (relative cell volume of 0.42) after exposing human RBCs to 0.8 M saline solution. From this experiment, Lovelock found that the majority of damage was not apparent when the cells were still in a hypertonic environment, rather only manifested once the cells were induced to swell back to isotonic conditions [53].

Studies reported in literature indicate that various factors like pH [47, 54], temperature [47, 49, 54, 55], type of anticoagulant used [49, 50], alterations to the cell membrane [56], and age of cells [57, 58] can have an effect on the osmotic fragility.

Beutler and colleagues conducted experiments on RBCs that have been stored in the preservative citrate phosphate dextrose adenine for 42 days and found an increase in hypotonic osmotic fragility. The cells that have been refrigerated for a prolonged period was found to incur 50% hemolysis when induced to swell to 1.5 times the osmotically active cell volume (1.36 times the total isotonic cell volume). Meryman and Douglas examined the osmotic fragility of RBCs equilibrated in glycerol solution of various concentrations [59]. Analysis on the raw data from this study revealed that 50% hemolysis was attained when RBCs in 5 M glycerol was induced to swell to 1.97 times the osmotically active isotonic cell volume (1.69 times the total isotonic cell volume).

To our knowledge, a study that examines the osmotic fragility of cryopreserved RBCs has never been conducted. The membrane of thawed cryopreserved RBCs is expected to be the most osmotically sensitive after enduring the effects of glycerolization, freezing, and thawing. The results of osmotic fragility studies presented thus far have reported the hypo- or hypertonically induced cell volume changes that resulted in a considerable amount of hemolysis at ~50%. Because we intend to minimize hemolysis during the deglycerolization process, the osmotic tolerance limits chosen for any modeling approach should be set at a more conservative value to ensure that osmotic damage is avoided.

2.3 CURRENT EFFORTS TO IMPROVE DEGLYCEROLIZATION

Although more modern approaches exist in optimizing the deglycerolization method, there has been no improvement in the current clinical standard since the

introduction of the ACP 215 Cell Processor. Studies published in the last fifteen years have reported various methods that have the potential for being applicable in improving the deglycerolization process.

Studies using hollow fiber dialysis modules have shown potential for extracting CPA from thawed cryopreserved RBCs. In most studies, the hollow fiber modules are used in a dilution-filtration system. The cryopreserved RBCs are pumped out of the blood bag and diluted with a small volume of diluting solution (usually isotonic saline) to facilitate mass transfer of glycerol to the extracellular solution. The diluted mixture is then flowed through an ultrafiltration hollow fiber module to remove a portion of the extracellular solution and hence glycerol from the suspension. The cells are recirculated back into the blood bag to be diluted and filtered repeatedly until sufficient CPA is removed. Castino and Wickramashinge developed a mass transfer model to predict the glycerol removal capability of a dilution-filtration system [60]. Experiments conducted with prediluted thawed cryopreserved blood (initial concentration of approximately 1.57 M glycerol) and the commercially available Sepracor 300 hollow fiber module indicated good agreement between model predictions and actual results. The authors proposed that by optimizing the dimensions of the hollow fiber module, glycerol can be removed completely from prediluted thawed cryopreserved RBCs (1.57 M) in approximately 30 minutes. A follow up study also found this system to be effective in removing 5-10% DMSO from cryopreserved peripheral blood hematopoietic progenitor cells and platelets in approximately 20 minutes [61].

Another dilution-filtration system using hollow fibers was tested by Zhou and colleagues [62]. The system uses a commercially available hemofilter, the Plasmaflo TM AP-05H/L, and optimizes the washing protocol to obtain the most favorable result. The authors were able to completely remove glycerol from cryopreserved RBCs in 40% w/v glycerol (without predilution) to the levels approved by AABB while achieving 90% cell recovery in approximately one hour. Although the system does not necessarily reduce washing time in comparison to the ACP 215, the authors argue that the equipment cost of the dilution-filtration system is lower than an automated cell washer, and therefore can be applied in more areas [62].

Even though some studies have shown that it is theoretically possible to reduce the washing time if an optimized hollow fiber module is used, the dilution-filtration system is still a batch process. The number of washed units using this method will still need to be planned to meet the daily unpredictable clinical demands for transfusion. As previously mentioned, batch processing of cryopreserved RBCs for unscheduled transfusion could create logistical issues. Washing too many units could result in outdated units that must be discarded, whereas not enough washed units could result in failure to perform life-saving medical procedures like emergency surgery.

If enough CPA could be removed from cryopreserved RBCs without the need to repeatedly recirculate the cells, the use of hollow fiber modules for deglycerolization may be more realistic. Arnaud performed experiments where cryopreserved platelets in 5% DMSO were flowed counter-current to isotonic saline in several hollow fiber modules [63]. In this study, it was concluded that in order to remove enough DMSO in a single

pass (over 95% of the original amount), the flow rate must be set at a value that is too slow to be used in practice [63]. The main mass transfer limitation in conventional hollow fiber modules is the non-uniformity of the dialysate flow path caused by non-uniform packing of the fibers inside the shell of the module [64]. Non uniform packing in the shell of the module can cause the development of stagnant regions of flow, significantly hindering mass transfer [65]. To reduce the tendency for stagnant regions to develop, the shell side flow rate can be increased. However, increasing the shell side flow rate would necessitate the use of a larger volume of washing solution, increasing the economic cost of the process and possibly making it impractical depending on the necessary increase to maintain efficient mass transfer.

Recently, the development of technology has extended to the use of microfluidic devices for biological application. As explained by Brody et al. different forces become dominant at the microscale level than those experienced in bulk systems [66]. These forces include laminar flow, diffusion, fluidic resistance, surface area to volume ratio, and surface tension [67]. These dominant phenomena can be exploited to create microfluidic devices that are extremely efficient at manipulating cell populations using various different principles. For example, cell populations have been manipulated in microfluidic devices based on cell size [68, 69], using electromagnetic deflection [70], magnetic forces [71], acoustic fields [72, 73], gravitational settling rates [74], cell-capturing structures [75-77], vacuum channels [78], and hydrodynamic filtration [79].

For deglycerolization, one dominant force that can be exploited is diffusion. Microfluidic devices feature a large surface area to volume ratio, intensifying the

microscale transport phenomena by decreasing the path length for diffusion. As a result, mass transfer processes carried out in microfluidic platforms are expected to be more efficient compared to bulk systems. Several studies using microfluidic devices have shown potential as an alternate blood washing method to centrifugation. Song has developed a microfluidic device that minimizes osmotic shock to the cells by progressively changing the CPA concentration through controlled mass transfer during CPA loading and unloading [80]. The polydimethylsiloxane (PDMS) based microfluidic device consists of three inlet ports: one for the cells and two for the washing solution. As the cells travel down the channel (100 μm wide, 100 μm high, 1.5 m long), CPA is removed continuously and progressively by diffusion, thereby minimizing osmotic shock. Avoidance of osmotic shock by using this device has been shown to improve the post-wash survival of human hepatocellular carcinoma cells cryopreserved in the presence 3M propylene glycol by ~10% compared to the conventional step-wise CPA removal approach [80]. However, the success of this method has only been demonstrated using a cell suspension that is very dilute (0.3% cell volume fraction). Cryopreserved cell products used in practice have much higher cell densities (up to 75% cell volume fraction for cryopreserved RBCs). The performance of this device with a higher density cell suspension has yet to be examined.

Another diffusion based CPA extraction microfluidic device was developed by the Hubel group at the University of Minnesota. This device consists of two streams, a cell-laden CPA rich stream on the bottom and a cell-free wash stream on top, flowing in parallel within a rectangular channel of constant cross-sectional area. The laminar nature

of fluid flow inside this device makes diffusion based extraction while maintaining separation between the cell-laden stream and the wash stream possible. A theoretical model of the device gave an understanding of the functional relationship between critical operating parameters: flow rate fraction (flow rate ratio of cell stream and wash stream), fluid velocity in the channel, and the cell density [81]. Experiments carried out using Jurkat cells in 10% DMSO in a prototype revealed the device performed as predicted by the model [82, 83]. However, the target of 95% removal of DMSO in approximately 30 minutes was not experimentally achieved using the prototype device as high cell recovery can only be achieved with a moderately fast flow rate, restricting the fluid residence time for DMSO diffusion. A scale up analysis was conducted using the theoretical model to design an optimized prototype that would be capable of achieving the desired outcome (~30 minute processing time with 95% removal of DMSO, >10% cell loss) [84]. However, the footprint of the optimized device was found to be too large for practical use [85].

Recently, the Hubel group has developed a vertical microchannel device for diffusion based extraction of DMSO [86]. The cell stream is flowed in the middle of a vertical rectangular channel (500 μm wide, 25 mm deep and 80 mm long) flanked by two streams of wash solution. Similar to the device designed by Song, DMSO will diffuse from the cell stream to the wash stream as the cells travel down the length of the channel. The vertical design of the device leverages gravitational forces to recapture the cells at the end of the channel, improving cell recovery. Single trial experiments using Jurkat cells in 10% DMSO (15% cell volume fraction) and various flow rates show that the

current prototype is capable of 45% removal of DMSO. If the channel was lengthened or the cells were passed through multiple devices, 95% removal of DMSO would be possible. One drawback to this method is that it uses at least twice as much volume of washing solution compared to cell suspension. This drawback can be considered minor as the cost of saline solution is assumed to be much less than the cost of the cryopreserved cell product. Reliable high recovery of cells downstream when using this system in conjunction with extremely dense cell suspensions (higher than 40% hematocrit) still needs to be demonstrated. Although these studies all demonstrate the potential of microfluidics for cell processing, none of these techniques are currently used in a clinical setting.

The main focus of this dissertation is to present preliminary work on the feasibility of continuous removal of glycerol from cryopreserved RBCs using a membrane-based microfluidic device. The microfluidic device consists of two parallel channels separated by a semi-permeable membrane. The cell and the wash streams are flowed on either side of the membrane in a counter-current configuration allowing efficient mass transfer of glycerol from the cell stream into the wash stream. The presence of the membrane as a clear partition between the cell and the wash stream also enables 100% recovery of the cells, assuming no cells are lost to lysis during the process. Precisely controlling the fluid path inside of the device also eliminates stagnant regions of flow, mitigating the need for increasing the volumetric flow rate of the wash stream to maintain high mass transfer rates. More importantly, the rigidly defined fluid path also allows precise control of mass transfer in the device to avoid damaging osmotically

driven cell volume excursion during the removal process. Although in this study the main focus is to use the device for the deglycerolization of cryopreserved RBCs, the microscale size of the device could also potentially be suitable for processing smaller volume cryopreserved cell-based therapeutics such as umbilical cord blood and hematopoietic stem cells.

Chapter 3: Rapid Removal of Glycerol from Frozen-Thawed Red Blood Cells

Ratih E. Lusianti, James D. Benson, Jason P. Acker, Adam Z. Higgins

Journal: American Institute of Chemical Engineering *Biotechnology Progress*

Address: http://onlinelibrary.wiley.com/journal/10.1021/%28ISSN%291520-6033

Date: Published March 29, 2013.

3.1 ABSTRACT

The storage of red blood cells (RBCs) in a refrigerated state allows a shelf life of a few weeks, whereas RBCs frozen in 40% glycerol have a shelf life of 10 years. Despite the clear logistical advantages of frozen blood, it is not widely used in transfusion medicine. One of the main reasons is that existing post-thaw washing methods to remove glycerol are prohibitively time consuming, requiring about an hour to remove glycerol from a single unit of blood. In this study, we have investigated the potential for more rapid removal of glycerol. Using published biophysical data for human RBCs, we mathematically optimized a three-step deglycerolization process, yielding a procedure that was less than 32 s long. This procedure was found to yield 70% hemolysis, a value that was much higher than expected. Consequently, we systematically evaluated three-step deglycerolization procedures, varying the solution composition and equilibration time in each step. Our best results consisted of less than 20% hemolysis for a deglycerolization time of 3 min, and it is expected that even further improvements could be made with a more thorough optimization and more reliable biophysical data. Our results demonstrate the potential for significantly reducing the deglycerolization time compared with existing methods.

3.2 INTRODUCTION

Transfusion of red blood cells (RBCs) has been accepted as a method of therapy since the early 1900s [87-90]. Today, millions of patients receive blood transfusions, with over 15 million RBC units transfused per year in the United States alone [1]. Because of

the enormous clinical need for RBC products, a preservation method that maintains the viability and function of the cells for an extended period of time is crucial. Currently, almost all RBC units are stored in a refrigerated state using special hypothermic storage solutions, which allows a storage shelf life of up to 6 weeks [2, 3, 91] Although the blood inventory is carefully managed, outdating and inventory shortages are still significant issues [1]. Moreover, recent reports indicate that "old" blood may be associated with a higher incidence of transfusion-related complications [6-8], suggesting that the acceptable refrigeration period may be as short as 2 weeks [6, 9]. Such a reduction in shelf life would have a dramatic impact on the RBC supply chain, leading to more frequent shortages, higher incidence of outdating, and increased cost.

Cryopreservation has the potential to mitigate these logistical challenges by extending the acceptable storage period to years instead of weeks [92]. Currently, two different strategies are used clinically for cryopreservation of RBCs, and both involve the use of glycerol as a cryoprotectant (CPA) to prevent damage during freezing and thawing. In Europe, RBCs are routinely stored in 20% glycerol in liquid nitrogen, whereas in the United States and Canada it is more common to use 40% glycerol, which allows storage in a mechanical freezer at -80 °C [2]. Although RBCs frozen in 40% glycerol have an FDA-approved storage limit of 10 years, cryopreservation is typically only used for storage of rare or autologous units. One of the main obstacles to more widespread use of cryopreserved RBCs is that post-thaw processing to remove glycerol is prohibitively time consuming, requiring about 1 h for a single unit of blood [2, 28, 93].

Current deglycerolization methods are time consuming in part because of limitations in how fast glycerol can be removed without damaging the cells. Damage during addition and removal of CPAs such as glycerol can be attributed to two major causes. First, CPAs can be cytotoxic. For human RBCs, cytotoxicity is not expected to be a major issue because RBCs can be exposed to 40% glycerol for hours without incurring significant damage [30]. Second, addition and removal of CPAs result in large osmotic gradients, which may lead to damaging cell volume changes [45, 94, 95]. Human RBCs have been shown to undergo hemolysis if they swell beyond a limiting maximal volume or if they are returned to isotonic conditions after shrinking below a limiting minimal volume [47, 52]. The high glycerol concentrations used for RBC cryopreservation necessitate multistep removal protocols to avoid hemolysis caused by excessive cell volume changes. The most commonly used method involves an initial wash with 12% saline, an intermediate wash with 1.6% saline, and a final wash with isotonic saline, ultimately bringing the glycerol concentration down to less than 1% [23]. This method was empirically developed more than 30 years ago using the rationale that slow, gradual changes in solution composition would enable avoidance of osmotic damage [30]. More recently, a method has been introduced that only involves washes with 12% saline and isotonic saline; this method requires that the supernatant be removed from the glycerolized RBCs before initiating the washing process [23, 27].

To implement the multistep glycerol removal procedures described above, centrifugal cell washers are typically used. Historically, these centrifugal cell washers have been open (non-sterile) systems, and consequently post-wash storage periods have

been limited to 24 h. In recent years, a functionally closed centrifugal cell washing system—the ACP 215 Automated Cell Processor—has been introduced [27]. The primary advantage of this new cell washer is that it allows sterile operation, which has enabled the post-wash storage period to be extended to 2 weeks [27, 96]. However, even with the ACP 215, the washing process still requires about 1 h per RBC unit [29].

Mathematical models of cell membrane transport can be used to guide design of CPA addition and removal procedures, offering the potential for significantly reducing the deglycerolization time. Classically, mathematical optimization approaches have primarily focused on avoidance of osmotic damage and protocol expediency [45, 94, 95, 97-99]. More recently, Benson [100] and Benson et al. [99] have used optimal control theory to determine the time-varying solution composition that would minimize the duration of the procedure, while keeping the cell volume within osmotic tolerance limits. In general, minimal time protocols achieved using this theory have been at least an order of magnitude faster than the conventional step-wise approaches [99-101]. This study was motivated by the dramatic reductions in deglycerolization time that are predicted using this optimization theory. As shown in Figure 1, the minimal time deglycerolization procedure for human RBCs is predicted to take less than 20 s. The mathematically optimized procedure involves an extracellular solution composition that varies nonlinearly with time, such that the cell volume is maintained at the lower osmotic tolerance limit through the majority of the glycerol removal process. This cell shrinkage maximizes the concentration-driving force for glycerol removal, allowing the procedure to be completed as quickly as possible. Despite the promise of the mathematically

optimized deglycerolization method shown in Figure 3.1, the rapid nonlinear concentration changes are challenging to carry out, making it difficult to evaluate experimentally.

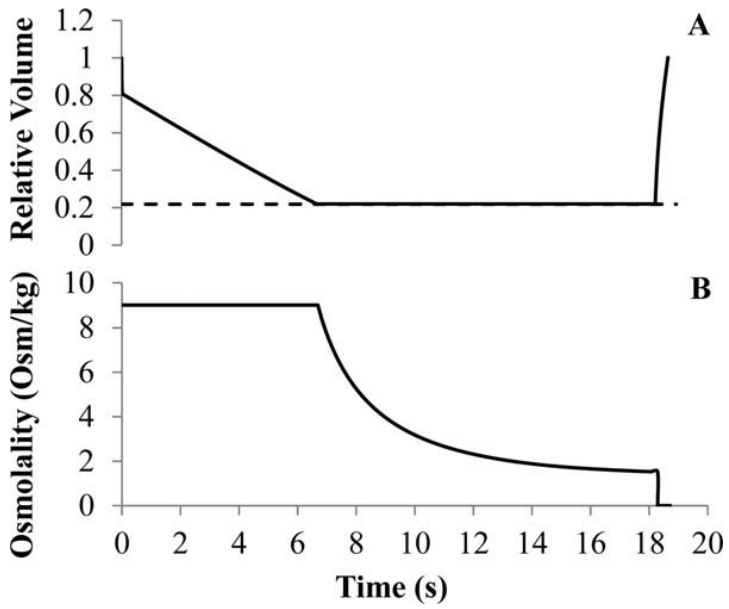

Figure 3.1. Mathematically optimized deglycerolization method determined using published biophysical data for human RBCs [33, 39-42, 47, 52, 102-104]. (see Table 1) and the optimization approach described in Benson et al [99]. The top panel (A) shows predictions of the relative osmotically active cell volume (i.e., the osmotically active volume normalized to the isotonic volume) during exposure to the optimal time-varying solute concentration shown in the bottom panel (B).

In this study, we have undertaken a preliminary investigation of glycerol removal from cryopreserved RBCs using a mathematically optimized three-step removal procedure. Our general approach was to dilute the sample with saline solution in each step, which allowed us to accurately control the timing of changes in solution

composition. Our results demonstrate that it is possible to rapidly remove glycerol from frozen-thawed RBCs, as long as the solution composition is appropriately controlled throughout the deglycerolization process. In future studies, we will focus on development of practical methods for implementation of the controlled changes in solution composition that are required for rapid deglycerolization. Ultimately, this work has the potential to substantially reduce the deglycerolization time compared with existing methods, which will facilitate more widespread use of frozen blood in transfusion medicine.

3.3 MATERIALS & METHODS

Mathematical optimization of the deglycerolization method

We wish to minimize the total time to remove glycerol while maintaining RBC volumes between osmotic tolerance limits. Although time-optimal concentration controls are already known for the case of continually varying concentrations (see Figure 3.1) [99, 100], they are presently impractical to implement. Therefore, we will attempt to define an optimal protocol with three piecewise constant steps: starting with cells equilibrated with the cryopreservation solution, we will expose them to three different media compositions for varying lengths of time. Using the known biophysical behavior of RBCs, we are able to formulate and solve this problem mathematically. Previous studies of glycerol transport in RBCs have used several modeling approaches, including the Kedem–Katchalsky formalism [31] and the two-parameter formalism [105]. We chose to work with the two-parameter model defined by

$$\frac{dW}{dt} = -L_p ART\left(M_n + M_s - \frac{N+S}{W}\right)$$
$$\frac{dS}{dt} = P_s A\left(M_s - \frac{S}{W}\right) \quad [1]$$

where W and S are the volume of osmotically active water and moles of glycerol, respectively, L_p and P_s are the hydraulic conductivity and solute permeability, respectively, A, R, and T are the cell surface area (which was assumed constant), gas constant, and absolute temperature, respectively, M_s and M_n are the extracellular osmolalities of glycerol and nonpermeating solute, respectively, N is the osmoles of nonpermeating solute, and t is time. Note that here we model only two permeating components of the solution: glycerol and water. Although there is a large body of literature discussing ionic transport in RBCs, the relative permeability of the components of salts, even under large electrochemical potential gradients, is six orders of magnitude less than that of glycerol, which is in turn three orders of magnitude less than that of water [106]. Thus, salts may be safely considered relatively nonpermeating in this context. Because nonpermeating solutes do not cross the cell membrane, the Boyle–van't Hoff equation applies and $= M^{iso}W^{iso}$, where M^{iso} and W^{iso} are the isotonic osmolality and water volume, respectively.

For practicality of implementation, we have chosen to consider three-step protocols involving ten-fold dilutions of the sample in each step, with isotonic conditions at the end of the third step. Such a protocol can be described using the following set of parameters: t_j, $M_{n,j}$, and $M_{s,j}$, indicating the durations, concentrations of nonpermeating

solutes, and concentrations of permeating solutes in steps j = 1, 2 and 3 respectively. Because our goal is to remove glycerol from the cells as quickly as possible, the solution being added to dilute the sample in each step should not contain any glycerol. Thus, the concentration of glycerol in each step can be estimated given the composition of the original sample (i.e., 40% w/v glycerol or an osmolality of about 6,500 mOsm/kg). After a ten-fold dilution (by volume) in the first step, the glycerol concentration is about $M_{s,1}$ = 410 mOsm/kg, and after an additional ten-fold dilution in the second step the glycerol concentration is is $M_{s,2}$ = 40 mOsm/kg. After the third step, the glycerol concentration is negligibly low (less than 5 mOsm/kg) and we have assumed $M_{s,3} \sim 0$. To achieve isotonic conditions at the end of the procedure, the nonpermeating solute concentration in step 3 must be the isotonic concentration, i.e., $M_{n,3}$ = 300 mOsm/kg. Consequently, the following five parameters remain to be optimized: t_1, t_2, t_3, $M_{n,1}$ and $M_{n,2}$.

If we let $\lambda = (t_1, t_2, t_3, M_{n,1}, M_{n,2})$, then we may formally define the optimization problem as finding minimal time $t_f = t_1 + t_2 + t_3$ over the parameter parameter set λ, subject to System 1, an end time constraint (as defined below) and cell volume constraints (as defined below). The end time constraint is defined as

$$\left\| \left((W(t_f), S(t_f)) - (W^{\text{iso}}, 0) \right) \right\|^2 < \epsilon \qquad [2]$$

where the parameter ϵ represents the acceptable squared error between the actual final state and the desired final state. The volume constraints are defined as

$$V_{low} - V_b \leq W(t) + \bar{v}S(t) \leq V_{high} - V_b \qquad [3]$$

where V_{low} and V_{high} are the lower and upper total volume osmotic tolerance limits for RBC, V_b is the osmotically inactive volume, and $\bar{v}$ = 71 mL/mol is the molar volume of glycerol. The constraints defined in Eq. 3 represent upper and lower osmotic tolerance limits on the osmotically active cell volume, which comprises the sum of volumes occupied by osmotically active water and glycerol. The parameter values used for mathematical optimization of the deglycerolization method are given in Table 3.1, and the details of our numerical optimization approach are provided in Appendix A. A flow chart illustrating the modeling strategy is also provided in Figure 3.2.

Table 3.1. Parameters for Optimization of the Deglycerolization Method

Parameter	Parameter Definition	Value	Reference
W^{iso}	Water volume at isotonic conditions	60 μm^3	[103, 104]
V_b	Osmotically inactive volume	40 μm^3	[103, 104]
A	Cell surface area	130 μm^2	[103]
V_{low}	Lower osmotic tolerance limit	53 μm^3	[52]
V_{high}	Upper osmotic tolerance limit	138 μm^3	[47]
L_p	Hydraulic conductivity	9 μm min^{-1} atm^{-1}	[33]
P_s	Glycerol permeability	1.8 μm/min	[39-42, 102]
T	Absolute temperature	295 K	

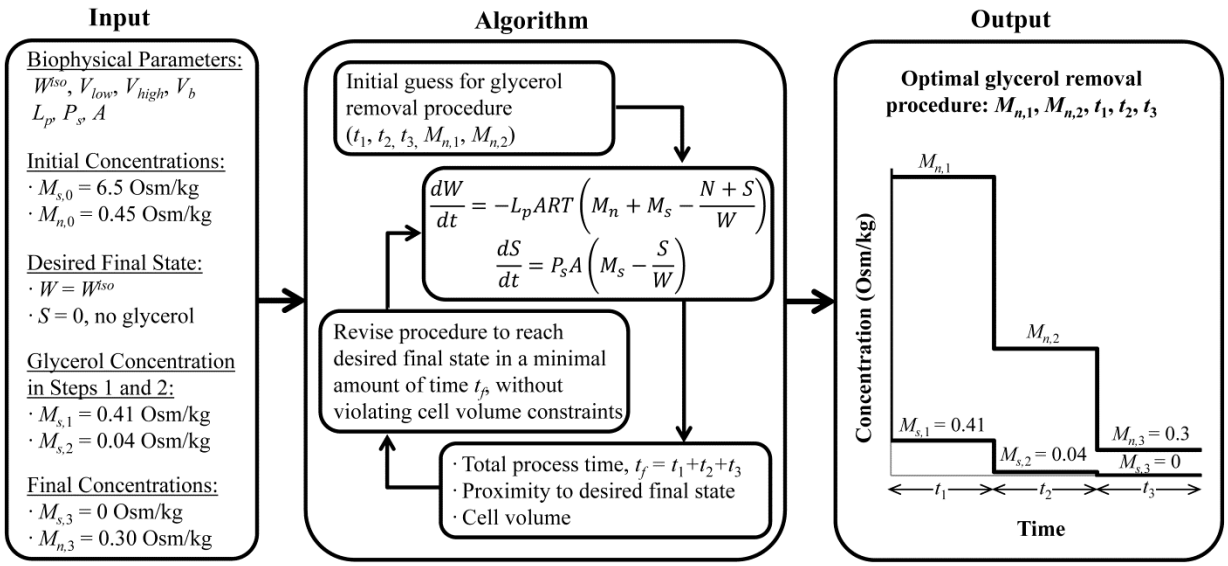

Figure 3.2. Schematic illustrating mathematical optimization strategy.

Glycerolization, freezing, and thawing

The methods for glycerolization, freezing, and thawing were adapted from Meryman and Hornblower [30]. Whole human blood in citrate phosphate dextrose (purchased from Bioreclamation, NY) was glycerolized and frozen within 4 days of collection. To prepare glycerolized RBCs, approximately 10 mL of whole blood was first centrifuged at 1,400g for 10–15 min, and the plasma was removed. The resulting packed cells were then glycerolized in two steps using an aqueous glycerol solution with the following composition: 57.1 g glycerol, 0.03 g potassium chloride, 0.085 g magnesium chloride hexahydrate, 0.08 g disodium phosphate, and 1.6 g sodium lactate in a total volume of 100 mL, adjusted to a pH of 6.8 [107]. In the first step, 1.5 mL of this glycerol solution was added dropwise to the packed cells with gentle agitation over a period of 3 min. The mixture was then allowed to equilibrate undisturbed for at least 5 min. In the

second glycerolization step, 5 mL of the glycerol solution was added dropwise while the mixture was gently agitated over a 3-min period, yielding a final glycerol composition of ~ 40% w/v. The entire glycerolization process was carried out at room temperature. The glycerolized RBCs were then divided into aliquots of 0.6–1.1 mL in cryogenic vials, placed in a Nalgene® Cryo 1 ºC "Mr. Frosty" freezing container (Thermo Scientific, NC), and stored in a -80 ºC freezer for at least 12 h. Frozen RBCs were thawed by placing the cryogenic vial in a 37 ºC water bath for ~1 min. All glycerolized blood samples were used in deglycerolization experiments within 2 h of thawing.

Implementation of the mathematically optimized deglycerolization method

We evaluated the mathematically optimized deglycerolization method, as well as procedures in the vicinity of the optimum. Table 3.2 provides the detailed experimental approach for carrying out the mathematically optimized method. A small volume of glycerolized blood was placed in a round-bottomed flask on a linear shaker, and diluted first with 20.4% w/v saline, then with 3% w/v saline solution, and finally with hypotonic 0.2% w/v glucose solution to bring the resulting concentration to isotonic. All solutions were buffered with 0.012 molal disodium phosphate and adjusted to a pH of 7. The deglycerolization process was carried out at room temperature (between 21 and 22 °C). Hemolysis was measured at the completion of the deglycerolization procedure as described below. Although the mathematical optimization approach assumed a ten-fold dilution in the third step and a corresponding glycerol concentration of $M_{s,3}$~ 0, we chose to use a five-fold dilution instead. This was done to avoid excessive dilution of

hemoglobin, which would reduce the accuracy of hemolysis measurements. The fivefold dilution in the third step brought the glycerol osmolality to 7 mOsm/kg, which is still low enough to assume that that $M_{s,3} \sim 0$.

Standard deglycerolization method

As a standard deglycerolization method, we used the serial dilution procedure described by Meryman and Hornblower [108]. This procedure is a manual adaptation of the deglycerolization procedure listed in the AABB Technical Manual [23]. The procedure was carried out as described in the literature except that it was scaled down for a smaller working volume. First, 0.51 mL of 12% saline was added slowly to 3 mL of 75% hematocrit glycerolized blood over 5 min and the resulting mixture was allowed to equilibrate undisturbed for 3 min. The mixture was then slowly diluted using 3.7 mL of 1.6% saline over 5 min and centrifuged at 1,400g for 10 min. The resulting cell pellet was resuspended by adding 5 mL of 0.9% saline, 0.2% glucose over a 3 min period, and the sample was again centrifuged at 1,400g for 10 min. This isotonic wash process (i.e., addition of 5 mL of 0.9% saline, 0.2% glucose solution followed by centrifugation) was repeated a second time, after which the cells were resuspendedin 1.8 mL of 0.9% saline, 0.2% glucose to achieve a 50% hematocrit mixture. The entire deglycerolization process was carried out at room temperature and took approximately 1 h. The hemoglobin content in the supernatant collected from each step was analyzed and compared to the initial hemoglobin content to obtain the percent hemolysis.

Systematic investigation of the deglycerolization process

To systematically investigate the glycerol removal process, we evaluated a range of procedures based on the standard deglycerolization method described above. The detailed experimental methods are provided in Table 3.2. The basic approach involved dilution of glycerolized cells in three steps, with the first step consisting of addition of 12% w/v saline, the second step consisting of addition of 3.4% w/v saline, and the final step consisting of addition of the appropriate volume of 0.2% w/v glucose to bring the mixture to isotonic conditions. Each of these dilution steps was carried out at room temperature. The conditions in the first step were varied as follows. The extent of dilution was varied between two-fold and ten-fold and the equilibration time was varied between 5 s and 2 min. All solutions were buffered with 0.012 molal disodium phosphate and adjusted to a pH of 7. These experiments were carried out in a 100-mL round-bottomed flask on a linear shaker, which was operated at a shaking rate of ~3 Hz. Samples were collected for hemolysis measurements at two different points during the deglycerolization process. One minute into the second equilibration period, a sample was collected to assess hemolysis under hypertonic conditions. A sample was also collected at the end of the procedure to assess hemolysis after the cells had been returned to isotonic conditions.

After systematically investigating three-step deglycerolization procedures, we evaluated the potential for achieving improved results by adding an additional step. We considered four-step procedures that were identical to the threestep procedures that yielded the lowest hemolysis, with the following exception. In the four-step procedures, the volume of 3.4% saline was divided into two different aliquots, which were added to

the sample at different times. We evaluated four-step procedures with either a tenfold or twofold dilution with 12% saline in the first step, as described in Table 3.2.

Table 3.2. Experimental Methods for Investigation of the Deglycerolization Process

Step	Mathematically Optimized	Systematic 3-Step Deglycerolization			4-Step Deglycerolization	
		2-fold	4-fold	10-fold	2-fold	10-fold
Initial	0.1 ml thawed RBC	0.5 ml thawed RBC	0.25 ml thawed RBC	0.1 ml thawed RBC	0.5 ml thawed RBC	0.1 ml thawed RBC
1	Add 0.9 ml 20.4% saline, wait 8.5 s	Add 0.5 ml 12% saline, wait 20-120 s	Add 0.75 ml 12% saline, wait 20-120 s	Add 0.9 ml 12% saline, wait 5-60 s	Add 0.5 ml 12% saline, wait 60 s	Add 0.9 ml 12% saline, wait 15 s
2	Add 9 ml 3% saline, wait 22 s	Add 9 ml 3.4% saline, Wait 120 s	Add 9 ml 3.4% saline, wait 120 s	Add 9 ml 3.4% saline, wait 120 s	Add 1 ml 3.4% saline, wait 30 s	Add 1 ml 3.4% saline, wait 15 s
3	*Add 45 ml 0.2% glucose	*Add 37 ml 0.2% glucose	*Add 35 ml 0.2% glucose	*Add 35 ml 0.2% glucose	Add 8 ml 3.4% saline, wait 90 s	Add 8 ml 3.4% saline, wait 105 s
4	n/a	n/a	n/a	n/a	*Add 37 ml 0.2% glucose	*Add 35 ml 0.2% glucose

* The appropriate volume of 0.2% buffered glucose was added to bring the final concentration to isotonic.

Measurement of hemolysis

To measure hemolysis, samples were centrifuged at 1,400g for 10 min to separate the supernatant from the surviving cells. A portion of the supernatant was then diluted appropriately to fall within the linear absorbance measurement range at 415 nm. The concentration of hemoglobin was measured using Harboe's direct spectrophotometric method with a three-point Allen correction, which converts the absorbance values to hemoglobin concentration (Hb) using the following equation [109]:

$$Hb(g/ml) = 167.2A_{415} - 83.6A_{380} - 83.6A_{450} \quad [4]$$

where A_{415}, A_{380} and A_{450} are absorbance values measured at 415 nm, 380 nm and 450 nm, respectively. The percent hemolysis was calculated by dividing the mass of the free hemoglobin present in the supernatant by the mass of total hemoglobin in a 100% lysed control sample containing the same number of RBCs. The 100% lysed sample was prepared by diluting 0.1 mL of the glycerolized blood 100-fold using distilled water followed by three freeze-thaw cycles to ensure complete lysis. A small portion of the lysed suspension was also viewed under the microscope to further confirm that no intact cells remained. To determine the total mass of hemoglobin in the supernatant, the hemoglobin concentration from Eq. 4 was multiplied by the volume of the supernatant as well as the dilution factor.

Statistical analysis

All hemolysis data are reported as averages of three replicates, with each replicate from a different batch of blood. Error bars show the standard error of the mean. The data were analyzed using ANOVA, followed by Tukey HSD tests for pairwise comparisons. Differences were considered to be significant at a 95% confidence level. All analysis was performed using StatGraphics software.

3.4 RESULTS

Mathematically optimized deglycerolization method

The mathematically optimized deglycerolization procedure is given by the steps

in Table 3.3, and the corresponding cell volume predictions are given in Figure 3.3. In short, we predicted that a total deglycerolization time of less than 32 s is achievable given the three-step method used in this study. The procedure involves exposure to a relatively hypertonic solution in the first step, which is predicted to cause an initial period of rapid cell shrinkage because of exosmosis of water, followed by more gradual shrinkage as both glycerol and water exit the cells. The inset plot of Figure 3.3 shows the first 0.15 s of the deglycerolization process and illustrates this biphasic behavior. After the initial period of rapid shrinkage, a quasi-equilibrium is reached, upon which the rate-limiting factor is the glycerol permeability as water may leave only as fast as the glycerol leaves. To be precise, because there is quasi-equilibrium, $M_n + M_s \cong (N + S)/W$, so $(M_n + M_s)W \cong N + S$ and $(M_n + M_s)dW/dt \cong dS/dt = P_s A(M_s - S/W)$. The end of the first deglycerolization step corresponds with shrinkage to the lower osmotic tolerance limit. In the second step, the cells are predicted to initially swell because of water influx and then shrink as both glycerol and water exit the cells. The end of the second step also corresponds with shrinkage to the lower osmotic tolerance limit. In the third step, the cells are exposed to isotonic conditions, which causes water influx and concomitant swelling, followed by stabilization of the cell volume near its isotonic value. The mathematically optimized procedure can be understood conceptually in terms of the concentration-driving force for glycerol removal. Figure 3.3 shows that the cells are in a shrunken state through the majority of the deglycerolization process, reaching the minimum osmotic tolerance limit at the end of the first and second steps. This shrinkage is advantageous because it increases the concentration of intracellular glycerol and

consequently increases the driving force for glycerol removal.

Table 3.3. Mathematically Optimized Three-Step Deglycerolization Method

Step	Glycerol Concentration (mOsm/kg)	Nonpermeating Solute Concentration (mOsm/kg)	Equilibration Time (s)
Initial	6500	450	-
Step 1	410	7414	8.5
Step 2	40	1487	22.1
Step 3	0	300	0.7

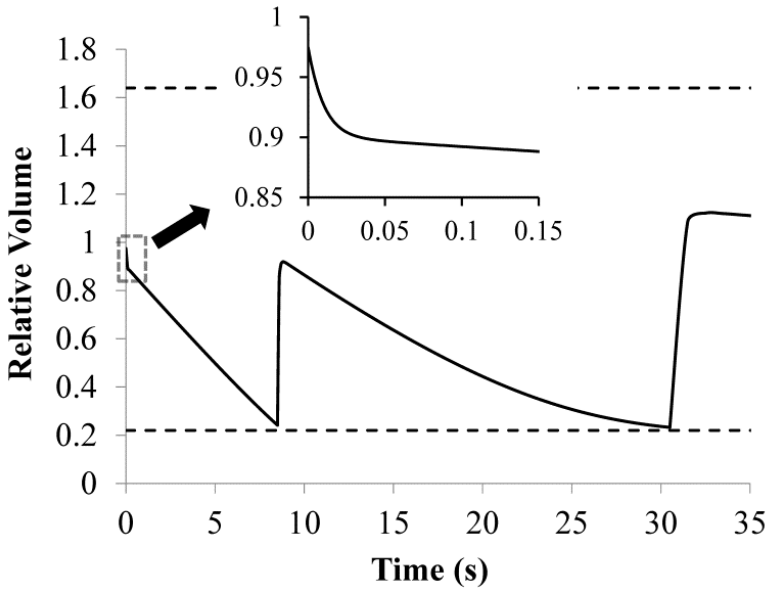

Figure 3.3. Predictions of relative osmotically active cell volume ($W/W^{iso} + \bar{v}S/W^{iso}$) for the mathematically optimized deglycerolization method (solid line). The dashed lines show the upper and lower osmotic tolerance limits on the osmotically active volume (see Eq. 3) and the inset shows an expanded view of the relative volume predictions in the first 0.15 seconds.

Numerical exploration of points around the optimum showed that the equilibration time in the first step was critical. When the first time step was too short, there was excessive swelling in the second step (which would be expected to cause hemolysis), and when the first time step was too long, there was excessive exosmosis of water (which would be expected to cause damage from shrinkage below the minimal volume limit).

To evaluate the mathematically optimized deglycerolization procedure, we exposed thawed RBCs to the optimal procedure, as well as procedures with slight variations in the equilibration times in steps 1 and 2. The hemolysis resulting from these procedures is shown in Figure 3.4. The mathematically optimized procedure resulted in 70.5±0.8% hemolysis, a value that was much higher than expected. Analysis of the data by two-way ANOVA revealed that the equilibration time in the first step of the procedure had a significant effect on hemolysis ($p = 0.0004$), but the duration of equilibration in the second step did not have a significant effect ($p = 0.16$). The interaction between equilibration times in steps 1 and 2 was also not significant ($p = 0.98$). In particular, pairwise comparisons show that the hemolysis incurred after a 5 s equilibration in the first step is significantly higher than the hemolysis for equilibration times of 8.5 and 15 s.

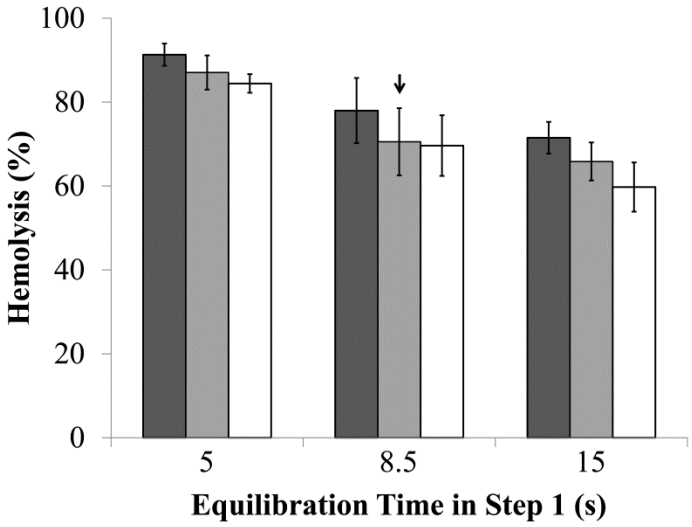

Figure 3.4. Hemolysis associated with the mathematically optimized deglycerolization procedure (indicated with the arrow) along with various similar procedures with slight time variations. In the second step of the procedure, RBCs were equilibrated for 15 seconds (dark gray bars), 22 seconds (light gray bars) or 30 seconds (white bars). Hemolysis was measured after the cells had been returned to isotonic conditions in the third step.

Standard deglycerolization method

To explore possible reasons for the unexpectedly high hemolysis resulting from the mathematically optimized procedure, the thawed blood was subjected to a standard deglycerolization procedure [108]. The standard method involves a series of washes over a time period of about 1 h, first with 12% saline, then with 1.6% saline, and finally with isotonic saline. Meryman and Hornblower found that this method resulted in high RBC recovery, with an average of around 95% [108]. In three replicate experiments (each representing a different batch of blood), we found that the standard deglycerolization method yielded a hemolysis of 8±2%. This demonstrates that high RBC recovery can be

achieved if an appropriate deglycerolization method is used.

Systematic investigation of the deglycerolization process

To systematically investigate the possibility of rapidly removing glycerol from thawed RBCs, a series of deglycerolization experiments was performed. The general experimental approach involved dilution of the thawed RBCs in three steps to achieve isotonic conditions at the end of the procedure (see Table 3.2). In the design of these experiments, one of our goals was to choose conditions in the second and third steps that would allow the RBCs to fully equilibrate without incurring damage. We chose to dilute the sample tenfold with 3.4% saline in the second step, which yielded a final saline concentration of ~1,400 mOsm/kg, before bringing the sample to isotonic conditions in the third step with the addition of hypotonic (0.2%) glucose solution. The concentration in the second step was chosen based on Lovelock's finding that RBCs can be exposed to saline concentrations of up to 1,500 mOsm/kg without significant damage [110]. To confirm that prolonged exposure to this concentration would not cause damage, a control experiment was carried out in which fresh RBCs, originally at 300 mOsm/kg, were exposed to a 1,400 mOsm/kg environment for 3 min before being brought back to isotonic conditions by addition of 0.2% glucose solution. In three replicate experiments, the average hemolysis was less than 1%. Two important conclusions can be drawn from these results. First, the results show that bringing RBCs to isotonic conditions by dilution with hypotonic glucose solution does not cause hemolysis. Second, the results indicate that exposure to a solution osmolality of 1,400 mOsm/kg in the second step of the

deglycerolization process is not expected to be damaging. Consequently, we focused on investigation of the first step of the deglycerolization process.

The first step of the deglycerolization process was carried out using equilibration times ranging from 5 s to 2 min and dilutions ranging from two-fold to ten-fold. To aid in the design and interpretation of these experiments, changes in cell volume were predicted using published membrane permeability parameters for human RBCs (see Table 3.1). Figure 3.5A illustrates the effect of the equilibration time in the first step on the predicted changes in cell volume. Only the first minute of the deglycerolization process is shown because predicted cell volume changes were most extreme in this regime. As shown in Figure 3.5A, an equilibration time of 20.5 s is expected to result in cell volumes that remain within the osmotic tolerance limits. However, even slight deviations in the equilibration time can dramatically affect the predicted changes in cell volume. If the addition of the second saline solution is too late, the cells will have shrunk past the lower osmotic tolerance limit. Conversely, if the addition of the second saline solution is premature, not enough glycerol will have been removed from the intracellular region causing the cells to swell beyond the upper osmotic tolerance limit.

Figure 3.5B shows cell volume predictions after dilution by ten-fold, four-fold, or two-fold in the first step of the deglycerolization procedure. The ten-fold dilution results in a substantial decrease in the extracellular glycerol concentration, which induces rapid efflux of glycerol from the cells. As a result, the cells shrink relatively rapidly, reaching the minimum osmotic tolerance limit after about 20 s. On the other hand, the two-fold dilution results in relatively slow cell shrinkage, with the RBCs reaching their minimum

osmotic tolerance limit after about 34 s. These predictions show that the maximum acceptable equilibration time in the first step of the procedure is expected to increase as the extent of dilution decreases.

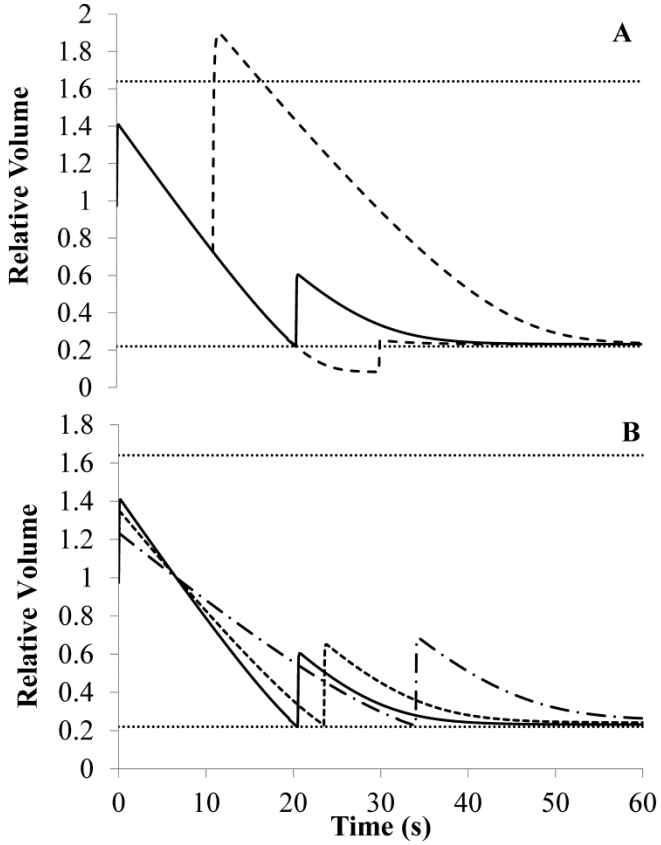

Figure 3.5. Theoretical predictions of relative osmotically active cell volume ($W/W^{iso} + \bar{v}S/W^{iso}$) after dilution with 12% saline in the first step and dilution with 3.4% saline in the second step. Osmotic tolerance limits (see Eq. 3) are shown with the dotted lines. (A) Effect of the equilibration time after a 10-fold dilution in the first step. The solid line shows predictions for an equilibration time of 20.5 seconds and the dashed lines show predictions for equilibration times of 11 and 30 seconds. (B) Effect of the extent of dilution in the first step. The dashed line shows predictions for a 10-fold dilution and a 20.5 second equilibration time, the solid line shows predictions for

a 4-fold dilution and a 23.5 second equilibration time, and the dash-dot line shows predictions for a 2-fold dilution and a 34 second equilibration time.

Figure 3.6A shows the results of experiments involving an initial tenfold dilution with 12% saline. The equilibration time in the first step of the procedure had a significant effect on the percent hemolysis ($p < 0.0001$), and so did the conditions under which hemolysis was measured ($p < 0.0001$). The interaction between these factors was also significant ($p < 0.0001$). When hemolysis was measured after the second deglycerolization step (under hypertonic conditions), hemolysis was found to decrease as the equilibration time in the first step increased. For example, when the equilibration time was 5 s, the hemolysis was 79.9±3.7% and it declined to 14.0±1.3% for an equilibration time of 30 s. In contrast, when hemolysis was measured at the end of the procedure (under isotonic conditions), it initially declined, reached a minimum of 32.1±2.4% at an equilibration time of 15 s, and then increased again.

The hemolysis data presented in Figure 3.6A can be explained in terms of the cell volume predictions shown in Figure 3.5A. Cell damage observed for short equilibration times is consistent with insufficient glycerol transport out of the cells during the first deglycerolization step. Excessive residual glycerol would be expected to cause influx of water upon addition of the second saline solution, consequently swelling the cells past their upper osmotic tolerance limit. This type of damage was apparent when hemolysis was measured under both hypertonic and isotonic conditions. The increase in hemolysis for long equilibration times is consistent with damage resulting from excessive cell shrinkage in the first deglycerolization step. This type of damage exhibited more complex

behavior that was dependent on whether hemolysis was measured under hypertonic or isotonic conditions. Our results are similar to those reported in previous studies of cell damage caused by exposure to hypertonic solutions. In particular, Lovelock reported that although some damage was observed from exposing RBCs to strong saline solutions, most of the damage became apparent once the RBCs were exposed to a more dilute saline solution and the cells were allowed to swell [110]. Figure 3.6A shows that the hypertonic hemolysis curve and isotonic hemolysis curve start to deviate from one another when the equilibration time exceeds 15 s. This separation is indicative of damage due to excessive shrinking, which manifests when the cells are induced to swell upon returning to isotonic conditions. The time at which the two curves deviate in Figure 3.6A (i.e., ~15 s) is approximately consistent with the predicted time to reach the minimum volume limit shown in Figure 3.5A, indicating a reasonable agreement between the predictions and the data.

The results from the four-fold and two-fold dilution experiments are shown in Figures 3.6B,C. In general, the hemolysis data are in agreement with the trends observed in the ten-fold dilution experiments. Statistical analysis revealed that the main effects (i.e., the equilibration time in the first step and the conditions under which hemolysis was measured), as well as the interaction between the factors, were all significant ($p < 0.023$). As with the ten-fold dilution experiments, the hemolysis data exhibited a minimum at an intermediate equilibration time. In the four-fold dilution experiments, a minimum hemolysis of 35.4±3.4 % was reached for an equilibration time of 30 s. In the two-fold dilution experiments, the hemolysis declined to 24.4±1.5% and 23.9±1.3% for

equilibration times of 60 and 90 s, respectively. These minimum hemolysis times approximately correspond with the cell volume predictions shown in Figure 3.5B.

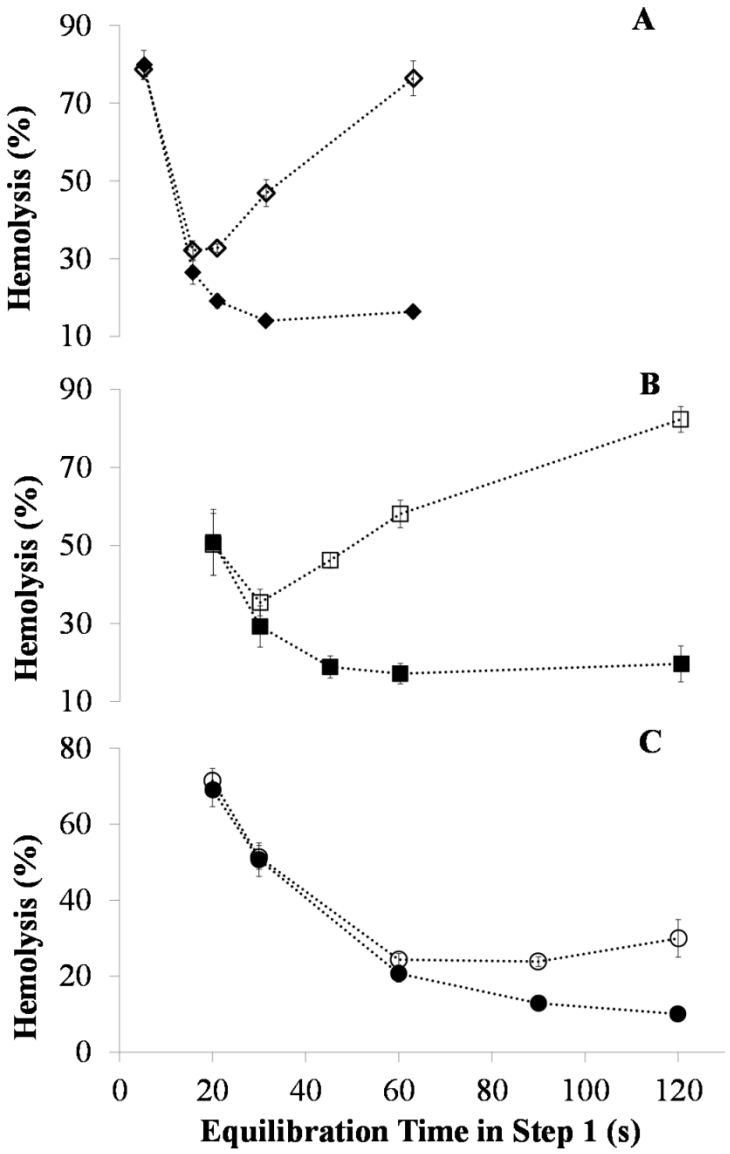

Figure 3.6. Effect of equilibration time after a 10-fold (A), 4-fold (B) or 2-fold (C) dilution with 12% saline in the first step of the deglycerolization process. Hemolysis was measured either at the end of the second step when the cells were in hypertonic

conditions (closed symbols) or at the end of the third step when the cells were in isotonic conditions (open symbols).

We also examined the effects of equilibration time and extent of dilution in the first step on the hemolysis incurred at the end of the deglycerolization process (under isotonic conditions). The effect of equilibration time in the first step was found to be significant ($p = 0.04$) but the extent of dilution was not ($p = 0.44$). However, the interaction between these factors was significant ($p < 0.0001$). For each extent of dilution, the hemolysis data reached a minimum value at a distinct equilibration time. The equilibration time corresponding with this minimum increased as the extent of dilution decreased. This trend is consistent with the theoretical predictions shown in Figure 3.5B, which show that as the extent of dilution decreases the cells can equilibrate for longer before shrinking beyond the lower osmotic tolerance limit

To further explore the possibility of decreasing damage during deglycerolization, the three-step procedures producing the best results from the ten-fold and two-fold experiments were expanded to four-step procedures. The results of these experiments are shown in Figure 3.7. In the case of tenfold dilution in the first step, the four-step procedure yielded an average hemolysis of 34.4±2.4%, which is not significantly different compared to the average hemolysis from the corresponding 3-step procedure ($p = 0.54$). For 2-fold dilution in the first step, the 4-step procedure yielded an average hemolysis of 19.2±1.0%. This value is significantly lower than the average hemolysis from the corresponding 3-step procedure ($p = 0.048$). Moreover, this value meets the AABB requirement of an *in vitro* RBC recovery of at least 80%.

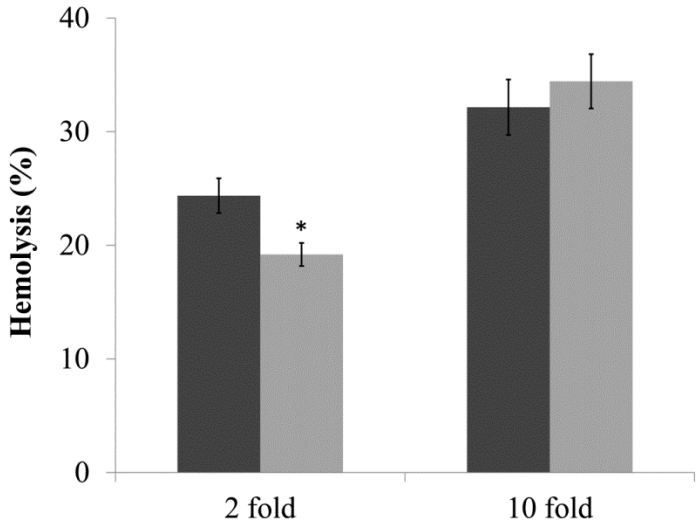

Figure 3.7. Hemolysis measured after deglycerolization using 3-step (dark gray bars) and 4-step (light gray bars) procedures with either 2-fold or 10-fold dilution in the first step. The asterisk shows a statistically significant difference between the 3-step and 4-step procedures.

3.5 DISCUSSION

The results of this study show that if the timing of changes in solution composition is appropriately controlled, it is possible to remove glycerol from frozen-thawed RBCs in a matter of minutes with less than 20% hemolysis. Although these results are promising, further improvements in cell recovery will be required before such rapid deglycerolization methods are adopted clinically. Thus, it is important to explore the possible causes for hemolysis in this study.

Although the trends observed in the deglycerolization experiments were reasonably consistent with theoretical predictions of cell volume changes, the magnitude

of hemolysis was higher than anticipated, particularly for the mathematically optimized procedure. To explore the reasons for this unexpectedly high hemolysis, we evaluated the sensitivity of the mathematically optimized deglycerolization procedure to the assumed values of the conductivity (L_p) and glycerol permeability (P_s). Over the range of values reported in the literature, the hydraulic conductivity had a negligible effect on the mathematically optimized solution compositions and equilibration times in each step of the procedure. This result is consistent with the cell volume predictions in the inset plot of Figure 3.3, which show that the hydraulic conductivity only has an effect for a short time period after exposure to a new solution composition until quasi-equilibrium is established. The optimal solution compositions in each step were also relatively insensitive to the assumed value of the glycerol permeability. However, the optimal equilibration times were highly sensitive to the glycerol permeability, as illustrated in Figure 3.8. There is considerable uncertainty in the accuracy of the glycerol permeability used in this study because published glycerol permeability values vary by more than an order of magnitude [39, 111], and in some cases the glycerol permeability has been found to decrease as the glycerol concentration increases [39, 40, 102]. In this study, we assumed that the glycerol permeability was constant and equal to the average of published permeability values corresponding with glycerol concentrations higher than 0.5 M. To improve the accuracy of the mathematically optimized procedure, a better understanding of glycerol transport in human RBCs is needed, particularly at high glycerol concentrations.

Another possible explanation for the unexpectedly high hemolysis following

deglycerolization is cell-to-cell variability, as underscored by the following points: (1) as shown in Figure 3.5A, it is critical to get the timing right in the first step of the procedure, and even slight changes in equilibration time lead to excessive shrinkage or swelling, and (2) the optimal equilibration time is highly dependent on the permeability of the cell membrane to glycerol, as shown in Figure 3.8. Therefore, in a cell population with a distribution of permeability values, there will also be a distribution of optimal equilibration times, and it may be difficult to select an equilibration time that is acceptable for all cells in the population. Jay and Rowlands measured the glycerol permeability in individual RBCs and found a wide spread in permeability values [44]. Thus, it will be important in future studies to adapt the mathematical optimization approach to account for this variability.

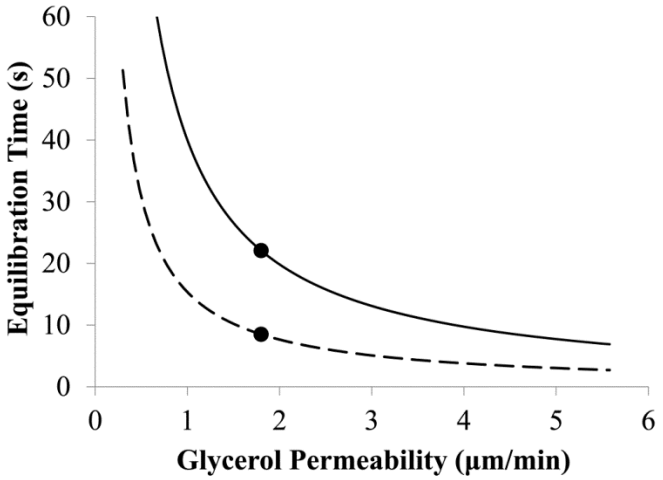

Figure 3.8. Effect of the assumed value of the glycerol permeability on the mathematically optimized equilibration times in step 1 (dashed line) and step 2 (solid line). The circles show the optimal equilibration times obtained using a glycerol permeability of 1.8 μm/min (see Table 1).

Limitations in the experimental method may have also contributed to hemolysis. The kinetics of mixing during deglycerolization would be expected to affect the agreement between model predictions and the experimental data. Although the model assumes instantaneous mixing, the experiments were done using a linear shaker that mixed the solution gently to avoid excessive mechanical stress to the RBCs. Qualitative observations suggest that mixing was complete in approximately 1–5 s. Such imperfect mixing could cause variability in the solution composition within the sample, potentially leading to damaging cell volume changes. In addition to imperfect mixing, the glass material of the roundbottomed flasks used in the deglycerolization experiments may have also caused damage. It has been shown that proximity to glass surfaces induces normal RBCs to form echinocytes, rendering them more susceptible to hemolysis [103].

We have primarily interpreted our hemolysis data in terms of cell volume changes induced by exposure to changes in solution composition during the deglycerolization process. For instance, our results show that improved cell recovery is achieved by dilution with a relatively small volume of 12% saline in the first step. Adding a small volume of 12% saline results in a relatively small change in glycerol concentration and relatively slow changes in cell volume (see Figure 3.5B). Thus, our interpretation is that the improved cell recovery is a result of slower volume changes during the first step and a concomitant increase in the time window during which the second saline solution can be added without causing excessive shrinkage or swelling. An alternative interpretation for this result is that dilution with a small volume of 12% saline is advantageous because it

prevents exposure to high and potentially toxic salt concentrations. We have interpreted our results in terms of cell volume predictions, rather than salt toxicity, for the following reasons. Previous studies show that cell shrinkage after exposure to hypertonic conditions causes damage to RBCs, not toxicity specific to salt solutions [112-114]. For instance, hypertonic solutions prepared with sodium chloride and sucrose both induce membrane damage at the same osmolality, whereas exposure to hypertonic solution containing DMSO (which is a permeating solute) is not damaging [113, 114]. The hypertonic solutions prepared with nonpermeating solutes cause shrinkage, whereas solutions prepared with DMSO do not; these results suggest that excessive cell shrinkage is what causes damage during exposure to hypertonic conditions. Further evidence for the damaging effects of cell shrinkage is provided by previous studies in which the amount of intracellular potassium was adjusted before exposing the cells to hypertonic conditions [112, 115]. These studies show that membrane damage manifests when the RBCs reach the same minimum volume, even though this minimum volume occurs at substantially different osmolalities because of the differences in intracellular potassium levels. These studies provide strong evidence that damage associated with exposure to hypertonic conditions is caused by excessive cell shrinkage, and not by salt toxicity. Nonetheless, it would be worthwhile in future studies to investigate the use of other nonpermeating solutes (e.g., sucrose) in the hypertonic wash solutions to rule out the potentially damaging effects of high salt concentrations.

The experimental method used for deglycerolization in this study was selected because it allowed good control over the timing of changes in solution composition.

However, it is not practical for use at large scale. Serial dilution of a full RBC unit using the methods described in this study would require over 30 L of wash solution and a mixing container capable of accommodating this volume. Moreover, the diluted RBC suspension would need to be centrifuged to bring the hematocrit back up to appropriate levels. Nonetheless, our experiments have identified solution compositions and equilibration times that allow rapid glycerol removal. In future studies, we will develop practical methods for implementation of these changes in solution composition, enabling rapid deglycerolization of full RBC units. Existing centrifugal cell washers are not appropriate for this purpose because of limitations in how fast the solution composition can be changed in these devices. Thus, we plan to develop microfluidic devices for imposing controlled changes in solution composition for rapid removal of glycerol from RBCs.

In addition, future studies will need to more fully characterize the quality of frozen-thawed RBCs after rapid deglycerolization. Although we only measured hemolysis levels immediately after deglycerolization, it will also be necessary to evaluate the stability of the washed RBCs during refrigerated storage. Additional in vitro assays will also need to be performed including measurement of potassium, ATP, 2,3-diphosphoglyerate, deformability, and p50 levels. Finally, it will be necessary to confirm that the RBCs survive after transfusion and meet the AABB standard for in vivo recovery of at least 75% after 24 h [23].

3.6 CONCLUSIONS

We have demonstrated that it is possible to deglycerolize frozen-thawed RBCs in 3 min with less than 20% hemolysis meeting AABB standards for in vitro cell recovery. This promising result shows that it is feasible to significantly reduce the deglycerolization time compared with existing methods, potentially removing one of the main barriers to more widespread use of frozen blood in transfusion medicine. In future studies, we will more thoroughly investigate the deglycerolization process, including the effects of temperature and the type of nonpermeating solute. These studies are expected to lead to further improvements in cell recovery and reductions in the deglycerolization time. We will also explore strategies for adapting the deglycerolization methods described here for use at large scale.

3.7 ACKNOWLEDGEMENTS

This work was supported by a National Science Foundation grant (#1150861) to Adam Higgins.

Chapter 4: Osmotic Tolerance Limits of Red Blood Cells from Umbilical Cord Blood

Mariia Zhurova*, Ratih E. Lusianti*, Adam Z. Higgins, Jason P. Acker

Journal: *Cryobiology*

Address: http://www.journals.elsevier.com/cryobiology/

Date: Submitted November 2013. Accepted with conditional revisions February 2014.

*These authors equally contributed to this work

4.1 ABSTRACT

Effective methods for long-term preservation of cord red blood cells (RBCs) are needed to ensure a readily available supply of RBCs to treat fetal and neonatal anemia. Cryopreservation is a potential long-term storage strategy for maintaining the quality of cord RBCs for the use in intrauterine and neonatal transfusion. However, during cryopreservation, cells are subjected to damaging osmotic stresses during cryoprotectant addition and removal and freezing and thawing that require knowledge of osmotic tolerance limits in order to optimize the preservation process. The objective of this study was to characterize the osmotic tolerance limits of cord RBCs in conditions relevant to cryopreservation, and compare the results to the osmotic tolerance limits of adult RBCs. Osmotic tolerance limits were determined by exposing RBCs to solutions of different concentrations to induce a range of osmotic volume changes. Three treatment groups of adult and cord RBCs were tested: 1) isotonic saline, 2) 40% w/v glycerol, and 3) frozen-thawed RBCs in 40% w/v glycerol. We show that cord RBCs are more sensitive to shrinkage and swelling than adult RBCs, indicating that osmotic tolerance limits should be considered when adding and removing cryoprotectants. In addition, freezing and thawing resulted in both cord and adult RBCs becoming more sensitive to post-thaw swelling requiring that glycerol removal procedures for both cell types ensure that cell volume excursions are maintained below 1.7 times the isotonic osmotically active volume to attain good post-wash cell recovery. Our results will help inform the development of optimized cryopreservation protocol for cord RBCs.

4.2 INTRODUCTION

Fetal and neonatal anemias are serious complications that may happen during pregnancy and post-natal development. Fetal anemia may be caused by immune hemolytic disease [116], defects in the hemoglobin structure and synthesis, fetomaternal or twin-to-twin hemorrhages, and parvovirus B19 infections [117]. Neonatal anemia may carry-over from fetal anemia, or develop after birth from hemorrhaging due to obstetric incidents, frequent blood draws for laboratory testing, or impaired red blood cell (RBC) production by the bone marrow [117]. The most common treatment for fetal and neonatal anemia is intrauterine or intravenous transfusion of RBCs derived from adult donors [116, 118-122]. However, adult RBCs are different from the cells present in the blood of a fetus or neonate in terms of membrane composition [117, 123], biophysical properties [117, 123], hemoglobin structure [117, 123-127], as well as metabolism and enzymatic profiles [124, 125]. In particular, fetal hemoglobin is present in high concentrations in fetal and neonatal RBCs, but is almost completely absent in normal adult RBCs [128]. Fetal hemoglobin facilitates the fetus' uptake of oxygen from the placenta due to a higher affinity for binding oxygen when compared to hemoglobin present in adult cells [126]. These differences between fetal and adult RBCs may contribute to complications arising after transfusion of adult RBCs to treat fetal and neonatal anemias, including retrolental fibroplasia [129-131] and bronchopulmonary dysplasia [132-134].

Recently, there has been interest in the transfusion of RBCs derived from umbilical cord blood to treat fetal and neonatal anemia[135-140]. RBCs in cord blood are commonly considered a waste product and are usually discarded after the isolation of

stem cells [141-143]. However, cord RBCs contain high levels of fetal hemoglobin and consequently may offer a superior treatment alternative for fetal and neonatal anemia compared to adult RBCs. Various studies have demonstrated the efficiency of autologous transfusion of cord RBCs for treatment of neonatal anemia [135-140, 144]; however, concerns have surfaced regarding the potential risk of bacterial contamination, low hypothermic storage stability, and the small harvestable volume of RBCs from umbilical cord blood [137, 145]. To overcome these concerns, an effective method for long-term preservation of cord RBCs is needed.

Adult RBCs are routinely stored at 1-6 ^{o}C in an anticoagulant/preservative solution for up to 42 days [2]. RBCs present in cord blood on the other hand, cannot be stored using the same hypothermic techniques as adult RBCs for more than 14 days without a significant decrease in quality [137]. Cryopreservation is a potential long-term storage strategy for maintaining the quality of cord RBC for the future use in intrauterine and neonatal transfusion as well as blood banking. Adult RBCs are routinely cryopreserved in the presence of 40% w/v glycerol for clinical use, with cryopreservation protocols described in the literature [10, 24]. However, to our knowledge, no protocol for the cryopreservation of cord RBCs has been reported.

During cryopreservation, cells are subjected to potentially damaging osmotic stresses. For instance, addition of a permeable cryoprotective agent (CPA) like glycerol results in osmotically-driven water efflux and a concomitant decrease in cell volume, followed by swelling as both water and CPA enter the cell. The converse happens during CPA removal. Freezing and thawing also result in osmotic stresses. During freezing,

growth of ice crystals removes water from the extracellular medium, concentrating the extracellular solution and creating an osmotic driving force for cell dehydration. Melting of ice crystals during thawing reverses this phenomenon. To design a successful cryopreservation procedure for cord RBCs, it will be necessary to avoid damaging osmotic stresses and the associated changes in cell volume. In particular, it will be necessary to maintain the cell volume within the osmotic tolerance limits, defined as the extent of volume excursions the cell can withstand before irreversible damage occurs [45].

This study investigates the osmotic tolerance limits of cord RBCs in conditions relevant to cryopreservation, and compares the results to the osmotic tolerance limits of adult RBCs. Our results will facilitate the development of a cryopreservation protocol specifically tailored for cord RBCs.

4.3 MATERIALS & METHODS

Collection of RBCs from umbilical cord blood

Cord RBCs were obtained from the Alberta Cord Blood Bank as a waste product after the isolation of stem cells from umbilical cord blood. The cord blood harvested from the placenta was stored at room temperature for up to 43 hours prior to the isolation of stem cells. A previous study showed that the storage period from harvest to the time of stem cell isolation does not cause a decrease in cord RBC quality [146]. The cord RBCs were then washed with isotonic saline and centrifuged at 2200 g, 4 ºC for 5 minutes. The washed cells were resuspended to a hematocrit of 60%, stored at 1-6 ºC, and used in

experiments within 24 hours. Ethics approval for the study was obtained from the University of Alberta Research Board (Biomedical Panel) and Canadian Blood Services Research Ethics Board.

Collection of adult RBCs

Adult RBCs were isolated from whole blood in citrate phosphate dextrose drawn from volunteer donors. Whole blood was centrifuged at 2200 g at room temperature for 6 minutes to separate the plasma and other components from the RBCs. The resulting packed cells were resuspended in isotonic saline, centrifuged at 2200 g at room temperature for 6 minutes, and the supernatant was removed. The RBCs were then resuspended in isotonic saline at a hematocrit of 60%, stored at 1-6 ºC, and used in experiments within 24 hours. Ethics approval for this study was obtained from the Oregon State University Institutional Review Board.

RBC glycerolization, freezing and thawing

Cord RBCs

The supernatant from washed cord RBCs was removed to attain an approximate packed cell hematocrit of 90%. The packed cells were then weighed to achieve a starting mass of 4.1-4.2 g. This was done to ensure that the desired final concentration of glycerol, non-permeating solute, and cell density was achieved. Glycerolite 57 was then added at room temperature in two separate steps. In the first step, 1.5 mL of Glycerolyte 57 was added to the packed cells slowly over a three minute period accompanied by

gentle agitation. The cells were then allowed to rest undisturbed for five minutes to ensure proper equilibration. In the second step, 5 mL of Glycerolyte 57 solution was added over a three minute period with gentle agitation to ensure proper mixing. After the second addition of Glycerolyte 57, the cord RBCs were either directly used for osmotic tolerance limit experiments or cryopreserved according to the following procedures. Glycerolized cord RBCs were transferred into cryovials (Thermo Fisher Scientific, Roskilde, Denmark) and frozen by placing them in a -80ºC freezer to achieve a freezing rate of approximately 1ºC per minute. Cord RBCs were left in a frozen state for at least 48 hours prior to being used in osmotic tolerance experiments. To thaw, the cryovials were placed in a 37ºC water bath for one minute. Thawed cord RBCs were used in experiments immediately.

Adult RBCs

The adult RBCs were glycerolized, frozen and thawed in the same way as the cord RBCs except that, instead of using Glycerolyte 57, the adult RBCs were glycerolized using an aqueous glycerol solution with the following composition: 57.1 g glycerol, 0.03 g potassium chloride, 0.085 g magnesium chloride hexahydrate, 0.08 disodium phosphate, and 1.6 g sodium lactate in a total volume of 100 mL, adjusted to a pH of 6.8 [147]. The two glycerolization solutions are essentially identical except that Glycerolyte 57 lacks magnesium chloride and instead has a slightly higher concentration of phosphate buffer.

Osmotic Tolerance Limit Experiments

The general method of investigating the osmotic tolerance limits involves exposing the cells to solutions of different concentrations to induce a range of osmotic volume changes. Three treatment groups of adult and cord RBCs were tested: 1) RBCs in isotonic saline, 2) RBCs in 40% w/v glycerol, and 3) frozen-thawed RBCs in 40% w/v glycerol.

Osmotic tolerance limits of RBCs in the presence of saline

To induce shrinkage or swelling, a 1 mL volume of buffered anisotonic saline solution was added to 0.1 mL of washed RBCs in isotonic saline while the sample was gently agitated. After a 5 min equilibration period, 0.1 mL of the resulting mixture was removed from the vessel for hemolysis testing under anisotonic conditions. The remaining mixture was then brought back to isotonic conditions by adding 19 mL of either hypo- or hypertonic buffered saline solution, resulting in a final volume of 20 mL. Once the suspension was homogeneously mixed, a sample was obtained for hemolysis testing under isotonic conditions. All solutions used were buffered with 12.5 mM disodium phosphate and adjusted to a pH of 7. The exact anisotonic saline concentrations added to the RBCs are tabulated in Table 4.1.

Table 4.1. Saline concentrations (in molal units) used for investigation of the osmotic tolerance limits of washed RBCs in isotonic saline.

Saline concentration in solution added to induce shrinkage or swelling (mmol/kg)	Saline concentration in solution added to return sample to isotonic conditions (mmol/kg)	Expected change in osmotically active cell volume (V_w/V_{w0})
0[a]	139	13
34	135	2.5
51	135	2.0
67	134	1.7
131	131	1.0
777	99[b]	0.20
1580	59[c]	0.10
2390	19[d]	0.067

[a] Whereas all other solutions were buffered with 12.5 mmolal disodium phosphate, this solution did not contain any phosphate buffer.
[b,c,d] In addition to the indicated saline concentration, these solutions also contained glucose at concentrations of 3 mmolal, 6 mmolal and 10 mmolal (b, c and d, respectively).

The Boyle-van't Hoff relationship was used to estimate the change in osmotically active cell volume after equilibration in each of the anisotonic solutions described in Table 4.1. In particular, the following equation was used to calculate the ratio of the final volume of osmotically active cell water (V_w) to the original, isotonic water volume (V_{w0}):

$$\frac{V_w}{V_{w0}} = \frac{M_0}{M} \qquad [1]$$

where M_0 is the is the isotonic osmolality and M is the osmolality of the anisotonic solution. To estimate the solution osmolality, each mole of sodium chloride was assumed to contribute two osmoles, and the phosphate buffer was assumed to contribute an

osmolality of 36 mOsm/kg (this is the measured osmolality of the buffer solution in the absence of saline). The expected volume changes calculated using Eq. 1 are also shown in Table 4.1.

Osmotic tolerance limits of RBCs in the presence of 40% w/v glycerol

The upper osmotic tolerance limit of RBCs in the presence of 40% w/v glycerol was measured – either immediately after glycerolization or after glycerolization, freezing and thawing – by inducing the cells to swell using a relatively hypotonic glycerol solution. The composition of the hypotonic glycerol solution was selected such that the equilibrium cell volume could be achieved by transport of water alone, avoiding the potentially confounding effects of glycerol transport (which occurs much more slowly than water transport). This was accomplished by preparing all solutions using a constant ratio of glycerol osmolality to non-permeating solute osmolality. The procedure for exposing the glycerolized RBCs to changes in solution composition was similar to that described above: a volume 0.1 mL of glycerolized RBCs was mixed with 1 mL anisotonic glycerol-saline solution, and the sample was gently agitated for 5 minutes to allow the cells to reach the expected volume change. Once the equilibration period was over, the cells were brought back to 'isotonic' conditions, the original starting concentration of the glycerolized RBCs, by adding the 18.9 mL of hypertonic glycerol-saline solution. After homogeneous mixing was achieved, a sample was obtained for hemolysis testing. All solutions were buffered with 12.5 mmolal disodium phosphate and

adjusted to a pH of 7. The saline and glycerol concentrations added to the RBCs in these experiments are given in Table 4.2.

To estimate changes in the osmotically active volume, we assumed that the cells had reached chemical equilibrium. Because both water and glycerol are membrane permeable, this results in two equilibrium relationships that equate intra- and extracellular osmolalities:

$$\frac{N_n}{\rho_w V_w} + \frac{N_s}{\rho_w V_w} = M_n + M_s \qquad [2]$$

$$\frac{N_s}{\rho_w V_w} = M_s \qquad [3]$$

where N is the moles of intracellular solute, ρ_w = 1 g/mL is the density of water and the subscripts n and s refer to non-permeating solute and glycerol, respectively. Given the subsidiary equations, $N_n = \rho_w V_{w0} M_0$ and $V_s = v_s N_s$ (where V_s is the intracellular volume of glycerol and v_s = 73 mL/mol is the molar volume of glycerol), the following expression for the relative osmotically active volume can be obtained:

$$\frac{V_w + V_s}{V_{w0}} = \frac{M_0}{M_n}\left(1 + v_s M_s \rho_w\right) \qquad [4]$$

To estimate the solution osmolalities for use in Eq. 4, each mole of sodium chloride was assumed to contribute two osmoles, each mole of glycerol was assumed to contribute 1 osmole and the phosphate buffer was assumed to contribute 36 mOsm/kg. The expected volume changes calculated using Eq. 4 are also shown in Table 4.2.

Table 4.2. Saline and glycerol concentrations (in molal units) used for investigation of the osmotic tolerance limits of glycerolized RBCs.

Composition of solution added to induce swelling		Composition of solution added to return sample to isotonic conditions		Expected change in osmotically active cell volume $[(V_w+V_s)/V_{w0}]$
Saline (mmol/kg)	Glycerol (mmol/kg)	Saline (mmol/kg)	Glycerol (mmol/kg)	
0*	0*	216	7010	12
41	1670	213	6870	2.5
63	2290	212	6820	2.0
86	2900	211	6740	1.7
206	6480	206	6480	1.0

* Whereas all other solutions were buffered with 12.5 mmolal disodium phosphate, this solution did not contain any phosphate buffer.

Hemolysis Measurement

Hemolysis was quantified by measuring the amount of free hemoglobin in the supernatant using Harboe's direct spectrophotometric method. The samples were first centrifuged at 2200 g for 6 minutes to separate the supernatant from the surviving cells. A portion of the supernatant was then diluted appropriately to fall within the linear absorbance measurement range at 415 nm. The concentration of the free hemoglobin (Hb) released by damaged cells into the supernatant was then measured using the following equation [109]:

$$Hb\ (g/mL) = (167.2A_{415} - \ 83.6A_{380} \ - 83.6A_{450}) \cdot dilution\ in\ H_2O \qquad [5]$$

where A_{415}, A_{380}, and A_{450} are absorbance values measure at 415, 380, and 450 nm respectively. The percent hemolysis was calculated by dividing the mass of free hemoglobin in the supernatant by the mass of total hemoglobin from a sample that had been intentionally lysed by 100-fold dilution in distilled water followed by three consecutive freeze-thaw cycles. The hematocrit in the final sample was always less than 1%, so it was not necessary to account for hematocrit when calculating percent hemolysis.

Statistical Analysis

The results of the experiments are reported as averages of five replicates, with each replicate originating from a different batch of blood, except for the data for cord RBCs in the presence of saline which was reported as averages of seven replicates. Error bars show the standard error of the mean. Statistical comparisons between adult and cord RBCs, as well as between different treatment groups, were performed using t-tests. Differences were considered to be significant at a 95% confidence level ($p < 0.05$).

4.4 RESULTS

Osmotic tolerance limits of untreated RBCs in the presence of saline

The osmotic tolerance limits of untreated cord and adult RBCs were evaluated to assess the osmotic sensitivity of the cell membrane in its natural state. The results for cord RBCs are shown in Figure 4.1A. To provide insight into the mechanisms of osmotic damage, hemolysis was measured while the cells were in anisotonic solutions, and after

the cells had been returned to isotonic conditions. Exposure to hypotonic conditions caused immediate damage to cord RBCs, the extent of which increased as the solution hypotonicity increased. On the other hand, the majority of damage from exposure to hypertonic conditions did not manifest until the cells were returned to isotonic conditions. For example, exposure to the most hypertonic solution that we tested resulted in less than 20% hemolysis, but subsequent return of the cells to isotonic conditions caused the hemolysis to increase to 100%. This trend is consistent with our results for adult RBCs, as shown in Figure 4.1B.

Figure 4.1C shows a comparison of the osmotic sensitivity of untreated cord and adult RBCs. Cord cells appear to be slightly less resistant to osmotic swelling and shrinking when compared to adult cells. A notable significant difference in hemolysis was seen when the cells were induced to swell to 1.7 times the isotonic osmotically active volume ($p = 0.0002$). Under these conditions, cord RBCs experienced a hemolysis of $10.2\% \pm 2.3\%$, which is significantly higher than value of $2.4\% \pm 0.6\%$ for adult RBCs. In addition, shrinkage to 10% of the isotonic osmotically active volume (and subsequent return to isotonic conditions) produced significantly higher hemolysis for cord RBCs ($60.1\% \pm 7.3\%$) than adult RBCs ($33.2\% \pm 3.7\%$).

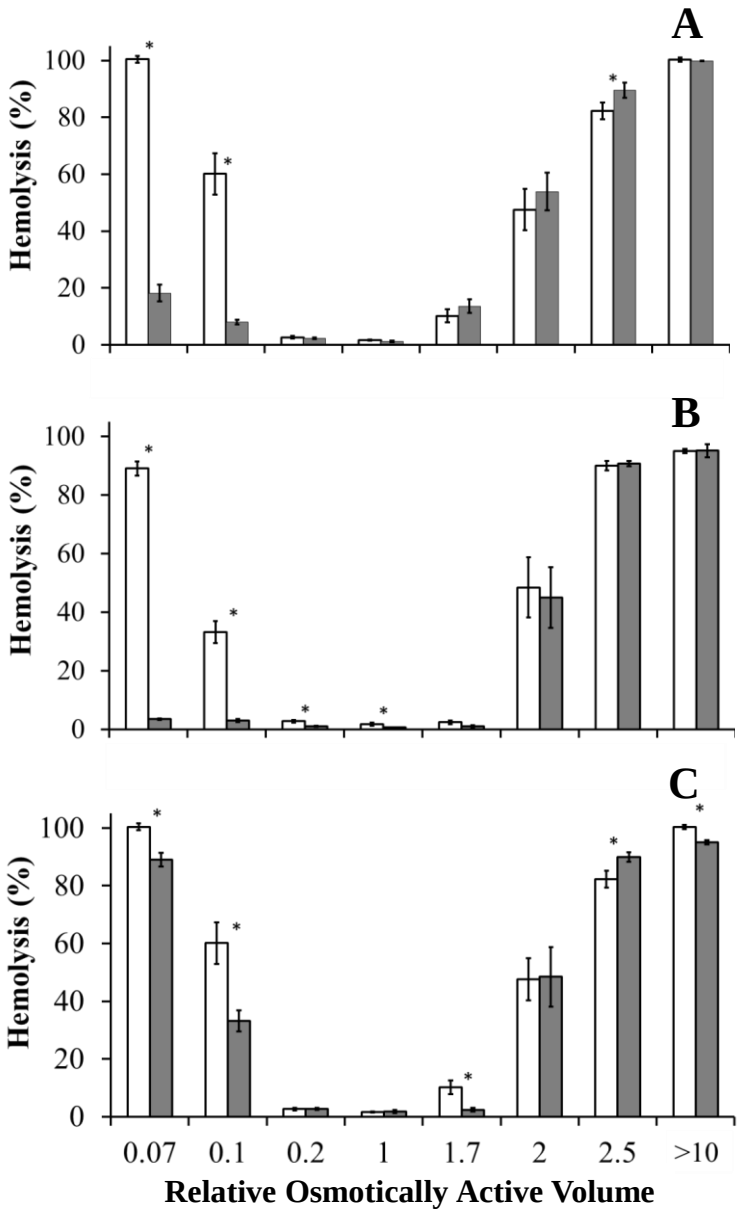

Figure 4.1. **Osmotic sensitivity of untreated RBCs in the presence of saline.**
(A) Hemolysis for cord RBCs measured under isotonic (white bars) and anisotonic (grey bars) conditions. (B) Hemolysis for adult RBCs measured under isotonic (white bars) and anisotonic (grey bars) conditions. (C) Comparison of hemolysis values for cord RBCs (white bars) and adult RBCs (grey bars) after the cells had been returned to isotonic conditions. Asterisks denote significant differences ($p < 0.05$).

Osmotic tolerance limits of glycerolized RBCs

To assess the effects of glycerol on osmotic sensitivity, RBCs were glycerolized to a final concentration of 40% w/v and then exposed to relatively hypotonic glycerol solutions to induce swelling to a range of final volumes. Figure 4.2A compares the resulting hemolysis measurements for cord RBCs to hemolysis measurements obtained for untreated cord RBCs in the absence of glycerol. The control data at the far left of Figure 4.2A shows that cord RBCs incur damage as a result of the glycerolization process. Hemolysis significantly increased from 1.6% ± 0.2% for untreated cord RBCs to 6.3% ± 1.8% for cord RBCs after glycerolization ($p = 0.02$). Subsequent exposure of the glycerolized RBCs to relatively hypotonic glycerol solutions caused damage that was similar to that observed for untreated RBCs induced to swell to the same final volume.

As shown in Figure 4.2B, adult RBCs also incur damage as a result of the glycerolization process. Hemolysis significantly increased from 1.8% ± 0.5% for untreated adult RBCs to 6.9% ± 0.3% for glycerolized adult RBCs ($p < 0.0001$). Figure 4.2B also shows that untreated and glycerolized adult RBCs have comparable susceptibility to hemolysis caused by swelling.

Figure 4.2C compares the osmotic sensitivity of cord and adult RBCs after glycerolization. The control data at the far left shows that cord and adult RBCs incur approximately the same amount of damage from the glycerolization procedure, as there is no significant difference between the hemolysis levels experienced by the two cell types. Glycerolized cord RBCs seem to be slightly more resistant to swelling when compared to glycerolized adult RBCs. In particular, there was a significant difference in hemolysis

between glycerolized cord RBCs and glycerolized adult RBCs when induced to swell to 2 ($p = 0.008$) and 2.5 ($p = 0.014$) times the isotonic osmotically active volume, with the difference being particularly large at a relative osmotic volume of 2.

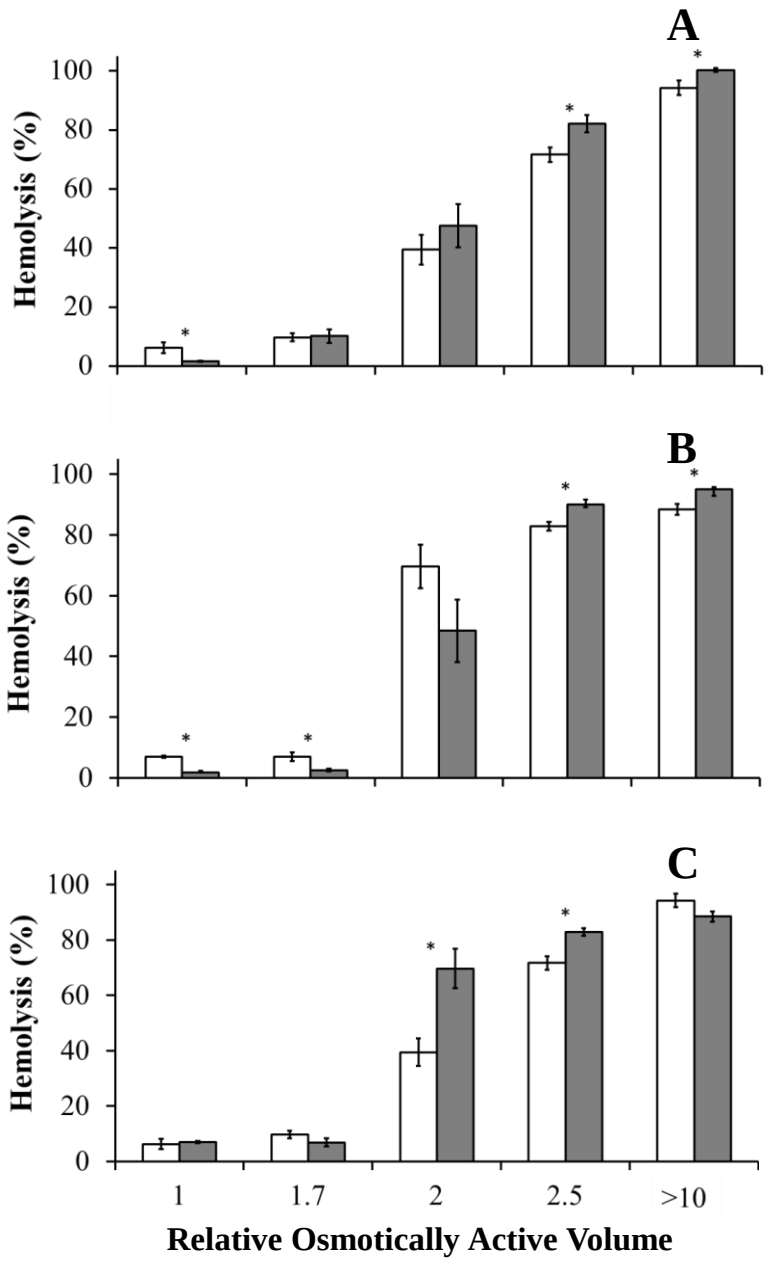

Figure 4.2. **Osmotic sensitivity of glycerolized RBCs.** (A) Cord RBCs after glycerolization (white bars) compared to untreated cord RBCs (grey bars). (B) Adult RBCs after glycerolization (white bars) compared to untreated adult RBCs (grey bars). (C) Glycerolized cord RBCs (white bars) compared to glycerolized adult RBCs (grey bars). Asterisks denote significant differences ($p < 0.05$).

Osmotic tolerance limits after glycerolization, freezing and thawing

The upper osmotic tolerance limit after glycerolization, freezing and thawing was evaluated to assess the osmotic sensitivity of the cell membrane in a state that most closely resembles the condition of thawed clinically cryopreserved RBCs. The control results in Figures 4.3A and 4.3B (far left) show that both cord and adult RBCs survive the freezing and thawing process, with no significant increase in hemolysis compared to unfrozen glycerolized cells. To assess the osmotic sensitivity of the frozen-thawed RBCs, the cells were induced to swell by exposure to relatively hypotonic glycerol solutions. Figures 4.3A and 4.3B compare the resulting hemolysis values to those obtained for RBCs that had been glycerolized, but not frozen and thawed. The results suggest that, for both cord and adult RBCs, freezing and thawing sensitizes the cells to swelling damage. In particular, frozen-thawed RBCs exhibited significantly higher hemolysis when induced to swell to 1.7 times the isotonic osmotically active volume than did glycerolized RBCs that had not been frozen and thawed.

Figure 4.3C compares the osmotic sensitivity of cord and adult RBCs after glycerolization, freezing and thawing. After the freeze-thaw process, cord RBCs exhibited a survival rate (5.5% ± 0.1%) that was only slightly lower than that of adult RBCs (3.8% ± 0.1%). The osmotic damage incurred by frozen-thawed cord RBCs and adult RBCs was comparable when the cells were induced to swell to 1.7 times the osmotically active isotonic volume. However, cord RBCs exhibited significantly lower hemolysis than adult RBCs when induced to swell to 2 times the osmotically active isotonic volume (52.8% ± 3.8% vs. 74.9% ± 5.0%, $p = 0.008$).

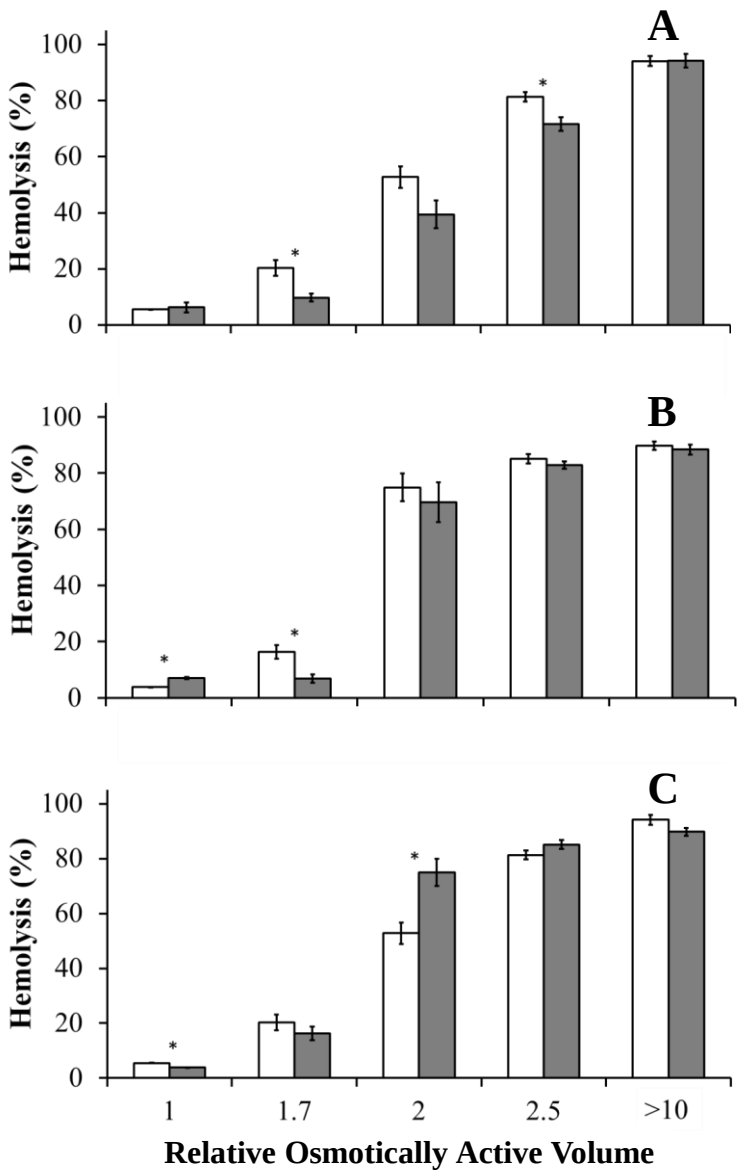

Figure 4.3. Osmotic sensitivity of RBCs after glycerolization, freezing and thawing. (A) Cord RBCs after glycerolization, freezing and thawing (white bars) compared to cord RBCs after glycerolization (grey bars). (B) Adult RBCs after glycerolization, freezing and thawing (white bars) compared to adult RBCs after glycerolization (grey bars). (C) Comparison of cord (white bars) and adult (grey bars) RBCs after glycerolization, freezing and thawing. Asterisks denote significant differences ($p < 0.05$).

4.5 DISCUSSION

To address the need for long-term storage of a cord RBC product, an obvious first step would be to use the 40% glycerol freezing method that was developed for adult RBCs. However, the 40% glycerol method yields lower cell recovery for cord RBCs than adult RBCs [148]. Therefore it is important to understand the biophysical differences between cord and adult RBCs in the context of the cryopreservation process. To this end, we investigated the osmotic tolerance limits of cord and adult RBCs, both in the presence of saline as is commonly done in the literature, as well as in the presence of 40% glycerol.

There have been many previous studies of the sensitivity of cord RBCs to swelling in hypotonic saline solutions [149-151]. Typically, the results of such osmotic fragility experiments are quantified in terms of the hypotonic saline concentration required to induce 50% hemolysis. Reported values are in the range 130-160 mOsm/kg for both cord and adult RBCs [47, 57, 149-151], which corresponds with a relative osmotically active volume V/V_{w0} between 1.9 and 2.3. We observed about 50% hemolysis for both cord and adult RBCs when the cells were induced to swell to V/V_{w0} = 2.0 (see Figure 4.1), which is in agreement with the previous literature. Whereas cord and adult RBCs do not appear to differ significantly in terms of the hypotonic concentration necessary to cause 50% hemolysis, previous studies do indicate that cord RBCs are more heterogeneous than adult RBCs and undergo hemolysis over a wider range of hypotonic concentrations [149-151]. Our results are consistent with this trend. As shown in Figure 4.1C, cord RBCs exhibited higher hemolysis than adult RBCs when

induced to swell to $V_w/V_{w0} = 1.7$, which suggests that a portion of the cord RBCs are more sensitive to swelling damage than the adult RBCs. On the other hand, lower hemolysis was observed for cord RBCs at $V/V_{w0} = 2.5$, which suggests that a subpopulation of cord RBCs is more resistant to swelling than adult RBCs. The osmotic tolerance limit for cord RBCs should be defined in order to ensure the all cells in the population are not damaged. Because cord RBCs exhibit about 10% hemolysis when induced to swell to 1.7 times the isotonic osmotically active volume, the upper osmotic tolerance limit in the presence of saline should be set somewhere below this value.

The upper osmotic tolerance limit is primarily useful for designing procedures that avoid excessive swelling during removal of cryoprotectant after freezing and thawing. Therefore, we also investigated the osmotic tolerance of cord and adult RBCs after freezing and thawing in the presence of 40% glycerol. There do not appear to be any previous reports of the effects of glycerol, or of freezing and thawing, on the osmotic tolerance limits of cord RBCs. However, Meryman and Douglas [59] investigated the osmotic fragility of adult RBCs in the presence of glycerol, and their data was later analyzed by Pegg [104] in terms of the RBC volume. These studies indicate that adult RBCs exhibit similar tolerance to swelling over a wide range of glycerol concentrations, with 50% hemolysis corresponding with a relative osmotically active volume of about $(V_w + V_s)/V_{w0} = 2.2$. We observed slightly higher hemolysis for unfrozen adult RBCs that had been glycerolized to 40% w/v: cells induced to swell to twice the isotonic osmotically active volume underwent about 70% hemolysis (see Figure 2).

Importantly, our results show that freezing and thawing makes both cord and adult RBCs more sensitive to swelling damage, which has implications for the design of post-thaw cell washing methods. The amount of damage experienced by both cell types was comparable when induced to swell to 1.7 times the isotonic osmotically active volume: hemolysis values were 16.3% ± 2.4% and 20.3% ± 2.8% for frozen-thawed glycerolized adult and cord RBCs, respectively. Because these hemolysis values are relatively high, the design of glycerol removal procedures for both cell types should ensure that cell volume excursions are at least maintained below 1.7 times the isotonic osmotically active volume to attain good post-wash cell recovery. Linear extrapolation of the data between relative volumes of 1.7 and 2.0 allows estimation of safe swelling limits for both cell types, yielding $(V_w + V_s)/V_{w0} = 1.5$ for frozen-thawed cord RBCs and $(V_w + V_s)/V_{w0} = 1.6$ for frozen-thawed adult RBCs.

Although the susceptibility of cord RBCs to damage in hypotonic solution has been fairly well studied, we are not aware of any previous reports of the sensitivity of cord RBCs to damage in hypertonic saline solutions. For both cord and adult RBCs, damage from exposure to hypertonic saline was not immediately apparent, and a significant increase in hemolysis was observed when the cells were returned to isotonic conditions (see Figures 4.1A and 4.1B). This trend is consistent with the observations of Lovelock, who postulated that the RBC membrane becomes permeable to ions at high saline concentrations, resulting in uptake of sodium ions and subsequent dilution stresses upon return to isotonic conditions [110]. The fact that cord and adult RBCs both exhibited this trend suggests that hypertonic exposure damages both cell types by a

similar mechanism. However, cord RBCs appear to be slightly more susceptible to hypertonic damage than adult RBCs, as evidenced by the higher hemolysis value for cord RBCs at $V_w/V_{w0} = 0.1$ (see Figure 1). The data in Figure 4.1 can be used identify the safe limits for shrinkage of cord and adult RBCs; because both cell types exhibited less than 3% hemolysis when induced to shrink to 20% of the isotonic osmotically active volume, a relative osmotic volume of 0.2 would be a conservative choice for the lower osmotic tolerance limit.

Our isotonic volume controls in Figures 4.2 and 4.3 provide useful information about the potential for cryopreservation of cord RBCs in the presence of 40% glycerol. While the glycerolization process significantly increased hemolysis from 1.6% to about 6%, subsequent freezing and thawing did not cause a further increase in hemolysis. These results indicate that 40% glycerol is adequate for protection of cord RBCs during freezing and thawing, and that glycerolization using the standard method (which was developed for adult RBCs) only causes modest damage to cord RBCs. These results, together with the previous observation that recovery of cord RBCs after cryopreservation in 40% glycerol is significantly less than recovery of adult RBCs [148], suggest that future efforts should primarily focus on refinement on the post-thaw washing process to maximize recovery of cord RBCs.

4.6 CONCLUSIONS

This study investigated the osmotic tolerance limits of cord and adult RBCs under conditions relevant to cryopreservation using high glycerol concentrations. We show that

cord RBCs are more sensitive to shrinkage and swelling than adult RBCs requiring that upper and lower osmotic tolerance limits are adjusted when considering protocols for the addition and removal of cryoprotectants. In addition, freezing and thawing resulted in both cord and adult RBCs becoming more sensitive to swelling damage requiring that glycerol removal procedures for both cell types ensure that cell volume excursions are at least maintained below 1.7 times the isotonic osmotically active volume to attain good post-wash cell recovery. Our results will help inform the development of optimized cryopreservation protocol for cord RBCs.

4.7 ACKNOWLEDGEMENTS

We would like to thank Dr. John Akabutu, Nanni Zhang and Sally Shahi from the Alberta Cord Blood Bank for providing cord RBC samples. We are also grateful to the Alberta Cord Blood Bank cord blood donors and the adult volunteers for providing samples for this study. We would also like thank Mary Garrard for performing blood collections. Mary was supported by funding from the National Institutes of Health (NIEHS #P30 ES000210).

Chapter 5: Continuous Removal of Glycerol from Frozen-Thawed Red Blood Cells in a Microfluidic Membrane Device

Ratih E. Lusianti and Adam Z. Higgins

Journal: Lab on a Chip

Address: http://pubs.rsc.org/en/journals/journalissues/lc#!recentarticles&all

Date: Manuscript is scheduled for submission March 2014

5.1 ABSTRACT

Human red blood cells (RBCs) are routinely cryopreserved in the presence of 40% w/v glycerol to extend the FDA approved shelf life to 10 years as opposed to only 6 weeks for conventional refrigerated RBCs. Although the use of cryopreserved RBCs is logistically more advantageous, refrigerated RBCs are more commonly used in clinical therapy due to the time consuming post-thaw wash process that is necessary to remove glycerol before the product can be used for transfusion. A more efficient method of glycerol removal is necessary to facilitate more widespread use of cryopreserved RBCs. In a previous study, we have proven that glycerol can be extracted rapidly from cryopreserved RBCs without excessively damaging the cells if the osmotically induced cell volume changes are restricted to the known safe osmotic tolerance limits. Presently, this study is focused on implementing the rapid extraction of glycerol from cryopreserved RBCs in a continuous manner, such that the cells will be glycerol-free and ready for transfusion after transiting through the device. Experimental efforts in this study have been centered on the use of a membrane-based microfluidic device. A mathematical model capable of predicting the mass transfer inside the device was developed to assist in experimental design as well as the development of a future device capable of carrying out the complete deglycerolization procedure. Preliminary results from this study have demonstrated the feasibility of rapidly removing glycerol in a continuous manner using a combined approach of microfluidics and mathematical modeling to improve the post-thaw wash process of cryopreserved RBCs.

5.2 INTRODUCTION

Transfusion of RBCs is one of the most commonly performed medical procedures with over 15 million RBC units transfused per year in the United States alone [1]. Because of the enormous clinical demand, a preservation method that maintains the viability and quality of the cells for long periods of time is essential for sustaining a high supply of transfusable RBC units. RBC units donated to blood banks and hospitals are most commonly preserved through refrigeration, which permits a short storage shelf life of up to 6 weeks [2, 3, 91]. Although the blood inventory is carefully managed, a reduction in the shelf life of refrigerated blood may cause serious logistical issues in blood banking; more units will have to be discarded due to outdating and the impact of seasonal shortages would be amplified [1, 5]. Cryopreserving RBCs has the potential to mitigate these logistical challenges by extending the product shelf life from weeks to years. RBCs are routinely cryopreserved in the presence of 40% w/v glycerol in North America [2, 29], enabling a FDA approved storage shelf life of 10 years in -80ºC [10]. Although effective at extending the product shelf life, cryopreservation is currently only used for long-term storage of rare or autologous units. One of the reasons for the limited clinical application of cryopreserved RBCs is the time consuming post-thaw processing required to remove the glycerol before the cells can be transfused.

The current state of the art method for deglycerolizing cryopreserved RBCs employs the use of the ACP 215 Automated Cell Washer, which extracts glycerol from the cells by employing multiple dilutions and washing steps using various saline solutions. In the deglycerolization process, RBCs are diluted with saline to facilitate the

slow permeation of glycerol out of the cells, followed by centrifugation to remove the permeated glycerol in the supernatant. The cells are then resuspended with fresh saline solution and the process is repeated until sufficient glycerol is removed [28]. The automated cell washer reduces the need for human labor and is capable of producing high post wash cell recovery [152]. However, the processing time still stands at 57 minutes per unit RBC, making it extremely challenging to use cryopreserved RBCs for unscheduled transfusions [28].

During deglycerolization, RBCs endure cell volume changes from the permeation of glycerol and water through the cell membrane as a response to osmotic gradients. Excessive cell shrinking or swelling as a result of changes in osmotic pressure are known to have detrimental effects to a cell's viability [112, 153]. The empirically developed conventional centrifugal based glycerol removal procedure was designed to induce gradual step-wise changes in solution composition to avoid osmotic damage [30]. However, because this procedure was not optimized, the total processing time may be longer than what is actually necessary to achieve the desired outcome. The cell membrane transport model can be used to design faster deglycerolization procedures, potentially enabling a significant decrease in total processing time [99, 100]. In a previous study, we used the cell membrane transport model to systematically determine a rapid deglycerolization procedure for RBCs [154]. Our results demonstrate that glycerol can be rapidly extracted from cryopreserved RBCs if the changes in the extracellular solution composition are precisely controlled to avoid damaging excessive cell volume excursions. From this study, we were able to achieve complete deglycerolization in three

minutes by diluting thawed cryopreserved RBCs with various saline solutions to induce rapid glycerol permeation out of the cells. The cell volume excursions were maintained to within safe osmotic tolerance limits by restricting the equilibration time after each dilution. Although we were able to achieve sufficiently high cell recovery in a short amount of time, direct implementation of this procedure is not practical as it would require over 40 L of diluting solution and result in an extremely dilute cell suspension. However, the general strategy used in this study is applicable for designing rapid CPA removal procedures for other systems capable of precisely controlling the extracellular solution composition.

Alternative microfluidic based strategies for the extraction of CPA have been developed and reported in various studies in recent years. A dilution-filtration method using hollow fiber modules has been reported to be successful in achieving complete deglycerolization of cryopreserved RBCs in less time compared to the ACP 215 [60]. The lower economic cost of a dilution-filtration system in comparison to the ACP 215 may also enable more widespread use of the system in remote areas [62]. Various diffusion based CPA extraction systems applicable to deglycerolizing cryopreserved RBCs have also been reported in literature [80-84, 86]. All of these systems have the potential to improve deglycerolization of cryopreserved RBCs; however, none of them are currently used in clinical practice. In this study, we attempted to adapt the rapid glycerol removal strategy into a continuous system using a microfluidic membrane device. The RBCs are flowed counter-current to the wash solution in two parallel rectangular channels separated by a membrane. A mathematical model of the mass transfer in the device was

developed to aid in selecting operating conditions that would achieve the desired results. Based on model predictions, it is possible to deglycerolize frozen-thawed RBCs completely using a continuous system in a reasonable amount of time.

5.3 MATERIALS & METHODS

Device Fabrication

The microfluidic device consists of three primary components: two laser patterned Kapton® sheets, an AN69 hemodialysis membrane, and a clear acrylic housing. An exploded view of the device with all of its primary components is shown in Figure 5.1. The channel design was first sketched in Solidworks®, and then laser patterned into the Kapton® sheets using an ESI Model 5330 UV Laser μVIA Drill [Portland, OR, USA]. The target channel width and length was 400 μm and 15 cm, respectively. The channels were cut into 50 μm and 130 μm thick Kapton® sheets to enable the creation of two devices with different channel depths. The housing was fabricated by machining ¼ inch thick acrylic plates to create screw holed aligning with the Kapton® sheets. Pins fashioned in the housing as well as the Kapton® sheets were used to ensure proper alignment of the channels when the device was assembled. Ports to introduce fluid into the device were made using Luer type fittings.

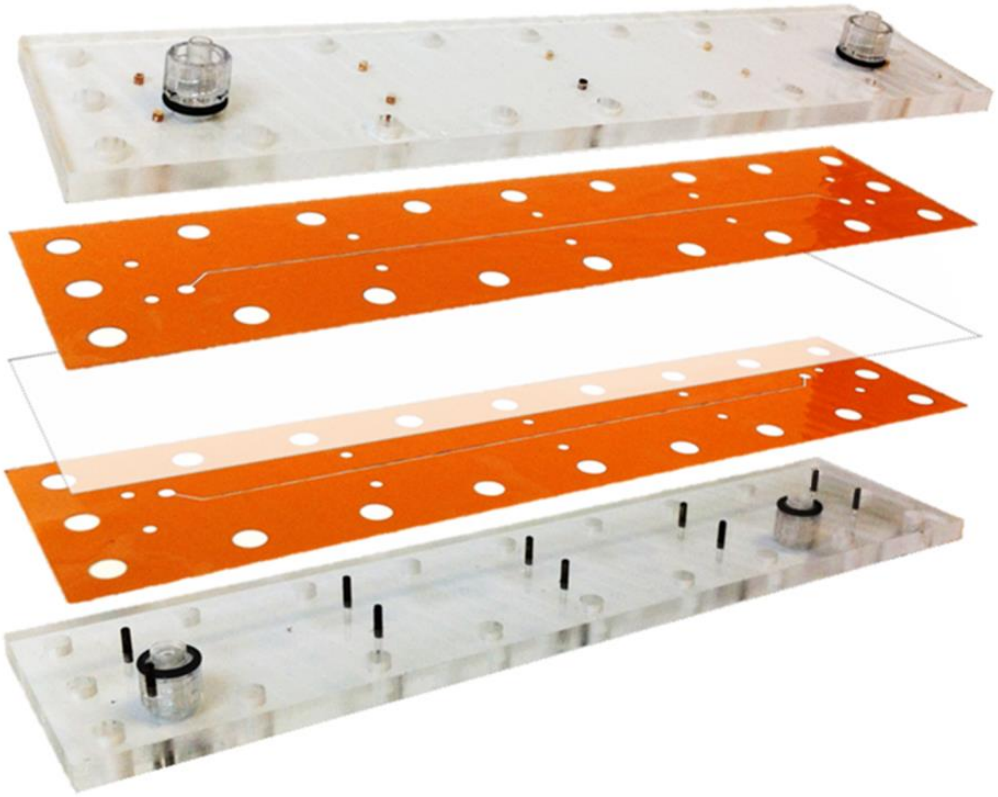

Figure 5.1 Exploded view of the microfluidic platform showing the primary components of the device.

Mathematical Model

To assist in selecting the appropriate operating conditions to attain the desired glycerol removal without incurring the unwanted osmotic damage, a mathematical model that can predict the transport of water, glycerol, and salt as well as the resulting cell volume changes was developed. To model the device, the system was divided into three different domains- the cell stream, the extracellular solution stream, and the wash stream. Figure 5.2 illustrates the differential volumes used to model the device. Symbols used in

the model are listed in Table 5.1. Detailed derivation of the mathematical model is presented in Appendix B.

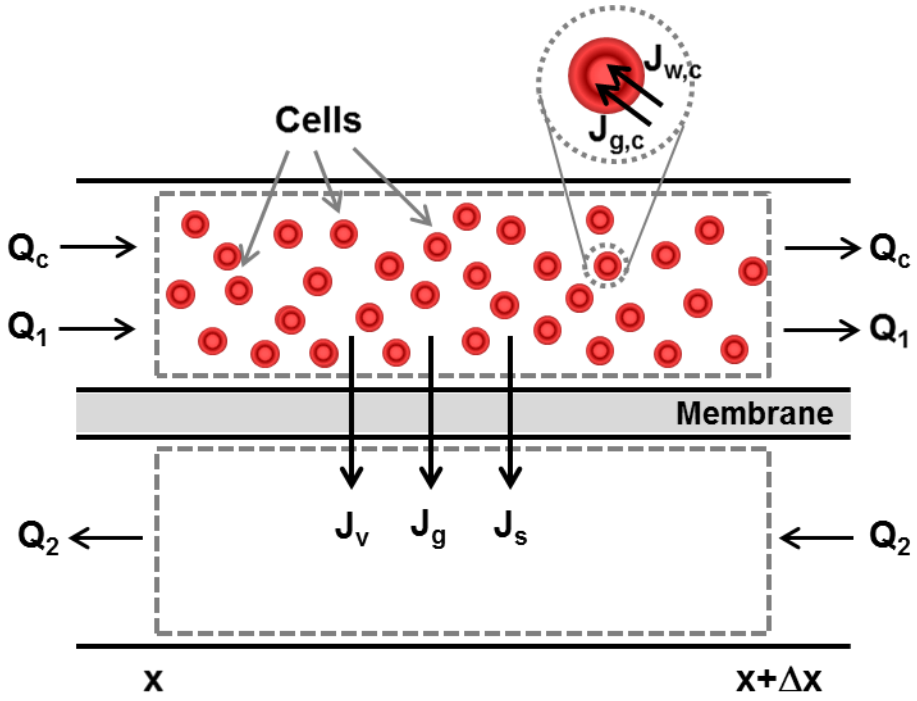

Figure 5.2 Diagram of the differential volume within the device used to develop the mathematical model.

Table 5.1. Nomenclature of symbols used in mathematical model

Symbol	Definition	Units	Value
$J_{w,c}$	Water flux across cell membrane	m^3/m^2 s	variable
$J_{g,c}$	Glycerol flux across cell membrane	mol/m^2 s	variable
J_v	Solution flux across AN69 membrane	m^3/m^2 s	variable
J_g	Glycerol flux across AN69 membrane	mol/ m^2 s	variable
J_s	Sodium chloride flux through AN69 membrane	mol/ m^2 s	variable
C	Concentration	mol/m^3	variable
Q	Flow rate	m^3/s	variable
P	Pressure	Pa	variable
μ	Viscosity	Pa s	-

g	Glycerol, subscript	-	-
s	Sodium chloride, subscript	-	-
c	Cell stream, subscript	-	-
1	Extracellular stream, subscript	-	-
2	Wash stream, subscript	-	-
$M_{s,c}$	Osmotic concentration of intracellular salts	osmoles/m^3	variable
$\dot{n}_c$	Cell flow rate	cells/s	variable
$n_{s,c}$	Osmoles salts per cell	osmoles/cell	$(2.0 \cdot 10^{-15})^a$
V_b	Osmotically inactive cell volume	m^3	$(2.7 \cdot 10^{-17})^a$
A_c	Cell surface area	m^2	$(1.3 \cdot 10^{-10})^a$
$L_{p,c}$	Hydraulic permeability of cell membrane	m/Pa s	$(1.5 \cdot 10^{-12})^a$
$P_{g,c}$	Glycerol diffusive permeability of cell membrane	m/s	$(3.0 \cdot 10^{-8})^a$
L_p	Hydraulic permeability of AN69 membrane	m/Pa s	variable
P_g	Glycerol diffusive permeability of AN69 membrane	m/s	variable
P_s	NaCl diffusive permeability of AN69 membrane	m/s	$(6.5 \cdot 10^{-6})^a$
σ_g	Glycerol reflection coefficient	-	$(0.009)^a$
W	Channel width	m	$350 \cdot 10^{-6}$
H	Channel height	m	50 or $130 \cdot 10^{-6}$
R	Gas constant	J/mol K	8.314
T	Temperature	K	295
γ	Osmotic coefficient	-	1.97
v_g	Molar volume of glycerol	m^3/mol	$71 \cdot 10^{-6}$

[a] Refer to text for references to these values

Cell membrane transport

Mass transfer of water and solute across a semi-permeable membrane can be predicted using various the two parameter (water and solute permeability) model, or the Kedem-Katchalsky model which incorporates a solute-solvent interaction term in addition to the water and solute permeability [32]. Evidence in literature indicates that water and glycerol are predominantly transported through the membrane using separate

pathways in human RBCs [155-158]. Because of this reason, we used the simpler two parameter model to describe water and glycerol flux across the RBC membrane [32]:

$$J_{w,c} = L_{p,c}RT(C_{g,c} + M_{s,c} - C_{g,1} - \gamma \cdot C_{s,1}) \quad [1]$$

$$J_{g,c} = P_{g,c}(C_{g,1} - C_{g,c}) \quad [2]$$

Transport across the AN69 membrane

Unlike RBC membranes, synthetic membranes transport water and solutes through the same pores. Therefore, the most appropriate formalism to describe the mass transfer through the synthetic membrane is the Kedem-Katchalsky model which incorporates the solute-solvent interaction term or reflection coefficient, σ. This model was used to predict the volume flux of solution and molar fluxes of glycerol and sodium chloride across the AN69 membrane.

$$J_v = L_p[(P_1 - P_2) - \sigma_g RT(C_{g,1} - C_{g,2})] \quad [3]$$

$$J_g = C_{m,g}J_v(1 - \sigma_g) + P_g(C_{g,1} - C_{g,2}) \quad [4]$$

$$J_s = C_{m,s}J_v + P_s(C_{s,1} - C_{s,2}) \quad [5]$$

where C_m is the mean intramembrane concentration [159, 160] as defined in equation 6 and 7 for glycerol and sodium chloride, respectively.

$$C_{m,g} = \frac{C_{g,2} - C_{g,1}exp\left(\frac{J_v}{P_g}\right)}{1 - exp\left(\frac{J_v}{P_g}\right)} - \frac{P_g}{J_v}(C_{g,1} - C_{g,2}) \quad [6]$$

$$C_{m,s} = \frac{C_{s,2} - C_{s,1} exp\left(\frac{J_v}{P_s}\right)}{1 - exp\left(\frac{J_v}{P_s}\right)} - \frac{P_s}{J_v}\left(C_{s,1} - C_{s,2}\right) \quad [7]$$

Volume Balances

The flux equations (eqns. 1-5) were used to predict the rate of volume transfer between streams, resulting in the following differential equations describing the volumetric flow rates of each stream:

$$\frac{dQ_c}{dx} = \left(J_{g,c} \cdot v_g + J_{w,c}\right) \cdot \frac{A_c \cdot \dot{n}_c}{Q_1 + Q_c} \cdot (W \cdot H) \quad [8]$$

$$\frac{dQ_1}{dx} = -\left(J_{g,c} \cdot v_g + J_{w,c}\right) \cdot \frac{A_c \cdot \dot{n}_c}{Q_1 + Q_c} \cdot (W \cdot H) - J_v \cdot W \quad [9]$$

$$\frac{dQ_2}{dx} = -J_v \cdot W \quad [10]$$

The volume of individual cells flowing through the channel can be determined by dividing the volumetric flow rate of the cell stream (Q_c) by the cell flow rate ($\dot{n}_c$).

Solute Balances

The flux equations can be used to derive differential equations describing the concentration of glycerol in each stream, resulting in:

$$\frac{dC_{g,c}}{dx} = \frac{1}{(Q_c - \dot{n}_c \cdot V_b)}\left[J_{g,c} \cdot \frac{A_c \cdot \dot{n}_c}{Q_c + Q_1} \cdot (W \cdot H) - C_{g,c}\frac{dQ_c}{dx}\right] \quad [11]$$

$$\frac{dC_{g,1}}{dx} = -\frac{1}{Q_1}\left[J_{g,c} \cdot \frac{A_c \cdot \dot{n}_c}{Q_c + Q_1} \cdot (W \cdot H) + J_g \cdot W + C_{g,1}\frac{dQ_1}{dx}\right] \quad [12]$$

$$\frac{dC_{g,2}}{dx} = -\frac{1}{Q_2}\left[J_g \cdot W + C_{g,2}\frac{dQ_2}{dx}\right] \quad [13]$$

The relative permeability of the components of salts to the RBC membrane is six orders of magnitude less than that of glycerol, which is in turn three orders of magnitude less than that of water [106]. Thus, in this study, the RBC membrane was assumed to be impermeable to salts. Nonetheless, the intracellular salt concentration may change throughout the process as a result of changes in cell volume. The salt concentration in the cell stream can be calculated by dividing the osmoles of intracellular salts by the osmotically active cell volume [42]:

$$M_{s,c} = \frac{n_{s,c}}{(Q_c/\dot{n}_c - V_b)} \quad [14]$$

The solute balance differentials for sodium chloride in the extracellular solution and wash streams are shown in equations 15 and 16, respectively.

$$\frac{dC_{s,1}}{dx} = -\frac{1}{Q_1}\left[J_s \cdot W + C_{s,1}\frac{dQ_1}{dx}\right] \quad [15]$$

$$\frac{dC_{s,2}}{dx} = -\frac{1}{Q_2}\left[J_s \cdot W + C_{s,2}\frac{dQ_2}{dx}\right] \quad [16]$$

Pressure Drop

The differential equations that describe the pressure in each stream were based on a published pressure drop equation for a rectangular channel [161]. The cell and the

extracellular solution were modeled as a combined stream and the viscosity of the combined stream was approximated using the composition of the extracellular solution, neglecting the effects of cells. The differential equations that describe the pressures in the combined stream and the wash stream are shown in equations 17 and 18, respectively.

$$\frac{dP_1}{dx} = \frac{Q_1 + Q_c}{\frac{(W \cdot H^3)}{4 \cdot \mu_1}\left[\frac{1}{3} - \frac{64 \cdot H}{W \cdot \pi^5} tanh \frac{W \cdot \pi}{2 \cdot H}\right]} \quad [17]$$

$$\frac{dP_2}{dx} = \frac{Q_2}{\frac{(W \cdot H^3)}{4 \cdot \mu_2}\left[\frac{1}{3} - \frac{64 \cdot H}{W \cdot \pi^5} tanh \frac{W \cdot \pi}{2 \cdot H}\right]} \quad [18]$$

Model parameter selection

Permeability properties of human RBC cell membrane

Published values of $L_{p,c}$ range between 0.8 to $2.0 \cdot 10^{-12} \frac{m}{Pa \cdot s}$ [34-38]. A value of $L_{p,c} = 1.5 \cdot 10^{-12} \frac{m}{Pa \cdot s}$ was used for model simulations in this study. Published value for $P_{g,c}$ vary by more than an order of magnitude [39-42, 102, 111]. The cell membrane glycerol permeability value used in this study was $P_{g,c} = 3 \cdot 10^{-8} \frac{m}{s}$, which is an average of published values excluding outliers.

Permeability properties of AN69 membrane

The permeability parameters for the AN69 membrane selected for use in model simulations were estimated from values published by Collins and Ramirez [162]. Collins

and Ramirez measured the hydraulic permeability of pure water across the AN69 membrane. We estimated the hydraulic permeability for the relatively viscous solutions used in this study by assuming that L_p was inversely proportional to the viscosity of the permeating solution. In particular, the local value of L_p was calculated by scaling the value of L_p for pure water by the average viscosity of solutions flowing on either side of the membrane. Viscosity was estimated using a polynomial expression based on published data for binary glycerol-water solutions [163]:

$$\mu = (3.0 \cdot 10^{-14}) \cdot {C_g}^3 - (8.2 \cdot 10^{-11}) \cdot {C_g}^2 + (3.4 \cdot 10^{-7}) \cdot C_g + 8.9 \cdot 10^{-4} \quad [19]$$

The effect of sodium chloride on viscosity is expected to be negligible for concentrations used in this study [164].

In their paper, Collins and Ramirez measured the permeability properties of various solutes, but not glycerol or sodium chloride. Their data showed a linear relationship between the membrane diffusive permeability and solute diffusivity [162]. Therefore, we estimated the permeability of glycerol and sodium chloride using published diffusivity data for these solutes. The diffusivity of glycerol is linearly dependent on the concentration [165], resulting in a linear relationship between the diffusive glycerol permeability (P_g) and the glycerol concentration:

$$P_g = (-6.6 \cdot 10^{-10}) \cdot C_g + 6.5 \cdot 10^{-6} \quad [20]$$

The local glycerol permeability was calculated based on the average of the glycerol concentrations of the solutions flowing on either side of the membrane. The diffusivity of sodium chloride in the concentrations used in experiments (0.15 to 0.57 M) does not vary

greatly [166]. Therefore, a single sodium chloride permeability value of $P_s = 6.5 \cdot 10^{-6}$ m/s was used based on the diffusivity of a 0.5 M sodium chloride solution.

Collins and Ramirez measured the reflection coefficient of urea and creatinine, two molecules that are of similar size to sodium chloride and glycerol, and reported reflection coefficients of zero and 0.009, respectively. The molecular weight of sodium chloride is less than that of urea; therefore, in this study it was assumed that the reflection coefficient of sodium chloride was zero. The reflection coefficient for glycerol was assumed to be $\sigma_g = 0.009$.

Dimensions of microfluidic channel

The channels used in the device were laser patterned into Kapton® sheets that are 130 μm ± 10 μm and 50 μm ± 8 μm thick, according to the manufacturer's specifications. Compression calculations for the Kapton® sheets as well as the AN69 membrane using the assembly conditions and published Young's modulus values [167, 168] resulted in a combined compression of less than 2 μm. Based on these results and the manufacturer's thickness tolerances, the compression due to the applied torque was assumed to be negligible. Although the fabrication of the single channel microfluidic device included pins to facilitate alignment, some overlap of the Kapton ® sheets during assembly is to be expected. To determine the average width of the channel that is available for mass transfer, the device was assembled, the channel was filled with fluid, and the width was measured at three points, the channel ends as well as the middle, to obtain an averaged value. This was done in triplicate, resulting in widths of 358 μm ± 11 μm and 351 μm ± 8

μm for the 50 μm and 130 μm thick Kapton® sheets, respectively. Based on these results, a channel width of 350 μm was chosen for model simulations.

Numerical simulation method

The differential equations describing the mass transfer process inside the device were solved numerically in MATLAB using the built-in function ODE45. Because the device is operated using a counter-current configuration, boundary conditions for one of the streams are unknown at x = 0. To solve the model, initial guesses for the unknown variables at x = 0 were set and the fminsearch function was used to iteratively revise the initial guesses until the model prediction at x = L matched the known target values. This solution strategy is similar to the shooting method which has been used previously in other studies to predict heat transfer parameters in counter-current heat exchangers [169, 170].

Collection, glycerolization, freezing and thawing of RBCs

Whole blood from participating volunteers was collected into citrate phosphate dextrose vacutainers using an IRB approved protocol. To isolate RBCs, whole blood was centrifuged at 2200 g at room temperature for 6 minutes, and the resulting packed cell pellet was resuspended in isotonic saline. The tube was then centrifuged again and the supernatant was removed. The resulting packed cells were prepared for experiments as described below.

To prepare fresh untreated RBCs, the isolated RBCs were simply resuspended in isotonic saline to achieve a hematocrit of 20%. Fresh untreated RBCs were prepared within 3 days of whole blood collection, and used in experiments within 24 hours. To prepare fresh 10% w/v glycerolized RBCs, isolated RBCs were glycerolized in two steps using an aqueous glycerol solution with the following composition: 16 g glycerol, 0.9 g sodium chloride, and 0.177 g disodium phosphate in a total volume of 100 mL, adjusted to a pH of 7. In the first step 1.25 mL of the glycerol solution was added drop-wise to 5 g of packed cell over 3 minutes with gentle agitation. The mixture was then left undisturbed for 5 minutes to equilibrate. In the second step, 6.25 mL of the glycerol solution was added drop-wise over a period of 3 minutes with gentle agitation, yielding a final glycerol concentration of approximately 10% w/v glycerol and approximately 40% hematocrit. RBCs glycerolized to 10% w/v were prepared within 3 days of collection and used in experiments within 8 hours of glycerolization. Frozen-thawed 40% w/v glycerolized RBCs were prepared according to the procedure detailed in our previous work [154]. All frozen-thawed RBCs were used in experiments within 4 hours of thawing.

To achieve a hematocrit of 20% used in experiments, fresh RBCs glycerolized to 10% w/v were diluted with a 10% w/v glycerol solution with the following composition: 12.2 g glycerol, 1.04 g sodium chloride, 0.177 g of disodium phosphate, and 100 mL of ultrapure water adjusted to a pH of 7. Frozen-thawed RBCs in 40% w/v glycerol were diluted with an aqueous 40% w/v glycerol solution with the following composition: 59.7 g glycerol, 1.23 g sodium chloride, 0.177 g disodium phosphate, in 100 mL of ultrapure

water adjusted to a pH of 7. All procedures conducted to prepare RBC samples were carried out at room temperature.

Operation of the Microfluidic Device

To assemble the device, the membrane was first laid between the two Kapton® sheets and then placed in between the two acrylic housing plates. To seal the device, screws around the perimeter of the housing were tightened to 80 cN-m using a torquewrench to ensure even pressure distribution around the plates. Syringes filled with the desired solutions were connected to the device using 0.02 inch ID Tygon® tubing and 20-gauge blunt dispensing needles. The connected syringes were then loaded onto syringe pumps (New Era Pump Systems, Farmingdale, NY, USA) to introduce fluids into the device. Before each experiment, the microfluidic device was flushed using a 2 g/L pluronic F108 solution (BASF, Florham Park, NJ, USA) to eliminate particle debris and air bubbles inside of the channels. The experimental solutions were then introduced into the channels and allowed to flow for a period of time until steady-state was reached. Steady-state was assumed to be attained once fluid equal to one hundred times the channel volume had passed through. After establishment of steady-state, the effluent from the cell and the wash stream was collected and analyzed as described below.

Hemolysis Measurement

Hemolysis was quantified by measuring the amount of free hemoglobin (Hb) in the supernatant using Harboe's direct spectrophotometric method [109]. A small volume of the cell stream effluent was used for measurement of hematocrit using a SpinCrit

hematocrit centrifuge (Indianapolis, IN, USA). A portion of the sample was also diluted by 500-fold with ultrapure water to prepare the total hemoglobin standard sample. The remaining sample was centrifuged at 2200 g for 6 minutes to separate the supernatant from the surviving cells. The supernatant was then diluted appropriately to fall within the linear absorbance measurement range at 415 nm. The concentration of free hemoglobin released by damaged cells into the supernatant was then estimated from absorbance measurements as follows:

$$Hb(g/mL) = (167.2 \cdot A_{415} - 83.6 \cdot A_{380} - 83.6 \cdot A_{450}) \cdot dilution\ in\ H_2O \quad [21]$$

where A_{415}, A_{380}, and A_{450} are absorbance values at 415, 380, and 450 nm, respectively. The percent hemolysis was then calculated using the measured sample hemoglobin (sHb), total hemoglobin (tHb) and hematocrit (Hct) values:

$$Hemolysis\ (\%) = \frac{sHb \cdot (100 - Hct\ \%)}{tHb} \cdot 100\% \quad [22]$$

Thermogravimetric Analysis

In addition to measuring the amount of free hemoglobin, the mass fractions of water, glycerol, and salt in the supernatant were also measured using thermogravimetric (TGA) analysis (TA Instruments, New Castle, DE, USA). Based on the pure species boiling points, water, glycerol, and salt have distinctively different volatilities. Through trial and error, a protocol that produced good separation between the evaporating species was determined. The sample was first heated at a rate of 5°C per minute until the

temperature reached 100°C and then maintained isothermal for 15 minutes to effectively evaporate the water. The sample was then heated again at a rate of 10°C per minute until the temperature reached 290°C and then maintained isothermal for 10 minutes to evaporate the glycerol. The remaining solid mass left at the end of the procedure is sodium chloride and soluble intracellular contents released into the supernatant from damaged cells. Hemoglobin makes up the vast majority (~98%) of the soluble intracellular contents [171]. To determine solute concentrations from the TGA data, the solution density was first estimated based on the measured mass fractions of glycerol and water, neglecting the contributions due to salt and hemoglobin. The concentration of glycerol was calculated directly from the measured glycerol mass fraction by multiplying by the solution density. The concentration of sodium chloride was obtained by calculating a concentration of solids from the TGA results, and then subtracting the concentration of hemoglobin measured from the hemolysis assay. Experimental results confirming the accuracy of the TGA analysis is presented in Appendix C.

Comparison of Model Predictions and Experimental Results

The model allows predictions of the conditions in each stream at the device outlet. However, as equilibrium has yet to be reached, mass transfer will continue to occur between the cells and the extracellular solution after they exit the device. The results from the TGA analysis reflect the concentrations of solutes after the cells have reached equilibrium with the extracellular solution. To accurately compare the model predictions to experimental data, additional calculations must be performed using the outlet

conditions from the model to find the concentrations of glycerol and sodium chloride in the cells and the extracellular solution after it has reached equilibrium. Assuming that the combined osmotically active volume remains constant and the concentration of solutes in the cells and the extracellular solution is equal once equilibrium is reached, the equilibrated concentration of glycerol ($C_{g,eq}$) and salt ($C_{s,eq}$) can be calculated from model predicted outlet conditions using equations as follows:

$$C_{g,eq} = \frac{C_{g,1} \cdot Q_1 + C_{g,c}(Q_c - \dot{n}_c \cdot V_b)}{Q_1 + (Q_c - Q_b)} \quad [23]$$

$$C_{s,eq} = \frac{C_{s,1} \cdot Q_1 + C_{s,c}(Q_c - \dot{n}_c \cdot V_b)}{Q_1 + (Q_c - Q_b)} \quad [24]$$

where $C_{s,c} = M_{s,c}/\gamma$.

Statistical Analysis

All experimental data are reported as averages of three replicates. Each replicate in experiments using RBCs was carried out with cells originating from different donors. Additionally, the device was reassembled with a fresh membrane for each experiment. Error bars show the standard error of the mean. Statistical analyses of the mechanical fragility control experiments were done using student t-tests. All other analyses were done using ANOVA, followed by Tukey HSD tests for pairwise comparisons. Differences were considered to be significant at a 95% confidence level. All statistical analyses were performed using StatGraphics software.

5.4 RESULTS & DISCUSSION

Mechanical Fragility Control Experiment

The microfluidic deglycerolization process subjects the cells to potentially damaging osmotic stresses, as well as mechanical stresses caused by shear and interactions with solid surfaces within the microfluidic channel. To isolate the effects of mechanical damage from osmotic damage, we perfused RBCs counter-current to an isosmotic wash solution. These control experiments were performed at the highest flow rates used in subsequent deglycerolization experiments in order to establish an upper limit for mechanical damage.

We first investigated mechanical damage to fresh RBCs by perfusing the cells through the 130 μm thick channel at a fluid velocity of 6.1 cm/s, using isotonic saline as the wash solution. These flow conditions – which correspond to a maximum apparent shear stress of approximately 25 dynes/cm^2 [172, 173] – resulted in a slight but statistically insignificant increase in hemolysis from 0.17% ± 0.02% at the device inlet to 0.69% ± 0.36% at the outlet ($p=0.22$). The low hemolysis observed under these conditions is consistent with previous studies of shear-induced damage to RBCs, which report a threshold of approximately 1500 dyne/cm^2 above which significant hemolysis occurs [174, 175].

Because cryopreservation of RBCs can heighten sensitivity to mechanical stresses [16], we also performed control experiments for frozen-thawed RBCs in 40% w/v glycerol using a wash solution with the same composition. We first subjected the frozen-

thawed RBCs to the same flow conditions as described above, corresponding in this case to a slightly higher maximum apparent shear stress of 100 dynes/cm^2 due to the increased solution viscosity. These flow conditions resulted in a small and statistically insignificant increase from 2.8% ± 1.3% to 3.2% ± 1.4% (p=0.84). We also perfused frozen-thawed RBCs through the 50 μm thick channel at a velocity of 4.0 cm/s, which corresponds to a maximum apparent shear stress of 170 dynes/cm^2. The cells used in these experiments had a starting hemolysis value of 5.3% ± 1.9% and an ending hemolysis value of 7.7% ± 1.4%. Once again, the increase in hemolysis was not statistically significant (p=0.34). The results of these experiments confirm that RBCs can be flowed through the device without incurring excessive membrane damage from mechanical stresses.

Continuous Removal Experiment and Model Predictions

Glycerol Removal

To facilitate design of a microfluidic deglycerolization process, we developed a mathematical model for predicting mass transfer and the resulting cell volume changes within the device. Experiments were conducted over a range of operating conditions to validate the model. Figure 5.3 shows the relative glycerol concentration at the device outlet as a function of inlet fluid velocity for two different channel heights (130 μm and 50 μm) and for two different inlet concentrations (RBCs in 10% w/v glycerol and frozen-thawed RBCs in 40% w/v glycerol: panels A and B, respectively). In general, the relative glycerol concentrations at the outlet decreased with flow velocity, consistent with the

expected increase in glycerol removal as fluid residence time in the device increases. The use of a shallower channel also increased the extent of glycerol removal for a given fluid velocity as mass transfer is intensified with the increase in the surface area to volume ratio. The predicted relative glycerol concentrations are in reasonable agreement for the 130 μm channel, but show slight discrepancies for the 50 μm channel, especially in regions of faster fluid velocities. This deviation could be caused by several factors. The channel depth used in model simulations was 50 μm, but manufacturer's specifications for the Kapton® sheet indicate tolerances of ± 8 μm. Simulations using a reduced channel height would increase mass transfer, decreasing the discrepancy between model predictions and experimental results at high fluid velocities. Additionally, fluid flow through the 50 μm channel would result in a relatively high pressure drop, particularly for higher fluid velocities. High pressures within the device may have caused the fluid to bleed from the confinement of the channel, resulting in an increase in the area available for mass transfer and a concomitant increase in glycerol removal. Despite the slight discrepancies, the model predictions match the general trends in the data with reasonable accuracy.

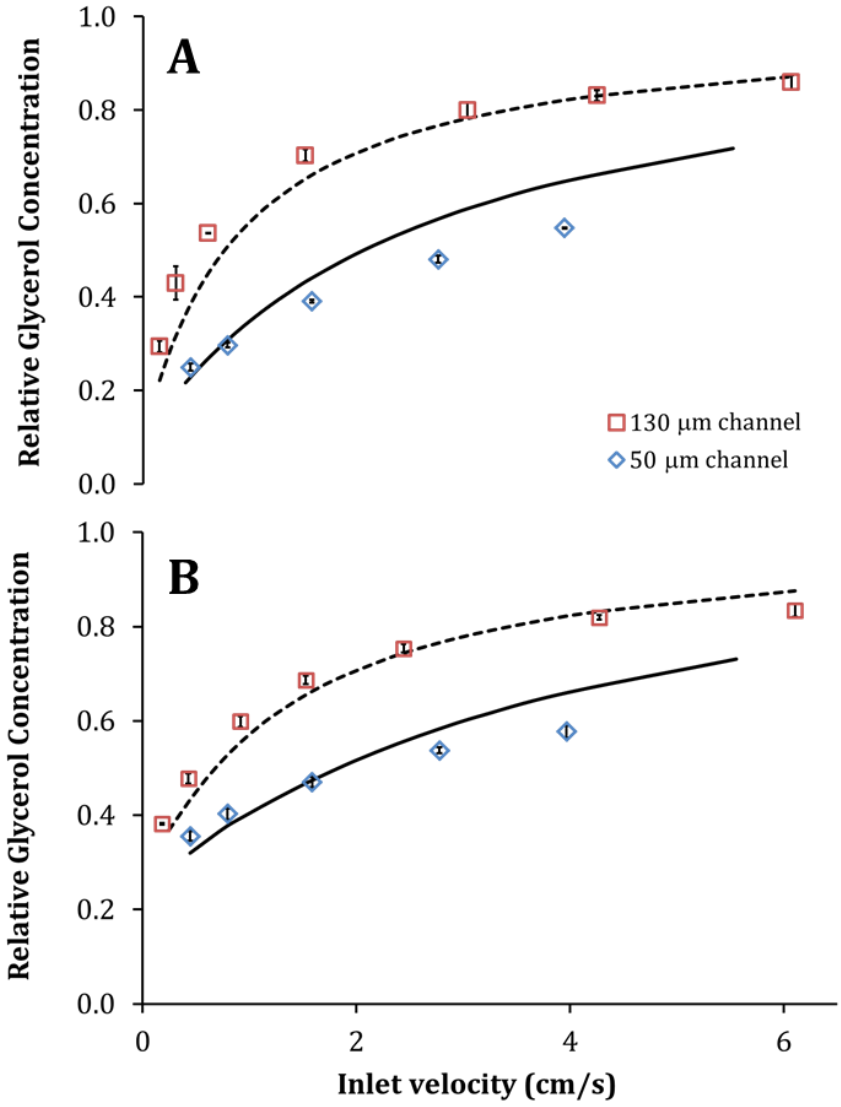

Figure 5.3. Removal of glycerol from RBCs glycerolized to 10% w/v with an isotonic saline wash (A) and frozen-thawed RBCs in 40% w/v glycerol with a 3.4% saline wash. The relative glycerol concentration was calculated by taking the ratio of the equilibrated glycerol concentration at the outlet (see Eq. 23) and the initial glycerol concentration in the inlet. Squares and diamonds are data points obtained from experiments conducted in the 130 and 50 μm device, respectively. The corresponding model predictions are represented by the dotted and solid lines, respectively

Measured Hemolysis and Maximum Cell Volume Predictions

The removal of glycerol from the extracellular medium creates an osmotic imbalance that drives water influx and concomitant cell swelling, resulting in a maximum cell volume at the device outlet. Figure 5.4A shows the predicted cell volume at the device outlet for RBCs glycerolized to 10% w/v. In general, the extent of cell swelling is predicted to increase under conditions that result in increased glycerol removal; that is, the maximum cell volume is higher for low fluid velocities and low channel heights. RBCs are known to undergo hemolysis if their volume exceeds a maximum threshold, known as the osmotic tolerance limit [47]. As shown in Figure 5.4A, the maximum cell volume is predicted to exceed the osmotic tolerance limit for the two slowest fluid velocities tested in the 130 μm channel and the three slowest fluid velocities in the 50 μm channel.

In Figure 5.4B, we compare these cell volume predictions to the measured hemolysis at the device outlet. Hemolysis was higher for the 50 μm channel than for the 130 μm channel, and hemolysis was observed to increase with decreasing fluid velocities, consistent with cell volume predictions shown in Figure 5.4A. For both the 50 μm and 130 μm channels, the effect of fluid velocity on hemolysis was found to be statistically significant ($p = 0.015$ and $p = 0.0008$, respectively). Pairwise comparisons revealed that hemolysis for the slowest fluid velocity in the 50 μm channel was significantly higher than hemolysis for the second fastest velocity. Pairwise comparisons for the 130 μm

channel revealed that the hemolysis for the slowest fluid velocity was significantly higher than the hemolysis values obtained for all other velocities.

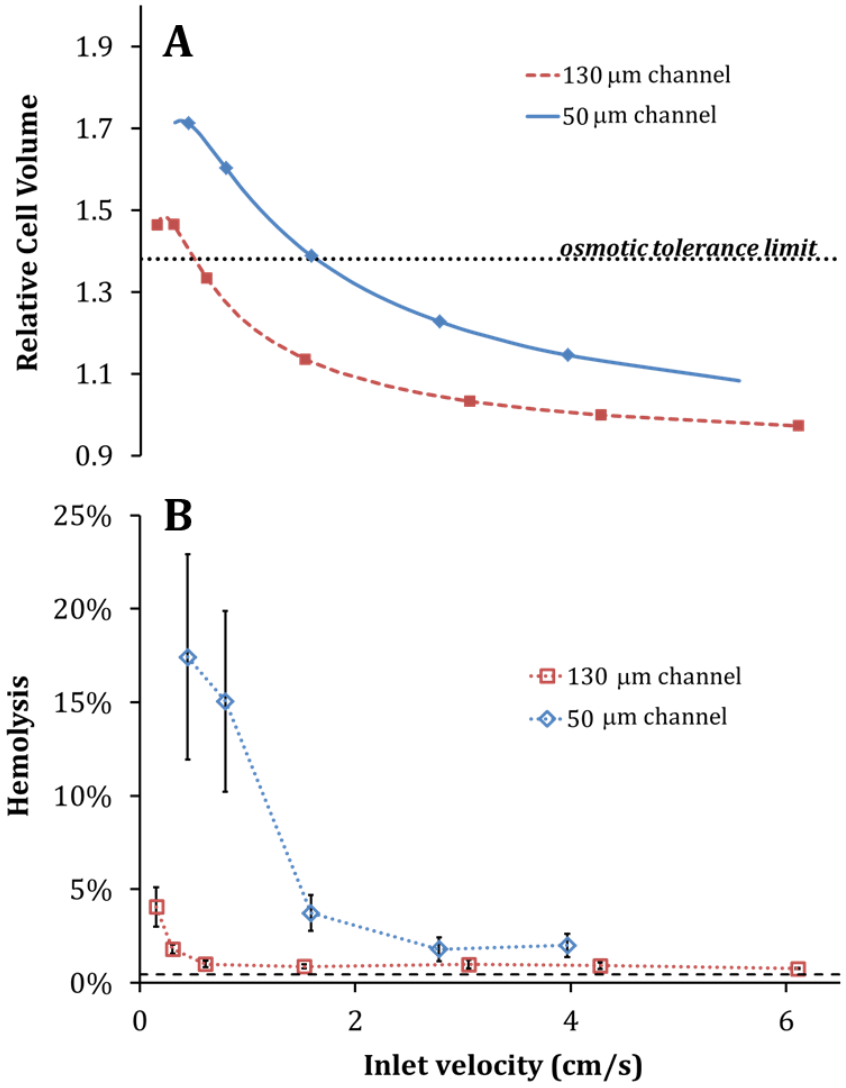

Figure 5.4. Predicted maximum cell volume (A) and measured hemolysis at the device outlet (B) after removal of glycerol from for RBCs in 10% w/v glycerol using an isotonic saline wash. The symbols in panel A correspond to the hemolysis data points in panel B. The dashed line in panel B shows the initial hemolysis of the RBCs at the device inlet

Predicted cell volume changes and the corresponding hemolysis values for experiments with the frozen-thawed RBCs in 40% w/v glycerol are presented in Figures 5.5 A and B, respectively. The maximum cell volume is predicted to exceed the osmotic tolerance limit for the three slowest fluid velocities in the 50 μm channel and the two slowest velocities in the 130 μm channel. Hemolysis measurements were consistent with these predictions. Fluid velocity was found to have a significant effect on hemolysis in both the 130 μm and 50 μm channels ($p = 0.0018$ and $p = 0.0075$, respectively). Pairwise comparisons of the hemolysis data for the 50 μm channel indicated a significantly higher hemolysis value at the slowest velocity (0.44 cm/s) than the two fastest velocities (2.9 and 4.0 cm/s), as well as a significantly higher hemolysis value for the second slowest velocity (0.79 cm/s) compared with the two fastest velocities. For the 130 μm channel, the hemolysis value measured at the slowest velocity (0.18 cm/s) was significantly higher than the hemolysis values measures at all other velocities.

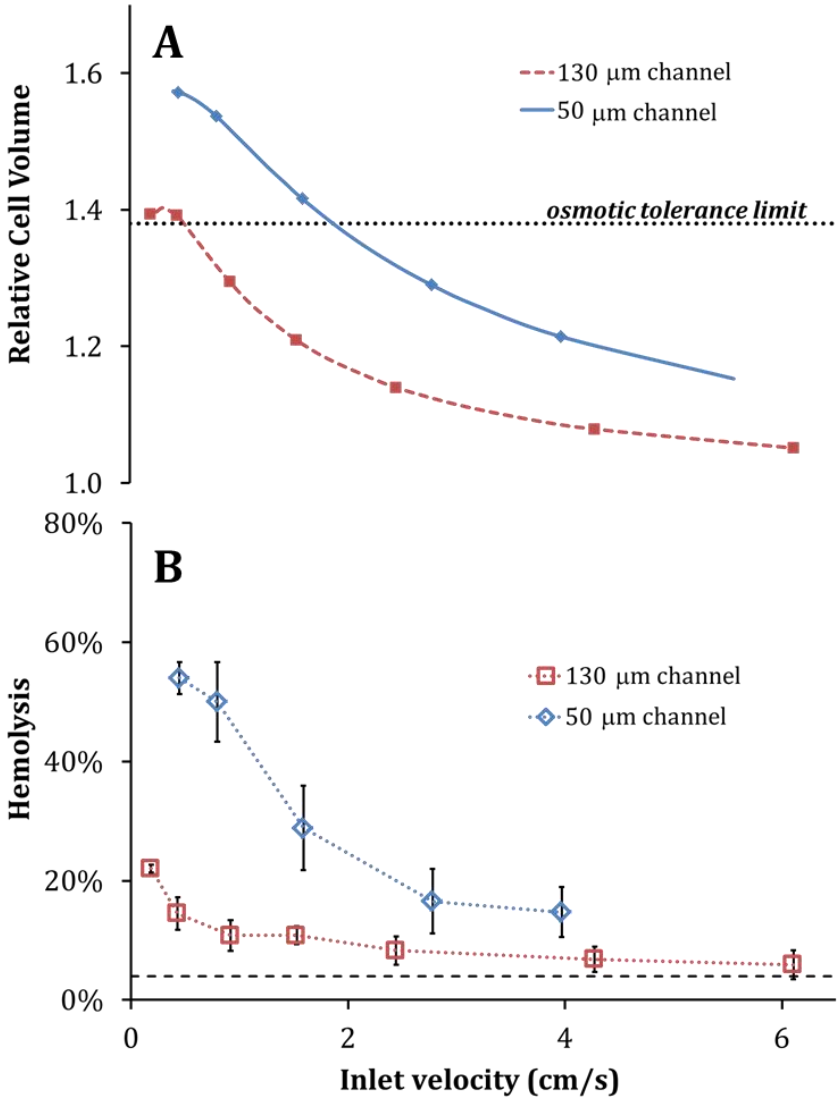

Figure 5.5. Predicted maximum cell volume (A) and measured hemolysis at the device outlet (B) after removal of glycerol from frozen-thawed RBCs in 40% w/v glycerol using a 3.4% saline wash. The symbols in panel A correspond to the hemolysis data points in panel B. The dashed line in panel B shows the initial hemolysis of the RBC at the device inlet.

The overall amount of measured hemolysis in experiments with frozen-thawed RBCs was higher than in experiments using fresh RBCs glycerolized to 10% w/v despite

lower predicted cell volumes for the velocities tested. The increased hemolysis may be attributed to increased sensitivity of frozen-thawed RBCs to osmotic and mechanical stresses as compared to unfrozen RBCs glycerolized to 10% w/v. Another possible explanation is the potential for an inaccurate selection of the value for cell membrane permeability to glycerol used in model simulations. Published values of $P_{g,c}$ vary by more than an order of magnitude [39, 111] and in some studies, $P_{g,c}$ has been found to decrease with increasing glycerol concentration [39, 40, 102]. The use of a lower $P_{s,c}$ in model simulations would result in an increased maximum relative cell volume, particularly for slower fluid velocities, which may explain the higher hemolysis values observed for frozen-thawed RBCs in 40% w/v glycerol.

Transport of Sodium Chloride

The amount of swelling the cells endure, particularly for slow velocities, can be easily controlled by increasing the saline concentration in the wash stream. An increase in saline concentration in the wash stream would allow more sodium chloride to permeate the AN69 membrane into the extracellular solution, effectively preventing excessive influx of water into the cells. Therefore, the ability to predict sodium chloride transport in the device is particularly important to design a washing procedure that avoids damaging osmotically induced changes in cell volume.

The experimentally measured concentration of sodium chloride at the outlet is compared to model predictions in Figure 5.6. The results from experiments using fresh RBCs glycerolized to 10% in the 50 μm and 130 μm channel are shown in panels A and

B, respectively, and results from experiments using frozen-thawed RBCs in 40% glycerol in the 50 μm and 130 μm channel are shown in panels C and D, respectively. As expected, the experiments with frozen-thawed RBCs in 40% glycerol show an increase in the outlet sodium chloride concentration with decreasing velocity. This is because more time is available for sodium chloride to permeate the AN69 membrane from the wash into the cell stream at slow velocities. The sodium chloride concentration in experiments conducted with RBCs in 10% glycerol remains relatively constant for all velocities tested. This was also expected, as in this case, the sodium chloride concentrations in the RBC stream and the wash stream are approximately equal.

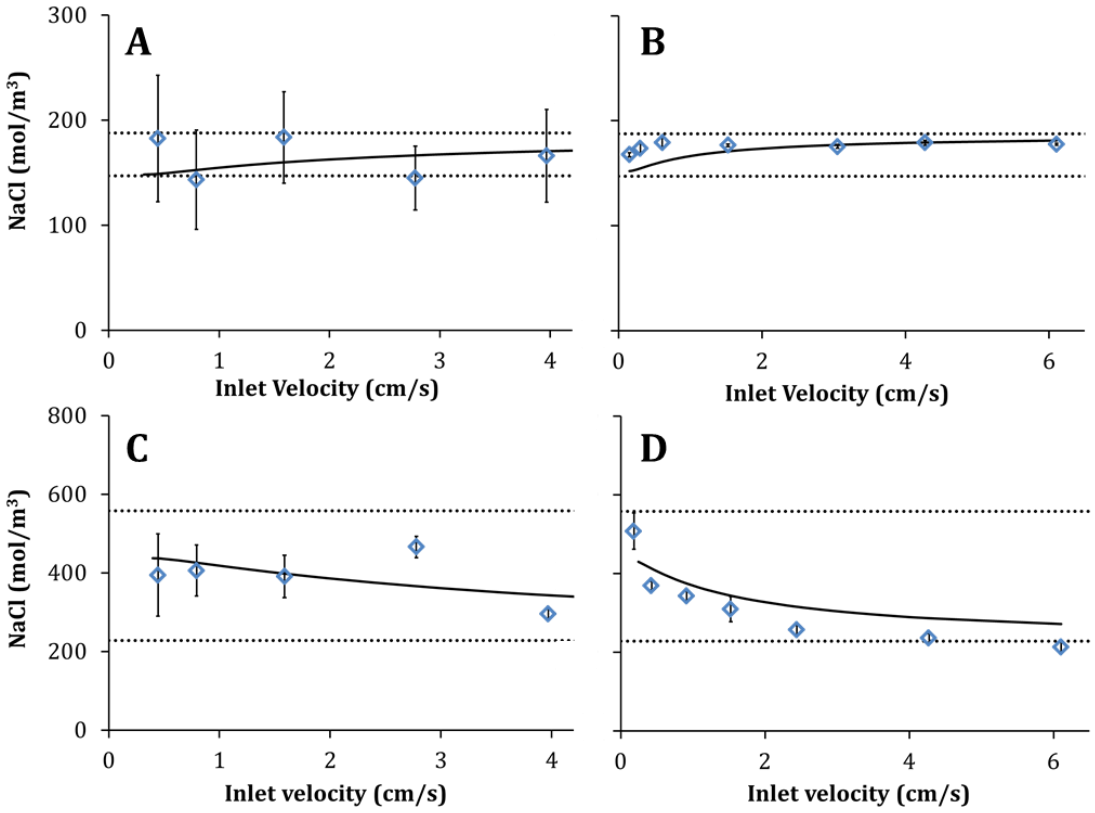

Figure 5.6. Thermogravimetric measurement of sodium chloride concentration in the RBC stream effluent. Panels A and B show measurements for removal of glycerol from RBCs in 10% w/v glycerol using an isotonic saline wash and the 50 and 130 μm channel, respectively. Panels C and D show measurements for removal of glycerol from frozen-thawed RBCs in 40% w/v glycerol using a 3.4% saline wash and the 50 and 130 mm channels, respectively. Solid lines show predicted sodium chloride concentrations in the RBC stream effluent (see Eq. 24) and dotted lines show the inlet concentrations in the RBC and wash streams.

Effect of Reflection Coefficient

As shown in Figure 5.7 A and B, the mass flow rate of the cell stream was higher at the outlet than in the inlet, and the relative increase in flow rate became more

pronounced with decreasing fluid velocity. This effect is consistent with model predictions and can be explained in terms of the glycerol reflection coefficient. Partial exclusion of glycerol from the membrane pores leads to a relatively low pressure inside the pore on the side of the membrane with the higher glycerol concentration. This drives flow of solution through the membrane pores towards the glycerol-rich stream. Reflection coefficients for small molecular cryoprotectants like glycerol and dimethyl sulfoxide have previously been neglected from the solution flux equation when modeling mass transfer through hemodialysis membranes as it is assumed that these molecules are small enough to pass through the membrane pores completely and easily [176, 177]. Although the glycerol reflection coefficient for the AN69 membrane is nearly zero, its effect on mass transfer is considerable when highly concentrated glycerol solutions are used and therefore cannot be neglected.

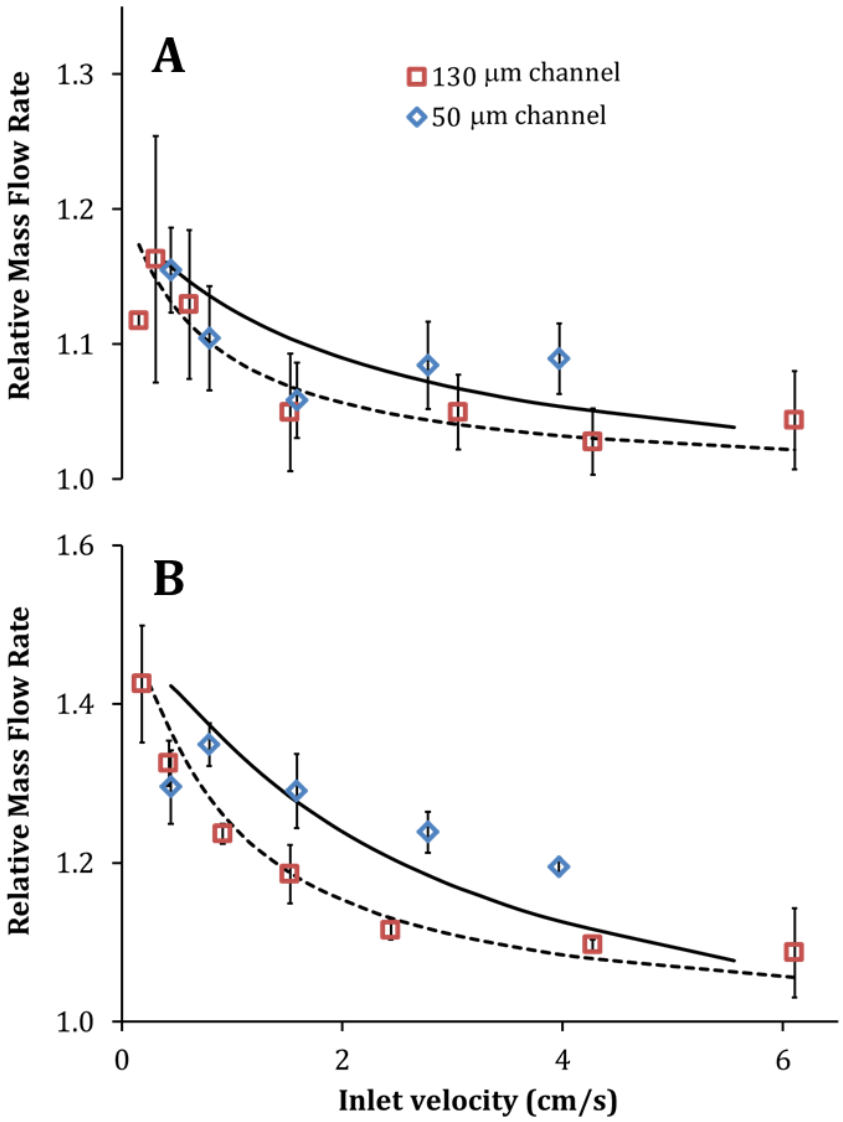

Figure 5.7 Increase in the outlet mass flow rate of the cell stream for glycerol removal experiments using RBCs glycerolized to 10% w/v with an isotonic saline wash (A) and frozen-thawed RBCs in 40% w/v glycerol with a 3.4% saline wash (B). The relative mass flow rate was calculated by taking the ratio of the cell stream mass flow rates at the outlet and inlet. Squares and diamonds are data points obtained from experiments conducted in the 130 and 50 μm channels, respectively. The corresponding model predictions are represented by the dotted and solid lines, respectively

Effect of Cell Density on Mass Transfer

To examine the effects of cell density of the glycerol removal capabilities of the device, experiments were performed using frozen-thawed RBCs with hematocrits ranging from 0% to 40%. The results of the experiments are shown in Figure 5.8. Hematocrit and fluid velocity were both found to have significant effects on the relative glycerol concentration at the device outlet ($p < 0.0001$ and $p = 0.0456$, respectively). However, the observed glycerol concentrations were similar for all the hematocrits that were tested. Therefore, cell density would most likely not have an apparent effect on the performance of the device from a practical standpoint.

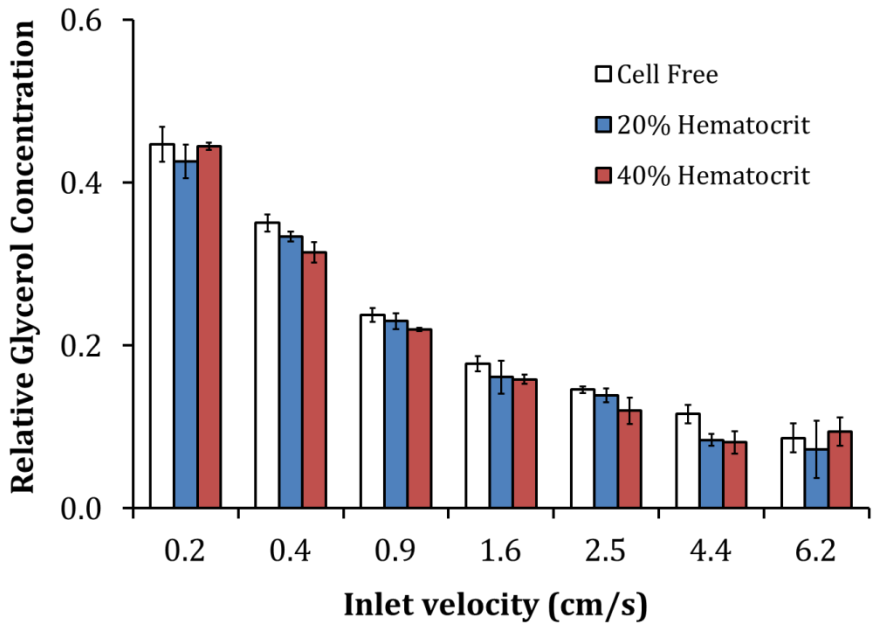

Figure 5.8. Effect of cell density on removal of glycerol from frozen-thawed RBCs in 40% w/v glycerol with a 3.4% saline wash and the 130 μm channel.

Steps Towards Rapid Continuous Deglycerolization

The design of an effective deglycerolization protocol must take into consideration two important criteria: the first is that the cell volume excursions are limited to the osmotic tolerance limits, and the second is to minimize the total process time as to satisfy the demands of clinical applications. The results presented thus far in this study have demonstrated successful partial deglycerolization of frozen-thawed RBC in a single channel microfluidic membrane device with reasonable agreement to the model predictions. By linking multiple devices in series and appropriately selecting the operating conditions in each device using the model, it is possible to design a complete continuous deglycerolization procedure that would achieve the desired ending glycerol concentration while maintaining the cell volume excursions to within the known safe osmotic tolerance limits in a reasonable amount of total washing time. The selection of the proper operating conditions in the first device is expected to be critical, as osmotic effects are expected to be the most damaging at the first stage of the removal process. Simulations indicate that it is possible to reduce the glycerol levels to a concentration that is comparable to what is attained using various AABB approved systems [152, 178, 179] in four passes using the 50 μm device and a fluid velocity of 0.8 cm/s. To maintain cell volume excursions to within the safe osmotic tolerance limits the saline concentration used in each step as well as the equilibration period as the cells flow from one device to the next must be selected and designed carefully. To achieve this, model simulations indicate that the cells may be washed with 5% saline in the first stage and allowed to equilibrate for 34 seconds, washed with 2.2% saline in the second stage and allowed to

equilibrate for 25 seconds, washed with isotonic saline in the third stage and allowed to equilibrate for 35 seconds, and finally washed with isotonic saline in the fourth and last stage for a total process time of 170 seconds. The model predicted decrease in glycerol concentration in the extracellular and the cell stream as well as cell volume predictions for the washing process is shown in Figure 5.9. To deliver the flow rate commonly used for transfusions in non-haemorrhagic patients (~4 ml/min) [23, 180] using this size channel and fluid velocity, the device must be scaled up to approximately 480 channels. Although the number of channels may seem large, the internal volume of cell suspension each device would only amount to approximately 1.3 mL of fluid due to the microscale dimensions of the channel. By optimizing the procedure, it may be possible to find operating conditions that would allow for faster processing while still achieving the desired outcome.

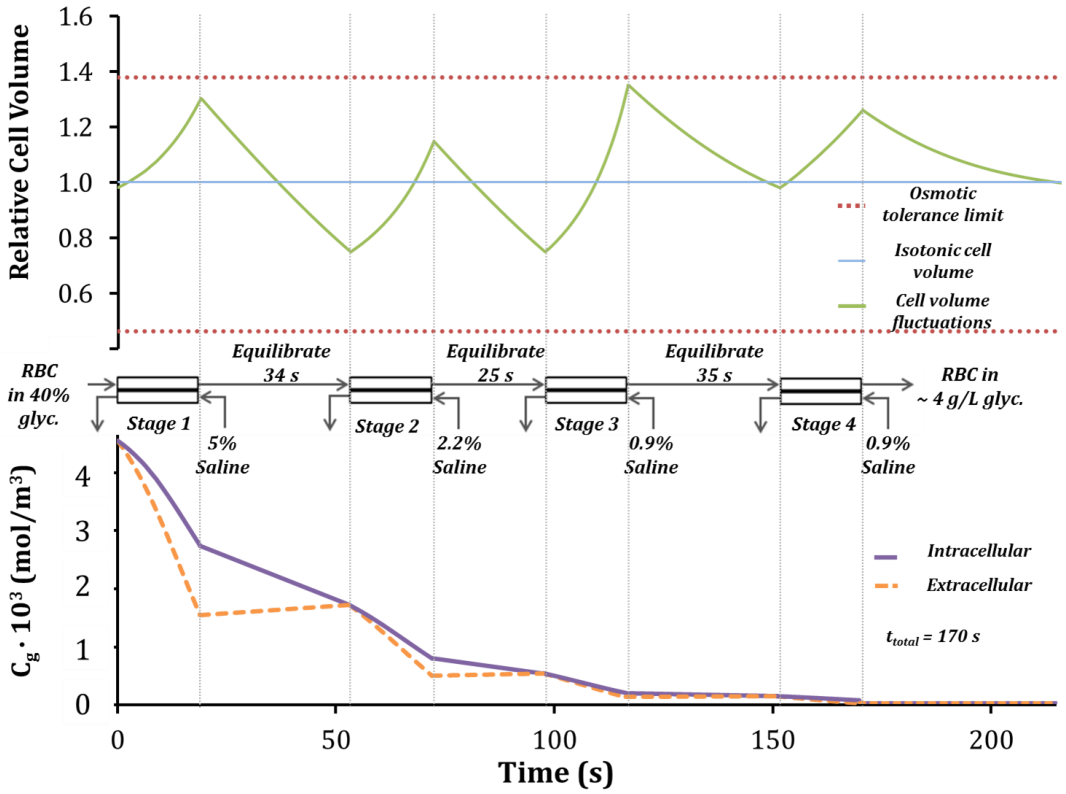

Figure. 5.9. Example of complete deglycerolization procedure designed using model predicted glycerol removal and resulting cell volume changes.

Because of the solute-solvent interaction in the AN69 membrane, experiments in this study show an increase in the outlet mass flow rate of the cell stream which leads to a decrease in cell density with each pass of the device resulting in an ending cell density that may be too dilute for direct transfusion at the end of the washing procedure. To mitigate excessive decrease of cell density, a membrane with larger pores could be used in the device to eliminate the effect of the reflection coefficient. Moreover, a backpressure may be applied to the cell stream so that the first term of the solution flux equation is comparable to the second. Lastly, the RBCs can also be passed through a

filtration membrane device at the end of the washing process to increase the cell density. The last membrane device would not induce any additional mass transfer; rather only remove the excess extracellular solution in the cell suspension via ultrafiltration to increase the hematocrit to an acceptable value for transfusion.

5.5 CONCLUSIONS

The results presented in this study demonstrated three main points relevant to continuous processing of cryopreserved RBCs:

1. Frozen-thawed cryopreserved RBCs can be flowed in the microfluidic membrane device without causing excessive mechanical damage.
2. The mathematical model developed was found to predict mass transfer trends and cell volume changes with reasonable accuracy as validated by actual experiments.
3. Using the mathematical model, a theoretical protocol for continuous rapid deglycerolization of frozen-thawed RBCs that avoids excessive cell volume changes to attain a high cell recovery can be designed.

5.6 ACKNOWLEDGEMENTS

We would like to thank Dr. Skip Rochefort for allowing us to conduct the TGA analysis at his rheology lab. We are grateful to the Oregon State University Student Health Center for performing blood collections. We would also like to thank the volunteers for providing blood samples for this study. This work was supported by a National Science Foundation grant (#1150861) to Adam Higgins.

Chapter 6: Lessons Learned, Future Directions, and Conclusions

6.1 INTRODUCTION

Lessons that were learned through the last three and a half years provide insight on future experimental design as well as missing pieces that need to be considered to develop a continuous rapid RBC deglycerolization system. In this chapter, the effects of various variables on the glycerol removal performance of the device and the resulting cell volume changes are presented. Preliminary experimental work on several side projects that are relevant to the deglycerolization of cryopreserved RBCs are also presented in this chapter. The main purpose of this chapter is to lay out pertinent information to facilitate the development of a complete deglycerolization procedure and potential optimization in the near future.

6.2 EFFECT OF SALINE CONCENTRATION

As mentioned in Chapter 5, a successful deglycerolization procedure must balance the amount of glycerol removed with the resulting cell volume changes to attain a high cell recovery. Using slower flow rates would increase glycerol removal by increasing the fluid residence time in the device, however it could also subject the cells to too much mass transfer and damaging cell volume changes. Because the AN69 membrane is much more permeable to glycerol in comparison to the cell membrane, glycerol is extracted more rapidly from the extracellular solution in comparison to the intracellular region. The imbalance in glycerol concentration between the intracellular

region and the extracellular solution causes an influx of water into the cells in an effort to equilibrate the glycerol concentration. Excessive influx of water would consequently cause over swelling of the cells, leading to osmotic damage. High concentrations of saline in the wash solution may be used to control the cell volume change as the RBCs transit through the device. The use of a higher saline concentration in the wash stream would allow more sodium chloride to permeate the AN69 membrane into the extracellular solution, effectively preventing excessive intracellular influx of water by reducing the osmotic pressure gradient across the cell membrane.

Figure 6.1 shows the predicted cell volume (panel A) and the relative glycerol concentration (panel B) at the device outlet for glycerol removal from RBCs in 40% w/v glycerol using a 3.4% and a 4.2% saline wash in the 130 μm channel. From panel A, it can be seen that washing the RBCs with a 3.4% saline solution causes the cells to swell past the upper osmotic tolerance limit in regions of slow fluid velocities. By using a higher saline concentration in the wash stream, the cell volume change can be kept to within the osmotic tolerance limits for all fluid velocities. From panel B, it can be seen that increasing the saline concentration does not have an apparent effect on the glycerol removal performance of the device. The selection of saline concentration used in each stage of the removal process is critical not only to prevent excessive cell swelling, but also to optimize the necessary equilibration time as the cells travel from one removal stage to the next in the design of a complete continuous deglycerolization protocol.

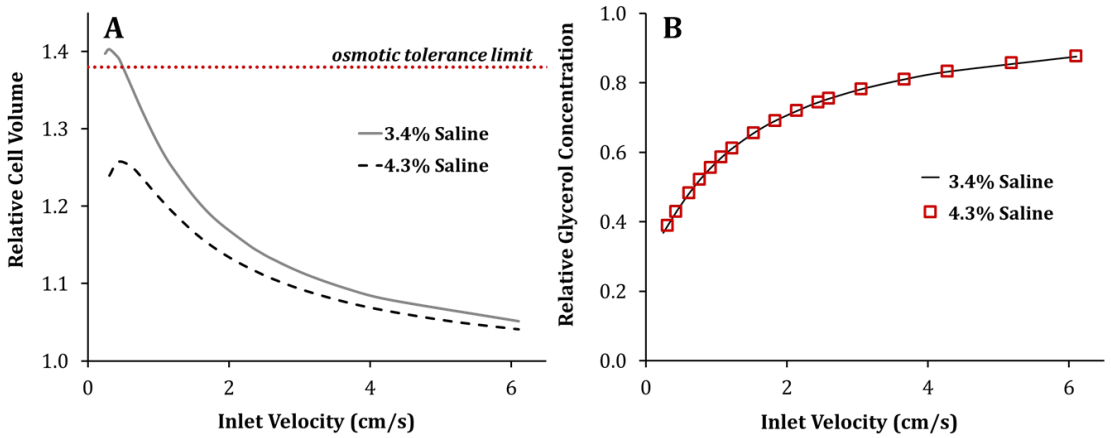

Figure 6.1. The effect of saline concentration used in the wash stream on predictions of cell volume (A) and glycerol removal (B) at the device outlet.

6.3 EFFECT OF CELL MEMBRANE GLYCEROL PERMEABILITY

As mentioned in Chapter 2, and briefly reiterated in Chapters 3 and 5, water transport across the RBC membrane occurs much more rapidly in comparison to glycerol. For this reason, the kinetics and magnitude of cell volume changes are primarily controlled by the cell membrane glycerol permeability. However, glycerol permeability values reported in literature vary by more than an order of magnitude. Selecting the most accurate cell membrane glycerol permeability value for use with the mathematical model is essential when generating cell volume predictions to design an optimized deglycerolization protocol. The use of a cell membrane glycerol permeability value that is too high would result in faster osmotic cell response and a lower predicted cell volume change at the device outlet. Conversely, the use of a value that is too low would under predict the osmotic cell response time, resulting in a cell volume at the device outlet that is too high. Selecting a cell membrane glycerol permeability that is too high would have

the most detrimental effect in practice as it would cause unexpected hemolysis. Selecting a cell membrane permeability that is too low could cause the unnecessary use of a highly concentrated saline wash as well as over estimation of the required equilibrating period between each removal stages, resulting in a sub-optimal deglycerolization protocol.

Figure 6.2 illustrates the effect of cell membrane glycerol permeability value on cell volume (panel A) and glycerol removal (panel B) predictions for glycerol removal from RBCs in 40% w/v glycerol using a 3.4% saline wash in the 130 μm channel. As can be seen from panel A, even a relatively small difference in the cell membrane glycerol permeability value used in the model could result in very different cell volume predictions. Panel B shows that the effect of the cell membrane glycerol permeability in glycerol removal, once the cells have exited the device and come to equilibrium with the extracellular solution, is negligible.

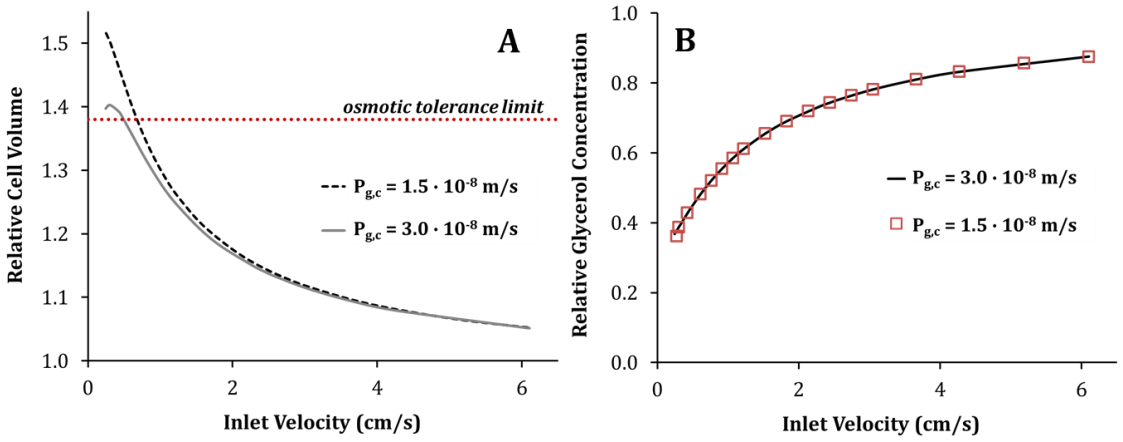

Figure 6.2. The effect of cell membrane glycerol permeability value on predictions of cell volume (A) and glycerol removal (B) at the device outlet.

6.4 EFFECT OF WASH FLUID FLOW RATE

The effect of channel dimension and operating fluid velocity in on glycerol removal and cell volume has been demonstrated in Chapter 5. One more factor that can be leveraged to improve glycerol removal that has yet to be discussed is the flow rate of the wash stream. All experiments conducted in Chapter 5 used a wash stream flow rate that is equal to the flow rate of the cell stream. The glycerol removal performance of the device can be increased by increasing the wash stream flow rate relative to the cell stream. The use of a higher wash stream flow rate would increase convective mass transfer, resulting in an increased concentration gradient across the AN69 membrane consequently improving the glycerol removal performance of the device. However, increased removal of glycerol also results in a greater magnitude of osmotically induced cell swelling.

Figure 6.3 shows the effect of doubling the wash fluid flow rate relative to the cell stream flow rate on predictions of cell volume (panel A) and relative glycerol concentration (panel B) at the device outlet for glycerol removal from RBCs in 40% w/v glycerol using a 4.3% saline wash in the 130 μm channel. From Figure 6.3 in can be seen that increasing the flow rate of the wash stream relative to the flow rate of the cell stream has an apparent effect on both glycerol removal as well as cell volume. The effects on cell volume must be considered carefully when using this strategy to improve glycerol removal in the design of an optimized deglycerolization procedure.

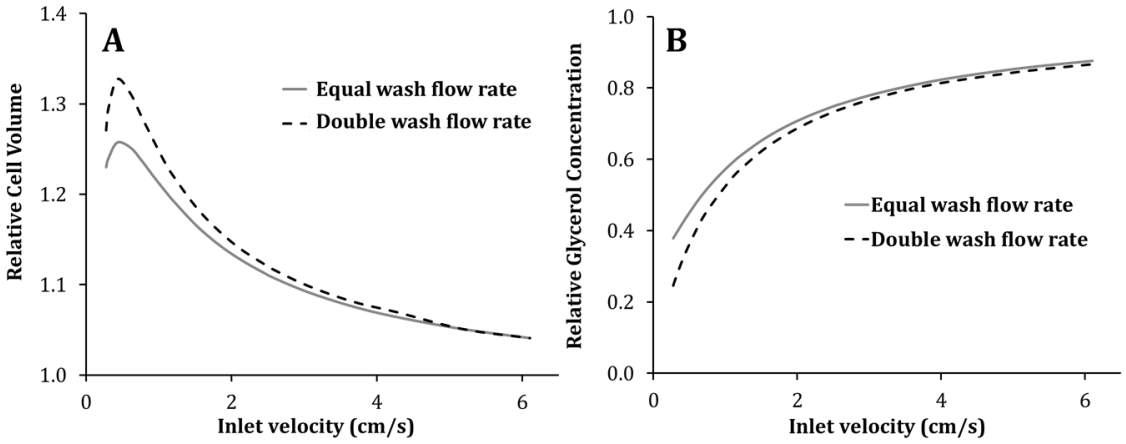

Figure 6.3. The effect of increasing the wash stream flow rate relative to the cell stream flow rate on predictions of cell volume (A) and glycerol removal (B) at the device outlet.

6.5 EFFECT OF REFLECTION COEFFICIENT

Glycerol removal experiments conducted in Chapter 5 all show an increase in the mass flow rate of the cell stream effluent as a result of the reflection coefficient. Because the partial exclusion of glycerol from permeating through the AN69 membrane drives the trans-membrane flow of solution towards the glycerol rich stream, the cell suspension at the device outlet becomes more diluted in comparison to the initial condition at the inlet. As the cells pass through multiple devices (removal stages), the cell density will become increasingly more dilute. This would result in a cell density that is too low for direct transfusion at the end of the deglycerolization procedure. As briefly addressed in Chapter 5, this may be mitigated by using a membrane with larger pores, by applying a backpressure to the cell stream, or by using an inline filtration device at the end of the deglycerolization process. This section of the chapter presents completed experimental work on a few separation techniques that has potential of being incorporated into a

complete deglycerolization system in future experiments. These separation techniques will probably be the most useful for the purpose of increasing cell density. However, with further development they could also potentially be used for glycerol removal.

Measurement of hydraulic conductivity of Millipore Isopore™ membranes

The structure and assembly of the membrane based microfluidic device easily allows the use of different membranes to fulfill certain mass exchange requirements. We were first interested in the Millipore Isopore™ membrane, for its relatively large pore size, enabling rapid mass transfer of glycerol from the cell stream to the wash stream. The Isopore™ HTTP membrane is a hydrophilic, track-etched polycarbonate membrane with cylindrical pores approximately 0.4 μm in diameter [181]. The larger pore diameter of the Isopore™ HTTP membrane would allow greater pressure driven solution flux across the membrane to improve mass transfer. However, experiments conducted using RBCs in isotonic saline with the Isopore™ HTTP membrane indicated a severe effluent imbalance. The effluent of the cell stream was observed to considerably increase whereas the effluent of the wash stream was severely decreased, almost to the point of being absent. This phenomena was not observed when we conducted experiments with 10% glycerol solution flowed counter-current to DI water. This effluent imbalance is unlikely to be caused by the reflection coefficient as the pores of the Isopore™ HTTP membrane are sufficiently large to allow complete clearance of sodium chloride molecules (or glycerol for that matter) present in the extracellular saline solution. We had hypothesized that this effluent imbalance is due to cell settling on the surface of the membrane

resulting from the trans-membrane pressure gradient of a counter-current flow configuration. Due to the extreme effluent imbalance, we concluded that the Isopore™ HTTP membrane is not a suitable membrane option for glycerol removal using counter-current flow configuration in the microfluidic device.

Although the Isopore™ HTTP membrane was found to be unsuitable for glycerol removal, it could still potentially be used in a deglycerolization system as a filtration device. The relatively large pores would allow ultrafiltration to remove a portion of the extracellular solution for the purpose of increasing the cell density. Once complete deglycerolization has been achieved, the cells may be passed through a device with the Isopore™ HTTP membrane. To avoid cell settling, the cells can be passed through the device co-current to an isosmotic solution set to flow at a lower fluid flow rate to maintain the direction of ultrafiltration. With this potential use in mind, the hydraulic conductivity of the Isopore™ HTTP membrane was experimentally determined for glycerol solutions of various concentrations.

We had previously attempted to measure the hydraulic conductivity of the Isopore™ HTTP membrane using a multichannel membrane microfluidic device in experimental work for the completion of a master's thesis [182]. However, the device used in this study was found to be difficult to flush free of air bubbles. The presence of air bubbles within the device led to inaccuracies in measuring the surface area of the membrane actually available for mass transfer. Air bubbles were more easily flushed with the present design of the microfluidic device, as the device only consists of a single channel per side of the membrane. Because the area can be more accurately measured

using the present microfluidic device, the hydraulic conductivity experiments for the Isopore™ HTTP membrane were repeated.

To measure hydraulic conductivity, the fluid of interest was perfused into the device in a co-current configuration for a period of time to eliminate particle debris and to flush any air bubbles residing in the channels. After the device was sufficiently primed, the syringe pump connected to the bottom channel was turned off while the syringe pump connected to the top channel remained in operation. The amount of filtrate across the membrane was collected and measured at the effluent of the bottom stream. The pressure drop in the channels was measured using pressure transducers (Utah Medical Deltran I, Midvale, UT, USA) and a data acquisition card (National Instruments USB-6210, Austin, TX, USA). The pressure drop in the channels and the resulting filtrate was measured for several different flow rates. The hydraulic conductivity (L_p) was then calculated using the equation below,

$$L_p = \frac{V_f}{A_x \cdot t \cdot (P_1 - P_2)} \quad [1]$$

where V_f is the volume of the filtrate collected, A_x is the surface area of the membrane available for mass transfer, t is the collection time, and $(P_1 - P_2)$ is the average transmembrane pressure between the top and bottom channel calculated as,

$$(P_1 - P_2) = \left(\frac{P_{1,i} - P_{1,o}}{2}\right) - \left(\frac{P_{2,i} - P_{2,o}}{2}\right) \quad [2]$$

where subscripts 1 and 2 denotes the top and bottom channel, respectively and i and o denotes channel inlet and outlet, respectively. The experiment was done in triplicate, using a fresh membrane for each experiment. Measurements of filtrate volume and

pressure drop were done in triplicates for each flow rate that was tested. The hydraulic conductivity of three solutions was tested: pure water, 10% w/v glycerol, and 40% w/v glycerol.

Table 6.1 presents the measured results of the hydraulic conductivity for the Isopore™ HTTP membrane. As expected, the measured hydraulic conductivity was found to be inversely proportional to solution viscosity. Millipore reports a hydraulic conductivity value of 12.1 m/Pa-s for the flow of pure water across the Isopore™ HTTP membrane [181]. As can be seen from Table 6.1, our experimentally measured value is in good agreement with the manufacturer's reported value. This general method for measuring the hydraulic conductivity may also be used in the future should we decide to employ a different type of membrane for use in the deglycerolization system.

Table 6.1 Measured hydraulic conductivity of the Isopore™ HTTP membrane to glycerol solution of various concentrations

Solution	L_p x 10^{-8} (m/Pa-s)
Water	11.5 ± 1.67
10% w/v glycerol	2.95 ± 0.25
40% w/v glycerol	1.91 ± 0.13

Post array deterministic lateral displacement microfluidic chip

We have initiated work on developing and constructing a post-array microfluidic chip for continuous cell separation using a relatively novel technique known as deterministic lateral displacement (DLD) first introduced by Huang and colleagues [68].

In this technique, particles follow a predetermined path as they flow through the device. The predetermined path is set by the size, spacing, and pitch of the post-array so that the asymmetry in the average fluid flow direction and the axis of the post-array will laterally displace particles larger than the critical diameter. This technique has been shown to be effective at fractionating the components of whole blood [183]. The main intent for using the DLD microfluidic chip was to be able to quickly change the extracellular medium of the RBC suspension for washing purposes as illustrated in Figure 6.4. Cell suspension flows on one half of the chip and the target medium is flowed on the other half. By selecting the appropriate post size, spacing, and pitch, it is hoped that we can rapidly exchange the extracellular medium by bumping RBCs across the width of the chip.

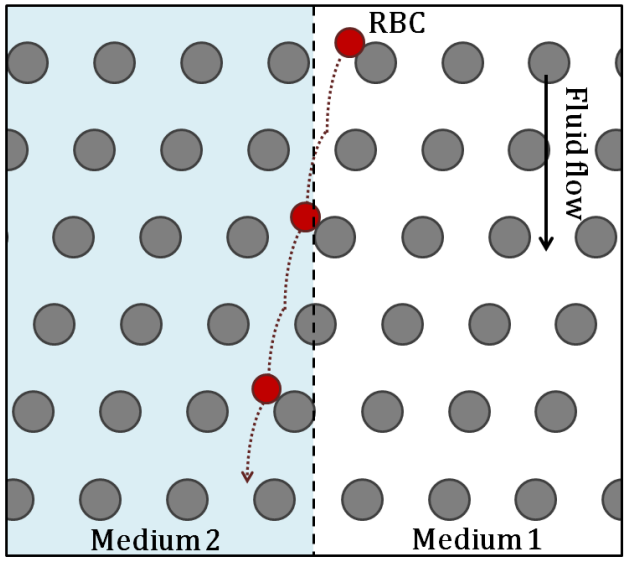

Figure 6.4. Proposed bumping of RBC across DLD device for rapid exchange of extracellular medium.

Photolithography was used to fabricate a silicon master. The chip design was created using AutoCAD and then printed into a photomask (CAD/Art Services, Bandon, OR, USA). Photoresist (SU-8 2050, MicroChem, Newton, MA, USA) was then spun into a 6 inch silicon wafer using the following recipe: accelerate at 100 rpm/s and spin at 500 rpm for 10 seconds, ramp by accelerating at 300 rpm/s to 4000 rpm and spin for 30 seconds to produce a film thickness of approximately 50 μm [184]. The photoresist coated wafer was then soft baked for 3 minutes at 65°C and 5 minutes at 95°C. The photomask was then placed on the hardened surface of the photoresist and exposed to a UV lamp for two and a half minutes at an intensity of 170 mW/cm^2. The wafer was then hard baked for 1 minute at 65°C and for 5 minutes at 95°C. The design was developed by immersing the wafer in the SU-8 developer while sonicating in 1 minute increments to ensure complete removal of photoresist that was not cross-linked. The developed wafer was then silanized using (tridecafluoro-1,1,2,2-tertahydrooctyl)-1-tricrhlorosilane (UCT Specialties, LLC, Bristol, PA, USA).

To fabricate the chip, PDMS and the curing agent (Sylgard 184 Silicone Elastomer Kit, Dow Corning, Midland, MI, USA) was mixed at a ratio of 10:1 and degassed in a dessicating chamber to eliminate air bubbles. The degassed mixture was then poured over the master and cured at 80°C for one hour. Once cured, the PDMS layer was carefully peeled away from the master and inlet and outlet ports were made by coring the PDMS using a large gauge blunt needle. The PDMS was then bonded to a microscope glass slide by oxygen plasma treatment. An image of the microfluidic chip is shown in Figure 6.5. The middle channel contains the micropost array designed to bump

RBCs. Fluid are introduced into the chip using Tygon® tubing and flowed through the prefilter (channels to the left and right side of the main channel) to remove large debris before arriving at the main channel.

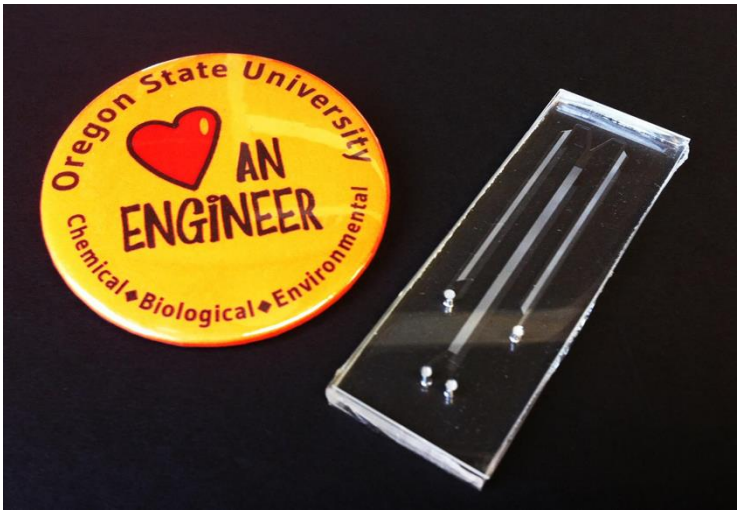

Figure 6.5. An image of the post array microfluidic chip.

Experiments to test the performance of the device were then conducted on a microfluidic chip with the following dimensions: 50 μm deep, 50 μm post diameter, 15 μm post spacing and 1° bump angle (pitch). Before each experiment, the device was flushed using a 2 g/L Pluronic F108 solution (BASF, Florham Park, NJ, USA) for 40 minutes to prime the surface of the device as well as to eliminate air bubbles using a flow rate of 2 ml/hr. The device was then perfused with isotonic saline with 3 g/L bovine serum albumin (BSA) (MP Biomedical New Zealand Limited, Auckland, New Zealand) for 20 minutes at a flow rate of 2 ml/hr to prep the channel for RBCs. BSA was added to the solution to maintain morphology of the cells as it is known that RBCs have a tendency to form echinocytes when contacted with glass surfaces [103]. Solutions were

introduced into the device using positive pressure via syringe pumps (New Era Pump Systems, Farmingdale, NY, USA). RBCs isolated from whole blood were resuspended in isotonic saline with 3 g/L BSA to reach a hematocrit of 20%. 2 mL of this RBC suspension was then mixed with 0.1 mL of 0.1 M Na_2EDTA solution. The resulting cell suspension was then flowed on one half of the chip with isotonic saline with 3 g/L BSA flowed on the other half. Observation of cell motion inside the device using high-speed microscopy indicates erratic cell flow pattern. At some regions of the device the cells appear to be travelling in DLD, whereas in other regions they appear to travel parallel to the flow of fluid. Cells were observed to exit the device mostly from the side that they entered, indicating that they did not bump or travel in DLD mode. Although some cells did exit out of the target outlet, the amount was variable from one chip to another. Observations of cell motion in the device indicate that DLD may be impeded by chip manufacturing flaws and inadequate experimental conditions. The chip features were measured and was confirmed to be close to the target size at the surface. However the chip was not analyzed using SEM to determine if the posts have perfectly vertical sidewalls. Posts that are thinner in the middle could allow RBCs to pass instead of traveling in DLD. Inadequate control of flow inside the device could also impede DLD. Videos of fluid flow inside the device replayed at super slow speeds reveals subtle pulses in the flow of fluid at the liquid-liquid laminar interface. These pulses, although subtle, could impede particles from travelling in DLD. Future experiments should be conducted using specialized pumps that deliver low, pulse-free flow rates.

Although we were unsuccessful in rapidly exchanging the RBC extracellular medium, we were still able to conduct mechanical fragility experiments inside the post array device. Cell damage from mechanical forces was determined by measuring the hemolysis at the device outlet for two operating fluid flow rates: 1.2 and 2.4 ml/hr. The measured hemolysis resulted in a value of less than 1% for both flow rates, indicating that RBCs can be flowed through the bump array microfluidic chip without incurring excessive damage from mechanical forces.

6.6 EFFECT OF FREE HEMOGLOBIN

Complete deglycerolization using the microfluidic membrane device is expected to cause hemolysis to a certain extent. Although our target is to limit the hemolysis to 20%, some of the cells are expected to undergo hemolysis during the deglycerolization process, releasing hemoglobin into the extracellular solution. The use of the AN69 membrane will cause retention of the free hemoglobin in the cell stream, as this membrane only allows the permeation of small molecular solutes. As a result of this retention, the hemoglobin concentration present in the extracellular solution after complete deglycerolization is achieved may be too high for immediate transfusion into patients. Hemoglobin is known to be toxic if present in high concentrations in blood plasma [185]. The concentration of hemoglobin present in the supernatant of transfusable RBC units must not exceed 2 g/L [23, 60]. Therefore, it may be necessary to incorporate a hemoglobin removal step after complete deglycerolization is achieved. Hemoglobin concentrations can potentially be reduced by ultrafiltration while

simultaneously increasing the cell density. Research has also been done in the development of an inline sorption column to bind free hemoglobin by coupling the hemoglobin binding protein, haptoglobin, onto sorption beads [186]. The use of such devices could be incorporated into the deglycerolization system to decrease the amount of free hemoglobin to a value acceptable for transfusion.

6.7 CONCLUSIONS

Through the course of this project, several discoveries relevant to the efforts of improving the deglycerolization process for cryopreserved RBCs were made. By using the mathematical model for cell membrane transport, it was found that glycerol can be rapidly extracted from cryopreserved blood without incurring excessive amounts of damage by precisely controlling the extracellular solution composition to maintain cell volume changes that are within the known safe osmotic tolerance limit. This was first demonstrated using a batch approach by step-wise dilution of the cells in various saline solutions to facilitate permeation of glycerol while restricting the equilibration time in each step to avoid damaging cell volume excursions. Our best result achieved complete deglycerolization in three minutes with less than 20% hemolysis. Osmotic tolerance limit experiments indicate that frozen-thawed RBCs glycerolized to 40% w/v are more sensitive to osmotic damage when compared to fresh RBCs and unfrozen RBCs glycerolized to 40% w/v. From these results, it can be inferred that in order to avoid hemolysis and attain high post-wash cell recovery, the osmotic tolerance limits used to design deglycerolization procedures for cryopreserved RBCs must be set to a value that is

much more conservative compared to values for fresh RBCs as reported in existing literature. A microfluidic membrane device was developed to adapt the rapid deglycerolization strategy into a continuous process. To assist in experimental design, a mathematical model that is capable of predicting the transport of water and solutes (glycerol and sodium chloride) was developed. Glycerol removal experiments using RBCs glycerolized to 10% w/v and 40% w/v using saline wash solutions demonstrated successful partial deglycerolization in a continuous process. Furthermore, experimental results were found to be in reasonable agreement with model predictions. By linking multiple devices in series and selecting the appropriate operating conditions for each device using the mathematical model, complete rapid continuous deglycerolization of cryopreserved RBCs would be possible. Model simulations suggest that complete deglycerolization can be achieved using the current device in four passes for a total processing time of approximately 170 seconds. With further optimization, it may be possible to determine operating conditions that would allow for even faster processing. Therefore, the work that has been done thus far has answered the two main questions that this study sought to answer: glycerol can be rapidly extracted from cryopreserved RBCs and the process can be done in a continuous manner.

Appendix A – Mathematical Modeling and Optimization of Three-Step Dilution Protocol

The primary advantage of the two-parameter cellular mass transport model (System 1) is that through a time-dependent change of variables, it can be made linear and thus analytically solvable when the extracellular concentrations are constant [187]. The analytical solution is critical to the optimization because during CPA removal, we expect to encounter conditions where there is minimal water volume in the cell. From System 1 it is clear that this leads to stiff differential equations (see, e.g., Burden and Faires [188]) where results depend sensitively to the precision of the estimation of the value of *W*. This type of differential equation is challenging and expensive to solve and thus is not ideal for optimization. Therefore, we begin by nondimensionalizing the model by defining $w = W/W^{iso}$, $s = S/(M^{iso}W^{iso})$, $m_n = M_n/M^{iso}$ and $m_s = M_s/M^{iso}$.

Combining terms, and defining a new unitless time variable $\sigma = t(L_p ARTM^{iso})/W^{iso}$, and relative permeability parameter $b = P_s\left(L_p RTM^{iso}\right)^{-1}$, yields the nondimensional model

$$\frac{dw}{d\sigma} = \left(m_n + m_s - \frac{1+s}{w}\right)$$
$$\frac{ds}{d\sigma} = b\left(m_s - \frac{s}{w}\right) \qquad \text{[A1]}$$

We now define a new "time" variable τ with the following relationship to the old time variable

$$\sigma = \int_0^{\tau} w(\xi) d\xi \qquad \text{[A2]}$$

In the new time τ we have the linear non-homogeneous system

$$\begin{aligned} \dot{w} &= -(m_n + m_s)w + s + 1, \\ \dot{s} &= b(m_s w - s), \\ w(0) &= w_0, \\ s(0) &= s_0. \end{aligned} \qquad \text{[A3]}$$

Through a simple change of variables $x = (w, s)^{\mathrm{T}} + A(M)^{-1}(1,0)^{\mathrm{T}}$, where

$$A(M) = \begin{bmatrix} -(m_n + m_s) & 1 \\ bm_s & -b \end{bmatrix}, \qquad \text{[A4]}$$

we end up with the autonomous, homogenous linear system

$$\begin{aligned} \dot{x} &= A(M)x, \\ x(0) &= (w_0, s_0)^{\mathrm{T}} + A(M)^{-1}(1,0)^{\mathrm{T}}. \end{aligned} \qquad \text{[A5]}$$

This system has the solution

$$x(\tau) = e^{A(M)\tau} x_0, \qquad \text{[A6]}$$

that may be determined analytically if the (easily determined in this case) eigenvalues of A are known. To find $x(\tau)$ in general, we may use the built in standard routine MatrixExp in our computational package (Mathematica, Wolfram Inc).

As stated above, we wish to minimize the total time to reach the desired state using three constant concentration steps. In our reparametrized-non-dimensional formulation with an exact solution, this problem becomes

$$\begin{aligned}
&\min_{\lambda\in A}\sum_{i=1}^{3}\int_0^{\tau_i} w_i(s;\lambda)ds \quad \text{subject to}\\
&\| x_3(\tau_3) - x_D \|^2 \le \text{tol},\\
&\dot{x} = A(M_i)x_i,\\
&x_1(0) = x(0) = \begin{pmatrix} w(0) \\ s(0) \end{pmatrix}, \quad x_2(0) = x_1(\tau_1), \quad x_3(0) = x_2(\tau_2),\\
&v_{min} \le \Gamma \cdot x_i(\tau) - \Gamma^{\mathrm{T}} A(M)^{-1}\begin{pmatrix} 1 \\ 0 \end{pmatrix} \le v_{max} \qquad i = 1,2,3
\end{aligned} \tag{A7}$$

where $x_D = (1,0)$, tol $= 10^{-3}$, $v_{min} = (V_{low} - V_b)/W^{iso}$, $v_{max} = (V_{high} - V_b)/W^{iso}$, and $\Gamma = \left(1, \bar{v}\, M^{iso}\right)^{\mathrm{T}}$.

Finally, because it is relatively difficult to check the inequality constraints for all τ, we note that the constraints will be satisfied for all time τ if they are satisfied at the endpoints and at the critical point if it exists. It is simple to show that there will be at most one critical point, and that for our protocols, it may only be a relative maximum, which makes determining the value

$$\begin{aligned}
&v_i^{max} := \Gamma \cdot x_i(\tau_i^{max}) - \Gamma^T A(M)^{-1}\begin{pmatrix} 1 \\ 0 \end{pmatrix}, \qquad i = 1,2,3\\
&\Gamma \cdot \frac{d}{dt} x_i(\tau_i^{max}) = 0,
\end{aligned} \tag{A8}$$

at this point easy to find either numerically or algebraically (see, for example Benson et al28), therefore, we may replace the inequality constraints in (A7) with $v_i^{max} \le v_{max}$ for i = 1,2,3 and

$$v_{min} \le \Gamma \cdot x_i(\tau_i) - \Gamma^{\mathrm{T}} A(M)^{-1}\begin{pmatrix} 1 \\ 0 \end{pmatrix} \le v_{max} \qquad i = 1,2,3. \tag{A9}$$

Finally, we note that given the solution $x_i(\tau) = \exp(A(M_i)\tau)x(0)$, we may find the integrals in the objective function exactly

$$\sigma_i = \int_0^{\tau_i} x_i\,(s)ds = A(M_i)^{-1}\left(e^{A(M_i)\tau_i}x_i(0) - x_i(0) - \tau_i\begin{pmatrix}1\\0\end{pmatrix}\right), \qquad \text{[A10]}$$

where σ_i is the step length in the nondimensional original time space. While a completely analytical solution to this optimization problem is possible, it is algebraically cumbersome at best, and fraught with potential clerical errors due to the number of parameters needed to resolve the inequality constraints. Because of the speed of the calculation of the solution of the linear ODE system and the subsequent integrals, we chose to use a numerical optimization, using the `FindMinimum` algorithm implemented in Mathematica (Wolfram Research, Inc, Champaign, IL) from a set of 100 random feasible starting points in the admissible set. Again, we reiterate that a numerical technique may not converge quickly in the non-rescaled time domain (e.g. solving System 1) due to stiffness problems as much of the optimal protocol occurs with $W(t) \ll W^{iso}$.

Appendix B – Mathematical Model of Microfluidic Membrane Device

The development of the mathematical model assumes the system has reached steady state conditions. Velocity, concentration, and pressure were assumed to be spatially uniform with respect to the channel height (plug flow conditions). Mass transfer was assumed to only occur between the cell stream and the extracellular solution, and between the extracellular solution and the wash stream (no direct mass transfer from the cell stream to the wash stream). Glycerol is assumed to be permeable through both the cell and synthetic membrane. The intracellular salt content is assumed to be composed of only sodium chloride. Sodium chloride is also assumed to be non-permeable to the cell membrane and only permeable to the synthetic membrane. We also assumed that no reaction takes place in the device, as well as constant molar volume and temperature.

The diagram of the differential volume used to model the device (Figure 5.2) as well as the flux equations (Eqns. 1-5) have been described in Chapter 5 and therefore will not be presented again in this Appendix. We begin by performing steady state volume balances of all the streams in the system. A volume balance of the cell stream yields the following equations.

In – Out + Generation = Accumulation

$$Q_c|_x - Q_c|_{x+\Delta x} + \left[J_{g,c} \cdot \nu_g + J_{w,c}\right] A_{Total} = 0 \qquad \text{[A1]}$$

A_{Total} is the surface area of all the cells in the differential volume and can be defined as a portion of the top stream volume that is occupied by cells as shown below,

$$A_{Total} = \frac{A_c}{V_c} \cdot \frac{Q_c}{Q_c + Q_1} \cdot (W \cdot H \cdot \Delta x) \quad [A2]$$

where A_c and V_c are the surface area and volume of a single cell, respectively. The total surface area of the cells is assumed to be constant. However, during the mass transfer process Q_c and V_c will not remain constant. To simplify the derivation, Q_c and V_c can be substituted by $\dot{n}_c$, the constant number of cells that passes through the differential volume per time as described below.

$$\dot{n}_c = \frac{Q_{c,0}}{V_{c,0}} \quad [A3]$$

Through this substitution, the total area can be expressed in terms of constant variables and reinserted back into equation A1 as shown below.

$$Q_c|_x - Q_c|_{x+\Delta x} + \left[J_{g,c} \cdot \nu_g + J_{w,c}\right] \frac{A_c \cdot \dot{n}_c}{Q_c + Q_1} \cdot (W \cdot H \cdot \Delta x) = 0 \quad [A4]$$

$$\frac{Q_c|_x - Q_c|_{x+\Delta x}}{\Delta x} + \left[J_{g,c} \cdot \nu_g + J_{w,c}\right] \frac{A_c \cdot \dot{n}_c}{Q_c + Q_1} \cdot (W \cdot H) = 0 \quad [A5]$$

Taking the limit as Δx approaches zero, we obtain the differential equation that describes the change in the volumetric flow rate of the cell stream as a function of channel length.

$$\frac{dQ_c}{dx} = \left[J_{g,c} \cdot \nu_g + J_{w,c}\right] \frac{A_c \cdot \dot{n}_c}{Q_c + Q_1} \cdot (W \cdot H) \quad [A6]$$

A similar volume balance approach can be performed on the extracellular solution and wash stream. A volume balance on the extracellular solution stream yields the following:

$$Q_1|_x - Q_1|_{x+\Delta x} - \left[J_{g,c} \cdot \nu_g + J_{w,c}\right] \frac{A_c \cdot \dot{n_c}}{Q_c + Q_1} \cdot (W \cdot H \cdot \Delta x) - J_v \cdot (W \cdot \Delta x) = 0 \quad [A7]$$

$$\frac{Q_1|_x - Q_1|_{x+\Delta x}}{\Delta x} - \left[J_{g,c} \cdot \nu_g + J_{w,c}\right] \frac{A_c \cdot \dot{n_c}}{Q_c + Q_1} \cdot (W \cdot H) - J_v \cdot W = 0 \quad [A8]$$

Taking the limit as Δx approaches zero, we get the differential equation that describes the change in the volumetric flow rate of the extracellular stream as a function of channel length.

$$\frac{dQ_1}{dx} = -\left[J_{g,c} \cdot \nu_g + J_{w,c}\right] \frac{A_c \cdot \dot{n_c}}{Q_c + Q_1} \cdot (W \cdot H) - J_v \cdot W \quad [A9]$$

A volume balance on the wash stream yields the following:

$$\frac{dQ_1}{dx} = -\left[J_{g,c} \cdot \nu_g + J_{w,c}\right] \frac{A_c \cdot \dot{n_c}}{Q_c + Q_1} \cdot (W \cdot H) - J_v \cdot W \quad [A10]$$

$$\frac{Q_2|_{x+\Delta x} - Q_2|_x}{\Delta x} + J_v \cdot W = 0 \quad [A11]$$

Taking the limit as Δx approaches zero, we get the differential equation that describes the change in the volumetric flow rate of the wash stream as a function of channel length.

$$\frac{dQ_2}{dx} = -J_v \cdot W \quad [A12]$$

To describe the mass transfer process in the device, steady state solute balances must be performed to derive the differential equations that describe the transport of glycerol and sodium chloride. In a given cell, there exist osmotically inactive components that occupy volume but to not play a part in the mass transfer process. Solutes are only

dissolved in the osmotically active portion of the cell which can be described as $V_c - V_b$, where V_c is the total volume of the cell and V_b is the osmotically inactive volume. Therefore, the flow rate of osmotically active cell volume can be defined as $Q_c - Q_b$, where Q_b is equal to $\dot{n}_c \cdot V_b$. The steady state solute balance of glycerol in the cell stream can then be performed as shown below.

$$\left[(Q_c - \dot{n}_c \cdot V_b) \cdot C_{g,c}\right]\Big|_x - \left[(Q_c - \dot{n}_c \cdot V_b) \cdot C_{g,c}\right]\Big|_{x+\Delta x} + J_{g,c} \cdot \frac{A_c \cdot \dot{n}_c}{Q_c + Q_1} \cdot (W \cdot H \cdot \Delta x) = 0 \quad \text{[A13]}$$

$$\frac{\left[(Q_c - \dot{n}_c \cdot V_b) \cdot C_{g,c}\right]\Big|_x - \left[(Q_c - \dot{n}_c \cdot V_b) \cdot C_{g,c}\right]\Big|_{x+\Delta x}}{\Delta x} + J_{g,c} \cdot \frac{A_c \cdot \dot{n}_c}{Q_c + Q_1} \cdot (W \cdot H) = 0 \quad \text{[A14]}$$

Taking the limit as Δx approaches zero,

$$C_{g,c}\frac{d(Q_c - \dot{n}_c \cdot V_b)}{dx} + (Q_c - \dot{n}_c \cdot V_b)\frac{dC_{g,c}}{dx} = J_{g,c} \cdot \frac{A_c \cdot \dot{n}_c}{Q_c + Q_1} \cdot (W \cdot H) \quad \text{[A15]}$$

The volume of the osmotically inactive portion of the cell is constant, hence the derivative is equal to zero. Simplifying and rearranging the equation we get the differential equation that describes the concentration of glycerol in the cell stream as a function of channel length.

$$\frac{dC_{g,c}}{dx} = \frac{1}{(Q_c - \dot{n}_c \cdot V_b)}\left[J_{g,c} \cdot \frac{A_c \cdot \dot{n}_c}{Q_c + Q_1} \cdot (W \cdot H) - C_{g,c}\frac{dQ_c}{dx}\right] \quad \text{[A16]}$$

The steady state glycerol balance in the extracellular solution yields the following,

$$\left[Q_1 \cdot C_{g,1}\right]\Big|_x - \left[Q_1 \cdot C_{g,1}\right]\Big|_{x+\Delta x} - J_{g,c} \cdot \frac{A_c \cdot \dot{n}_c}{Q_c + Q_1} \cdot (W \cdot H \cdot \Delta x) - J_g \cdot W \cdot \Delta x = 0 \quad [A17]$$

$$\frac{\left[Q_1 \cdot C_{g,1}\right]\Big|_x - \left[Q_1 \cdot C_{g,1}\right]\Big|_{x+\Delta x}}{\Delta x} - J_{g,c} \cdot \frac{A_c \cdot \dot{n}_c}{Q_c + Q_1} \cdot (W \cdot H) - J_g \cdot W = 0 \quad [A18]$$

Taking the limit as Δx approaches zero,

$$-\frac{d\left(Q_1 \cdot C_{g,1}\right)}{dx} - J_{g,c} \cdot \frac{A_c \cdot \dot{n}_c}{Q_c + Q_1} \cdot (W \cdot H) - J_g \cdot W = 0 \quad [A19]$$

Simplifying and rearranging we get the differential equation that describes the glycerol concentration change in the extracellular solution as a function of channel length.

$$\frac{dC_{g,1}}{dx} = -\frac{1}{Q_1}\left[J_{g,c} \cdot \frac{A_c \cdot \dot{n}_c}{Q_c + Q_1} \cdot (W \cdot H) + J_g \cdot W + C_{g,1}\frac{dQ_1}{dx}\right] \quad [A20]$$

The steady state glycerol balance in the wash stream yields the following,

$$\left[Q_2 \cdot C_{g,2}\right]\Big|_{x+\Delta x} - \left[Q_2 \cdot C_{g,2}\right]\Big|_x + J_g \cdot W \cdot \Delta x = 0 \quad [A21]$$

$$\frac{[Q_2 \cdot C_2]|_{x+\Delta x} - [Q_2 \cdot C_2]|_x}{\Delta x} + J_g \cdot W = 0 \quad [A22]$$

As Δx approaches zero, simplifying and rearranging we get the differential equation that describes the glycerol concentration change in the wash stream as a function of channel length.

$$\frac{dC_{g,2}}{dx} = -\frac{1}{Q_2}\left[J_g \cdot W + C_{g,2}\frac{dQ_2}{dx}\right] \quad [A23]$$

Because sodium chloride is assumed to be non-permeable through the cell membrane, the mass or moles of sodium chloride in the cells is constant through the mass transfer process. The concentration of sodium chloride, however, will change as glycerol and water can readily permeate in and out of the cell volume. The equation that describes the change in sodium chloride concentration is presented in Eq. 14 in Chapter 5. The sodium chloride balance can be performed on the extracellular solution and the wash stream to obtain differential equations that describe the change in sodium chloride concentration as a function of channel length. The steady state sodium chloride balance in the extracellular stream yields the following:

$$\left[Q_1 \cdot C_{s,1}\right]\Big|_x - \left[Q_1 \cdot C_{s,1}\right]\Big|_{x+\Delta x} - J_s \cdot (W \cdot \Delta x) = 0 \quad \text{[A24]}$$

$$\frac{\left[Q_1 \cdot C_{s,1}\right]\Big|_x - \left[Q_1 \cdot C_{s,1}\right]\Big|_{x+\Delta x}}{\Delta x} - J_s \cdot W = 0 \quad \text{[A25]}$$

Taking the limit as Δx approaches zero, and simplifying and rearranging the terms, we obtain a differential equation that describes the sodium chloride concentration change in the extracellular stream as a function of channel length.

$$\frac{dC_{s,1}}{dx} = -\frac{1}{Q_1}\left[J_s \cdot W + C_1 \frac{dQ_1}{dx}\right] \quad \text{[A26]}$$

The steady-state sodium chloride balance on the wash stream yields the following:

$$\left[Q_2 \cdot C_{s,2}\right]\Big|_{x+\Delta x} - \left[Q_2 \cdot C_{s,2}\right]\Big|_x + J_s \cdot W \cdot \Delta x = 0 \quad \text{[A27]}$$

$$\frac{\left[Q_2 \cdot C_{s,2}\right]\Big|_{x+\Delta x} - \left[Q_2 \cdot C_{s,2}\right]\Big|_x}{\Delta x} + J_s \cdot W = 0 \quad \text{[A28]}$$

Taking the limit as Δx approaches zero, we can simplify and rearrange the terms to get a differential equation that describes the sodium chloride concentration change in the wash stream as a function of channel length.

$$\frac{dC_{s,2}}{dx} = -\frac{1}{Q_2}\left[J_s \cdot W + C_{s,2}\frac{dQ_2}{dx}\right] \quad \text{[A29]}$$

The pressure drop in the channel was described using a pressure drop equation for a fully-developed, laminar flow in a rectangular channel [161] as shown in the equation below,

$$\bar{u} = \frac{\Delta P \cdot c^2}{\mu \cdot L}\left[\frac{1}{3} - \frac{64 \cdot \varepsilon}{\pi^5} tanh\frac{\pi}{2 \cdot \varepsilon}\right] \quad \text{[A30]}$$

where $\bar{u}$ is the analytical mean velocity in the channel and $c = \frac{H}{2}$, $b = \frac{W}{2}$, and $\varepsilon = \frac{c}{b}$. Through algebraic manipulation, the pressure drop equation for the cell and extracellular solution stream and the wash stream can be obtained, as shown in Equation 17 and 18, respectively in Chapter 5.

Appendix C – Validation of the Thermogravimetric (TGA) Analysis

To test the accuracy of the TGA analysis, the composition of twenty cell-free standard solutions containing different amounts of water, glycerol, and salt was measured using the TGA procedure. The compositions of the standard solutions are presented in Figure C1. The TGA procedure was carried out in 4 steps: (1) ramp 5°C /min to 100°C, (2) isothermal for 15 mins at 100°C, (3) ramp 10°C/min to 290°C, (4) isothermal for 10 mins at 290°C. A sample of the resulting thermogravimetric curve is shown in Figure C2. The error between triplicate measurements of the solution composition and the actual known composition was then calculated. The procedure was found to be reasonably accurate for measuring the water, glycerol, and salt composition of most of the standard solutions. The TGA measurements were found to not be accurate at measuring the composition of glycerol in solutions containing very high salt concentrations (10-25% w/w) and very low glycerol concentrations (less than 2% w/w). The inaccuracy in measuring the glycerol composition is not seen in solutions with high sodium chloride concentrations if the concentration of glycerol is similar or higher. In deglycerolization experiments, it is unlikely for an experimental run to produce an effluent with very high sodium chloride and very low glycerol concentration. Hence, the TGA results for these solutions were excluded from the average error calculations. The resulting average error in mass fraction for water, glycerol and sodium chloride using the TGA method was found to be 0.9%, 3.6%, and 7.6% respectively. The average error for sodium chloride is the largest because sodium chloride is only present in small amounts in most of the standard solutions. Figures C2, C3, and C4 show the measured mass fraction plotted

against the known value for water, glycerol, and sodium chloride, respectively. Error bars show the standard error of the mean in three triplicate measurements.

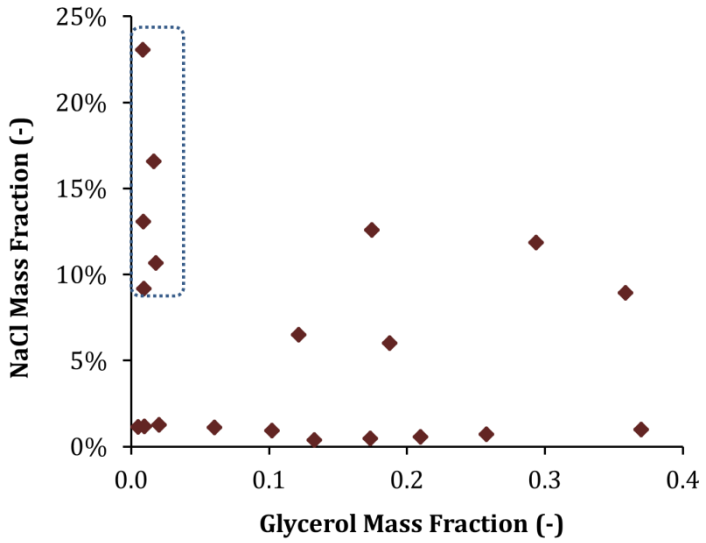

Figure C1. Composition of the standard solutions used to validate the TGA analysis. The composition of the standard solutions excluded from the average error calculations are indicated with the dashed rectangle.

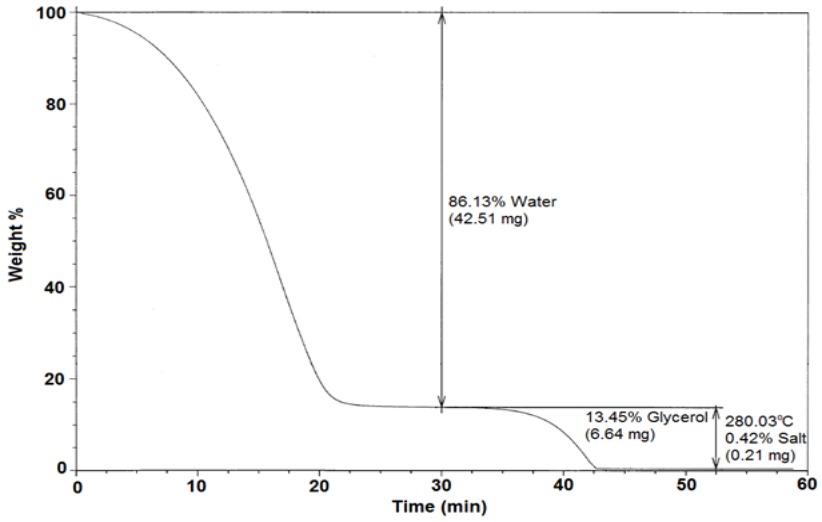

Figure C2. Thermogravimetric curve of concentrated ternary solution of water, glycerol, and sodium chloride

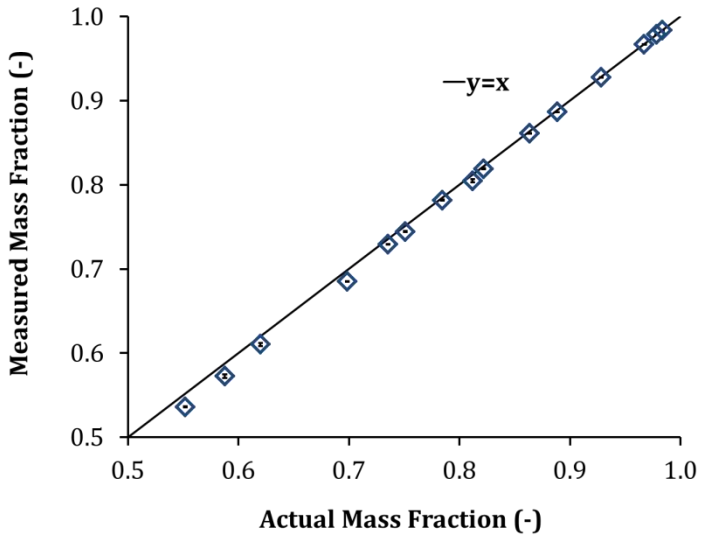

Figure C3. Thermogravimetrically measured mass fraction of water as a function of the actual water mass fraction.

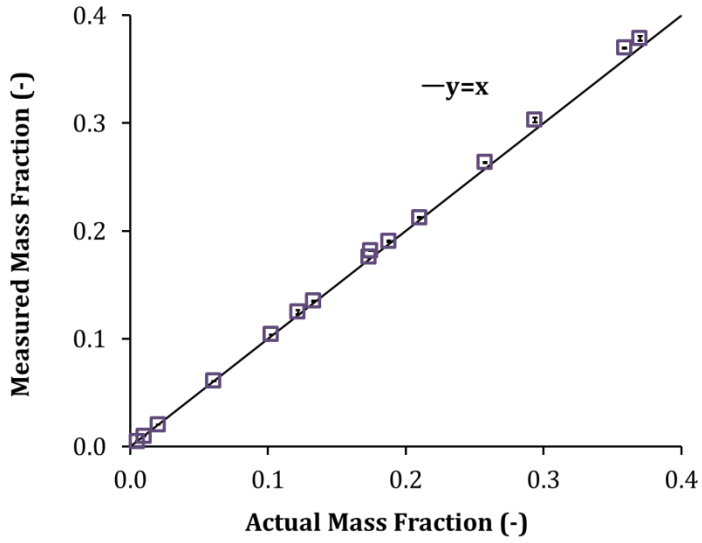

Figure C4. Thermogravimetrically measured mass fraction of glycerol as a function of the actual glycerol mass fraction.

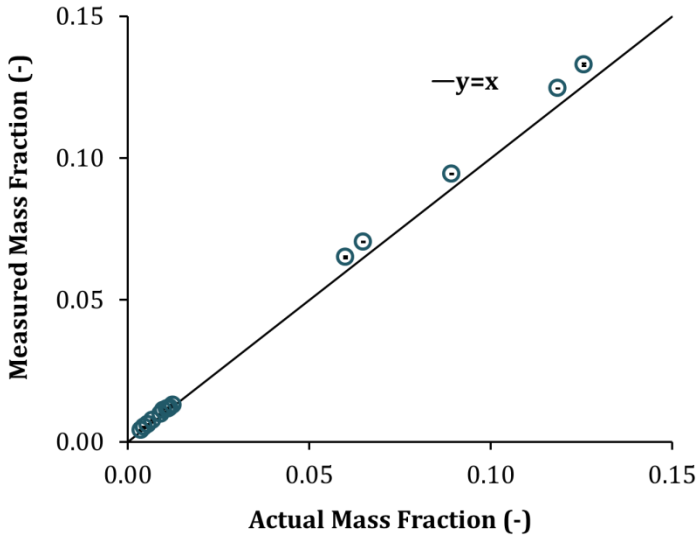

Figure C5. Thermogravimetrically measured mass fraction of sodium chloride as a function of actual sodium chloride mass fraction.

Actual samples from deglycerolization experiments contain cells, a portion of which may have hemolyzed, releasing soluble intracellular content (salts and hemoglobin) into the supernatant. These soluble intracellular content are not expected evaporate by heating the sample to 290°C and therefore is left along with the sodium chloride as a solid. To obtain the correct concentration of sodium chloride from mass transfer, the amount of soluble intracellular content must be subtracted from the solid mass at the end of the TGA procedure. It is known that a vast majority of the soluble intracellular content of human erythrocyte is made up of hemoglobin (~98%) [171]. Therefore, theoretically, the amount of sodium chloride present in the supernatant may be closely estimated by subtracting the amount of measured hemoglobin from the mass of solid.

An experiment where the free hemoglobin concentration as measured by spectrophotometry was compared to the solid mass concentration as measured by TGA analysis was conducted to validate the previously described theory. RBCs were isolated from whole blood and resuspended with isotonic saline to attain a hematocrit of approximately ~45%. 2 mL of this cell suspension was then mixed with 8 mL of DI water to osmotically shock the cells to lyse. Further, the mixture was subjected to three freeze-thawe cycles to ensure lysis of most of the cells in the suspension. After thawing for the third time, a portion of the cell suspension was used to measure the hematocrit and to make a total hemolysis sample (100-fold dilution with DI water). The rest of the sample was centrifuged at 2200 g for 6 minutes and the supernatant was isolated. Four samples with different hemoglobin concentration were then made by serial dilution of the isolated supernatant as shown in Table C1.

Table C1. Serial dilution to obtain samples with different hemoglobin concentration.

Sample	Supernatant	DI Water
1	Original supernatant	-
2	3 mL Sample 1	2 mL
3	3 mL Sample 2	2 mL
4	3 mL Sample 3	2 mL

The hemoglobin concentration of the samples measured using Harboe's direct spectrophotometric method and the solid concentration measured using TGA analysis was compared as presented in Figure C6. As shown in the figure, the resulting hemoglobin concentration measured by spectrophotometry is approximately equal to the

resulting solid concentration measured using TGA analysis. The results of this experiment confirm that the concentration of sodium chloride from experimental samples can be deduced by subtracting the hemoglobin concentration from the hemolysis assay.

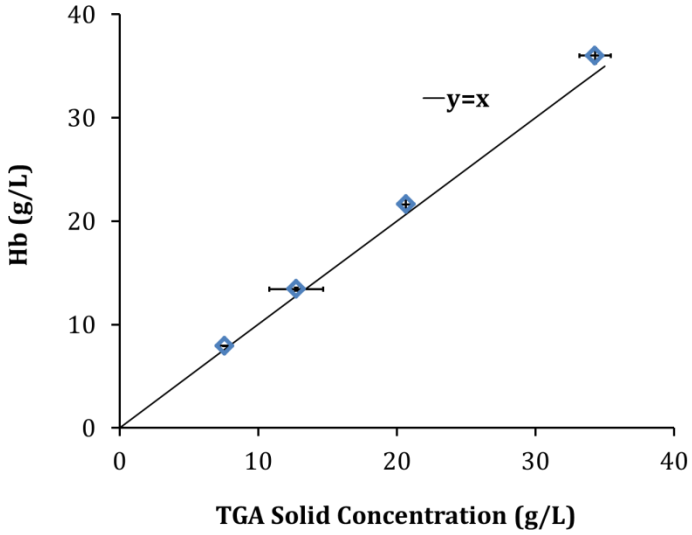

Figure C6. Concentration of hemoglobin (Hb) measured using spectrophotometry as a function of solid concentration measured using TGA analysis.

To further demonstrate that the sodium chloride concentration from experimental samples can be obtained by subtracting the hemoglobin concentration, the measured concentration of sodium chloride at the device outlet from deglycerolization experiments in Chapter 5 is compared to model predictions in Figure C7. In this figure, the squares show the concentration of sodium chloride as calculated directly from the mass fraction of solids obtained from TGA measurement of the supernatant. The diamonds show the concentration of sodium chloride after subtracting the amount of hemoglobin present in the supernatant. Concentrations of sodium chloride calculated directly from the mass

fraction of solids in the supernatant show much higher values than what is predicted by the model as well as what is physically possible based on inlet sodium chloride concentrations (dotted lines). This indicates that the soluble intracellular content released into the supernatant by damaged cells does not get evaporated during the TGA analysis, and is subsequently left as a solid along with sodium chloride at the end of the procedure. The mass of intracellular solids in the supernatant must be subtracted to obtain the true sodium chloride concentration in the samples collected from experiments. After subtracting hemoglobin, the concentrations of sodium chloride are in much better agreement with model predicted results.

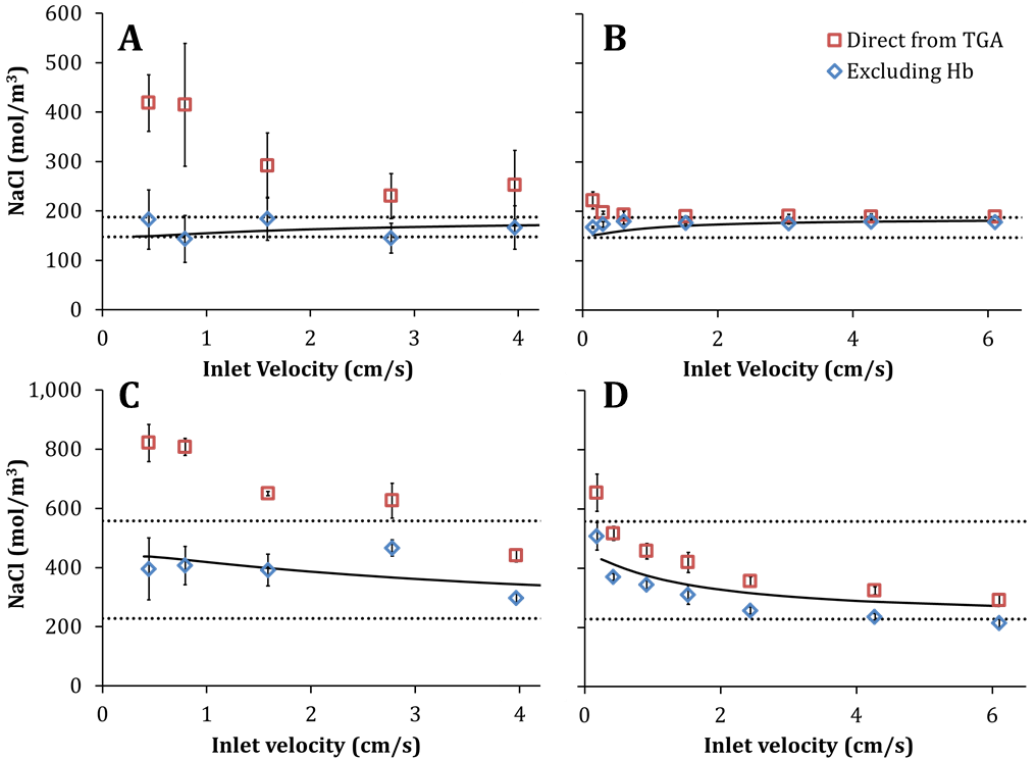

Figure C7. Thermogravimetric measurement of sodium chloride concentration in RBC stream effluent. Panels A and B show measurements from removal of glycerol

from RBCs in 10% w/v glycerol using an isotonic saline wash and the 50 and 130 mm channels, respectively. Panels C and D show measurements from removal of glycerol from frozen-thawed RBCs in 40% w/v glycerol using a 3.4% saline wash and the 50 and 130 mm channels, respectively. Solid lines show predicted sodium chloride concentrations in the RBC stream effluent (see Eq. 24 in Chapter 5) and dotted lines show the inlet concentrations in the RBC and wash streams.

Bibliography

1. *Report of the US Department of Health and Human Services. The 2009 national blood collection and utilization survey report*. 2011, Washington, DC: US Department of Health and Human Services, Office of the Assistant Secretary for Health.
2. Scott, K.L., J. Lecak, and J.P. Acker, *Biopreservation of red blood cells: Past, present, and future.* Transfusion Medicine Reviews, 2005. **19**(2): p. 127-142.
3. Hogman, C.F., *Preparation and preservation of red cells.* Vox Sanguinis, 1998. **74 Suppl 2**: p. 177-87.
4. Hess, J.R., *Red cell freezing and its impact on the supply chain.* Transfus Med, 2004. **14**(1): p. 1-8.
5. Gilcher, R.O. and S. McCombs, *Seasonal blood shortages can be eliminated.* Current Opinion in Hematology, 2005. **12**(6): p. 503-508.
6. Weinberg, J.A., et al., *Duration of Red Cell Storage Influences Mortality After Trauma.* Journal of Trauma, 2010. **69**(6): p. 1427-1430.
7. Spinella, P.C., et al., *Duration of red blood cell storage is associated with increased incidence of deep vein thrombosis and in hospital mortality in patients with traumatic injuries.* Critical Care, 2009. **13**(5).
8. Klein, S.R., et al., *The effect of older blood on mortality, need for ICU care, and the length of ICU stay after major trauma.* American Surgeon, 2005. **71**(9): p. 781-785.
9. Valeri, C.R., *Status report on the quality of liquid and frozen red blood cells.* Vox Sanguinis, 2002. **83 Suppl 1**: p. 193-6.
10. Valeri, C.R., et al., *An experiment with glycerol-frozen bed blood cells stored at -80 degrees C for up to 37 years.* Vox Sanguinis, 2000. **79**(3): p. 168-174.
11. Gage, F.H., *Cell therapy.* Nature, 1998. **392**(6679): p. 18-24.
12. Meryman, H.T., *Cryoprotective Agents.* Cryobiology, 1971. **8**(2): p. 173-&.
13. McGann, L.E., *Differing actions of penetrating and nonpenetrating cryoprotective agents.* Cryobiology, 1978. **15**(4): p. 382-90.

14. Mazur, P., *Freezing of living cells: mechanisms and implications.* Am J Physiol, 1984. **247**(3 Pt 1): p. C125-42.
15. Rall, W.F. and G.M. Fahy, *Ice-free cryopreservation of mouse embryos at -196 degrees C by vitrification.* Nature, 1985. **313**(6003): p. 573-5.
16. Lovelock, J.E., *The mechanism of the protective action of glycerol against haemolysis by freezing and thawing.* Biochimica et Biophysica Acta, 1953. **11**(1): p. 28-36.
17. Mazur, P., *Cryobiology: the freezing of biological systems.* Science, 1970. **168**(934): p. 939-49.
18. Meryman, H.T., *Freezing Injury and Its Prevention in Living Cells.* Annual Review of Biophysics and Bioengineering, 1974. **3**: p. 341-363.
19. Polge, C., A.U. Smith, and A.S. Parkes, *Revival of Spermatozoa After Vitrification and Dehydration at Low Temperatures.* Nature (London), 1949. **164**.
20. Smith, A.U., *Prevention of Haemolysis During Freezing and Thawing of Red Blood Cells.* Lancet, 1950. **2**: p. 910-11.
21. Mollison, P.L. and H.A. Sloviter, *Successful Transfusion of Previously Frozen Human Red Cells.* Lancet, 1951. **6689**: p. 862-864.
22. Meryman, H.T. and Hornblow.M, *Method for Freezing and Washing Red Blood-Cells Using a High Glycerol Concentration.* Transfusion, 1972. **12**(3): p. 145-&.
23. Brecher, M.E., ed. *Technical Manual*. 2005, AABB: Bethesda, MD.
24. Meryman, H.T. and M. Hornblower, *Simplified Procedure for Deglycerolizing Red Blood-Cells Frozen in a High Glycerol Concentration.* Transfusion, 1977. **17**(5): p. 438-442.
25. Rowe, A.W., E. Eyster, and A. Kellner, *Liquid Nitrogen Preservation of Red Blood Cells for Transfusion - a Low Glycerol-Rapid Freeze Procedure.* Cryobiology, 1968. **5**(2): p. 119-&.
26. Valeri, C.R., et al., *In vivo survival of apheresis RBCs, frozen with 40-percent (wt/vol) glycerol, deglycerolized in the ACP 215, and stored at 4 degrees C in AS-3 for up to 21 days.* Transfusion, 2001. **41**(7): p. 928-932.

27. Valeri, C.R., et al., *A multicenter study of in vitro and in vivo values in human RBCs frozen with 40-percent (wt/vol) glycerol and stored after deglycerolization for 15 days at 4 degrees C in AS-3: assessment of RBC processing in the ACP 215.* Transfusion, 2001. **41**(7): p. 933-939.

28. Valeri, C.R. *Standard Operating Procedure. Glycerolization and Deglycerolization of Red Blood Cells in a Closed System Using the Haemonetics ACP215. Retrieved October 1, 2011*. [cited 2011 October 1]; Available from: www.nbrl.org/SOP/ACP215.

29. Lelkens, C.C., et al., *Stability after thawing of RBCs frozen with the high- and low-glycerol method.* Transfusion, 2003. **43**(2): p. 157-64.

30. Meryman, H.T. and M. Hornblower, *Method for Freezing and Washing Red Blood-Cells Using a High Glycerol Concentration.* Transfusion, 1972. **12**(3): p. 145-156.

31. Kedem, O. and A. Katchalsky, *Thermodynamic analysis of the permeability of biological membranes to non-electrolytes.* Biochimica et Biophysica Acta, 1958. **27**: p. 229-246.

32. Kleinhans, F.W., *Membrane permeability modeling: Kedem-Katchalsky vs a two-parameter formalism.* Cryobiology, 1998. **37**(4): p. 271-289.

33. McGrath, J. and K. Diller, eds. *Low Temperature Biotechnology: Emerging Applications and Engineering Contributions*. 1988, American Society of Mechanical Engineers: New York. 203-211.

34. Terwilliger, T.C. and A.K. Solomon, *Osmotic water permeability of human red cells.* J Gen Physiol, 1981. **77**(5): p. 549-70.

35. Sha'afi, R.I., C.M. Gary-Bobo, and A.K. Solomon, *Permeability of red cell membranes to small hydrophilic and lipophilic solutes.* Journal of General Physiology, 1971. **58**(3): p. 238-58.

36. Papanek, T.H., *The Water Permeability of the Human Erythrocyte in the Temperature Range +25^{o}C to -10^{o}C, PhD Thesis*. 1978, Massachusetts Institute of Technology.

37. Rule, G.S., et al., *Water Permeability of Mammalian-Cells as a Function of Temperature in the Presence of Dimethylsulfoxide - Correlation with the State of the Membrane-Lipids.* Journal of Cellular Physiology, 1980. **103**(3): p. 407-416.
38. Mazur, P., W.F. Rall, and S.P. Leibo, *Kinetics of Water-Loss and the Likelihood of Intracellular Freezing in Mouse Ova - Influence of the Method of Calculating the Temperature-Dependence of Water Permeability.* Cell Biophysics, 1984. **6**(3): p. 197-213.
39. Carlsen, A. and J.O. Wieth, *Glycerol transport in human red cells.* Acta Physiol Scand, 1976. **97**(4): p. 501-13.
40. Stein, W.D. and J.F. Danielli, *Structure and function in red cell permeability.* Discussions of the Faraday Society, 1956. **21**: p. 238-251.
41. Du, J.Y., et al., *Human Spermatozoa Glycerol Permeability and Activation-Energy Determined by Electron-Paramagnetic-Resonance.* Biochimica et Biophysica Acta-Biomembranes, 1994. **1194**(1): p. 1-11.
42. Mazur, P. and R.H. Miller, *Permeability of Human Erythrocyte to Glycerol in 1 and 2 M Solutions at 0 or 20 Degrees C.* Cryobiology, 1976. **13**(5): p. 507-522.
43. Saari, J.T. and J.S. Beck, *Hypotonic hemolysis of human red blood cells: a two-phase process.* Journal of Membrane Biology, 1975. **23**(3-4): p. 213-26.
44. Jay, A.W. and S. Rowlands, *The stages of osmotic haemolysis.* J Physiol, 1975. **252**(3): p. 817-32.
45. Gilmore, J.A., et al., *Determination of optimal cryoprotectants and procedures for their addition and removal from human spermatozoa.* Human Reproduction, 1997. **12**(1): p. 112-118.
46. Creed, E., *The Estimation of the Fragility of Red Blood Corpuscles.* The Journal of Pathology and Bacteriology, 1938. **46**(2): p. 331-340.
47. Parpart, A.K., et al., *The osmotic resistance (fragility) of human red cells.* Journal of Clinical Investigation, 1947. **26**(4): p. 636-40.

48. Ito, Y., P. Carmeci, and R. Steele, *Continuous-Flow Method for Determination of Erythrocyte Osmotic Fragility.* American Journal of Hematology, 1977. **2**(4): p. 403-412.
49. Godal, H.C., N. Nyvold, and A. Rustad, *The osmotic fragility of red blood cells: a re-evaluation of technical conditions.* Scandinavian Journal of Haematology, 1979. **23**(1): p. 55-8.
50. Godal, H.C., et al., *The normal range of osmotic fragility of red blood cells.* Scandinavian Journal of Haematology, 1980. **25**(2): p. 107-12.
51. Guest, G.M. and M. Wing, *Osmometric Behavior of Normal Human Erythrocytes.* Journal of Clinical Investigation, 1942. **21**(3): p. 257-62.
52. Meryman, H.T., *Modified model for the mechanism of freezing injury in erythrocytes.* Nature, 1968. **218**(5139): p. 333-6.
53. Lovelock, J.E., *The protective action of neutral solutes against haemolysis by freezing and thawing.* Biochemical Journal, 1954. **56**(2): p. 265-70.
54. Murphy, J.R., *Erythrocyte Osmotic Fragility and Cell Water - Influence of Ph and Temperature.* Journal of Laboratory and Clinical Medicine, 1969. **74**(2): p. 319-&.
55. Richieri, G.V. and H.C. Mel, *Temperature Effects on Osmotic Fragility, and the Erythrocyte-Membrane.* Biochimica Et Biophysica Acta, 1985. **813**(1): p. 41-50.
56. Bruckdorfer, K.R., et al., *The effect of partial replacements of membrane cholesterol by other steroids on the osmotic fragility and glycerol permeability of erythrocytes.* Biochimica et Biophysica Acta, 1969. **183**(2): p. 334-45.
57. Beutler, E., W. Kuhl, and C. West, *The Osmotic Fragility of Erythrocytes after Prolonged Liquid Storage and after Reinfusion.* Blood, 1982. **59**(6): p. 1141-1147.
58. Rifkind, J.M., K. Araki, and E.C. Hadley, *The Relationship between the Osmotic Fragility of Human-Erythrocytes and Cell Age.* Archives of Biochemistry and Biophysics, 1983. **222**(2): p. 582-589.

59. Meryman, H.T. and M.S. Douglas, *Isotonicity in the presence of penetrating cryoprotectants.* Cryobiology, 1982. **l9**(5): p. 565-9.
60. Castino, F. and S.R. Wickramasinghe, *Washing frozen red blood cell concentrates using hollow fibres.* Journal of Membrane Science, 1996. **110**(2): p. 169-180.
61. Wickramasinghe, S.R., *Washing cryopreserved blood products using hollow fibres.* Food and Bioproducts Processing, 1999. **77**(C4): p. 287-292.
62. Zhou, X.M., et al., *A Dilution-Filtration System for Removing Cryoprotective Agents.* Journal of Biomechanical Engineering-Transactions of the Asme, 2011. **133**(2).
63. Arnaud, F., E. Kapnik, and H.T. Meryman, *Use of hollow fiber membrane filtration for the removal of DMSO from platelet concentrates.* Platelets, 2003. **14**(3): p. 131 - 137.
64. Tuhy, A.R., E.K. Anderson, and G.N. Jovanovic, *Urea separation in flat-plate microchannel hemodialyzer; experiment and modeling.* Biomedical Microdevices, 2012. **14**(3): p. 595-602.
65. Colton, C.K. and E.G. Lowrie, *The Kidney*. 2nd ed, ed. B.M. Brenner, F.C. Reactor, and W.B. Saunders. 1981: Jr. Philadelphia.
66. Brody, J.P., et al., *Biotechnology at low Reynolds numbers.* Biophysical Journal, 1996. **71**(6): p. 3430-3441.
67. Beebe, D.J., G.A. Mensing, and G.M. Walker, *Physics and applications of microfluidics in biology.* Annual Review of Biomedical Engineering, 2002. **4**: p. 261-286.
68. Huang, L.R., et al., *Continuous particle separation through deterministic lateral displacement.* Science, 2004. **304**(5673): p. 987-90.
69. Mohamed, H., et al., *Development of a rare cell fractionation device: Application for cancer detection.* Ieee Transactions on Nanobioscience, 2004. **3**(4): p. 251-256.
70. Huh, D., et al., *Microfluidics for flow cytometric analysis of cells and particles.* Physiological Measurement, 2005. **26**(3): p. R73-R98.

71. Pamme, N. and A. Manz, *On-chip free-flow magnetophoresis: Continuous flow separation of magnetic particles and agglomerates.* Analytical Chemistry, 2004. **76**(24): p. 7250-7256.
72. Hawkes, J.J., et al., *Continuous cell washing and mixing driven by an ultrasound standing wave within a microfluidic channel.* Lab on a Chip, 2004. **4**(5): p. 446-452.
73. Kumar, M., D.L. Feke, and J.M. Belovich, *Fractionation of cell mixtures using acoustic and laminar flow fields.* Biotechnology and Bioengineering, 2005. **89**(2): p. 129-137.
74. Huh, D., et al., *Gravity-driven microfluidic particle sorting device with hydrodynamic separation amplification.* Analytical Chemistry, 2007. **79**(4): p. 1369-1376.
75. Yang, M.S., C.W. Li, and J. Yang, *Cell docking and on-chip monitoring of cellular reactions with a controlled concentration gradient on a microfluidic device.* Analytical Chemistry, 2002. **74**(16): p. 3991-4001.
76. Wheeler, A.R., et al., *Microfluidic device for single-cell analysis.* Analytical Chemistry, 2003. **75**(14): p. 3581-3586.
77. Di Carlo, D., N. Aghdam, and L.P. Lee, *Single-cell enzyme concentrations, kinetics, and inhibition analysis using high-density hydrodynamic cell isolation arrays.* Analytical Chemistry, 2006. **78**(14): p. 4925-4930.
78. Sabounchi, P., et al., *Soft-state biomicrofluidic pulse generator for single cell analysis.* Applied Physics Letters, 2006. **88**(18).
79. Yamada, M., et al., *Millisecond treatment of cells using microfluidic devices via two-step carrier-medium exchange.* Lab on a Chip, 2008. **8**(5): p. 772-778.
80. Song, Y.S., et al., *Microfluidics for cryopreservation.* Lab on a Chip, 2009. **9**(13): p. 1874-1881.
81. Fleming, K.K., E.K. Longmire, and A. Hubei, *Numerical characterization of diffusion-based extraction in cell-laden flow through a microfluidic channel.*

Journal of Biomechanical Engineering-Transactions of the Asme, 2007. **129**(5): p. 703-711.

82. Mata, C., et al., *Experimental study of diffusion-based extraction from a cell suspension.* Microfluidics and Nanofluidics, 2008. **5**(4): p. 529-540.
83. Mata, C., et al., *Cell motion and recovery in a two-stream microfluidic device.* Microfluidics and Nanofluidics, 2010. **8**(4): p. 457-465.
84. Glass, K.K.F., E.K. Longmire, and A. Hubel, *Optimization of a microfluidic device for diffusion-based extraction of DMSO from a cell suspension.* International Journal of Heat and Mass Transfer, 2008. **51**(23-24): p. 5749-5757.
85. Hubel, A., *Advancing the preservation of cellular therapy products.* Transfusion, 2011. **51**: p. 82s-86s.
86. Hanna, J., A. Hubel, and E. Lemke, *Diffusion-based extraction of DMSO from a cell suspension in a three stream, vertical microchannel.* Biotechnology and Bioengineering, 2012. **109**(9): p. 2316-2324.
87. Hustin, A., *Note sure une nouvelle méthode de transfusion.* Annales et Bulletin des Séances Société des Sciences Médicales et Naturelles de Bruxelles, 1914. **72**: p. 104-111.
88. Rous, P. and J.R. Turner, *The preservation of living red blood cells in vitro. I. Methods of preservation.* Journal of Experimental Medicine, 1916. **23**: p. 219-238.
89. Rous, P. and J.R. Turner, *The preservation of living red cells in vitro. II. The transfusion of kept cells.* Journal of Experimental Medicine, 1916. **23**: p. 239-248.
90. Mollison, P.L., *The introduction of citrate as an anticoagulant for transfusion and of glucose as a red cell preservative.* Br J Haematol, 2000. **108**(1): p. 13-8.
91. Hess, J.R. and T.G. Greenwalt, *Storage of red blood cells: new approaches.* Transfus Med Rev, 2002. **16**(4): p. 283-95.
92. Lecak, J., et al., *Evaluation of red blood cells stored at-80 degrees C in excess of 10 years.* Transfusion, 2004. **44**(9): p. 1306-1313.

93. Nanu, A. and M. Lal, *Cryopreservation of Rh negative blood for improved storage & utilisation by means of indigenous freezing bags & solutions & manual deglycerolisation.* Indian Journal of Medical Research, 2001. **113**: p. 151-155.
94. Gao, D.Y., et al., *Prevention of Osmotic Injury to Human Spermatozoa during Addition and Removal of Glycerol.* Human Reproduction, 1995. **10**(5): p. 1109-1122.
95. Wusteman, M.C., et al., *Vitrification media: toxicity, permeability, and dielectric properties.* Cryobiology, 2002. **44**(1): p. 24-37.
96. Bandarenko, N., et al., *Successful in vivo recovery and extended storage of additive solution (AS)-5 red blood cells after deglycerolization and resuspension in AS-3 for 15 days with an automated closed system.* Transfusion, 2007. **47**(4): p. 680-6.
97. Karlsson, J.O.M., et al., *Permeability of the Rhesus Monkey Oocyte Membrane to Water and Common Cryoprotectants.* Molecular Reproduction and Development, 2009. **76**(4): p. 321-333.
98. Levin, R.L. and T.W. Miller, *An Optimum Method for the Introduction or Removal of Permeable Cryoprotectants - Isolated Cells.* Cryobiology, 1981. **18**(1): p. 32-48.
99. Benson, J.D., C.C. Chicone, and J.K. Critser, *A general model for the dynamics of cell volume, global stability, and optimal control.* Journal of Mathematical Biology, 2010.
100. Benson, J.D., *Mathematical Problems from Cryobiology*. 2009, University of Missouri.
101. Benson, J.D., A.J. Kearsley, and A.Z. Higgins, *Mathematical optimization of procedures for cryoprotectant equilibration using a toxicity cost function.* Cryobiology, 2012. **64**(3): p. 144-151.
102. Stein, W.D., *Spontaneous and enzyme-induced dimer formation and its role in membrane permeability. II. The mechanism of movement of glycerol across the human erythrocyte membrane.* Biochim Biophys Acta, 1962. **59**: p. 47-65.

103. Jay, A.W., *Geometry of the human erythrocyte. I. Effect of albumin on cell geometry.* Biophys J, 1975. **15**(3): p. 205-22.

104. Pegg, D.E., *Red cell volume in glycerol/sodium chloride/water mixtures.* Cryobiology, 1984. **21**(2): p. 234-9.

105. Jacobs, M.H. and D.R. Stewart, *A simple method for the quantitative measurement of cell permeability.* Journal of Cellular and Comparative Physiology, 1932. **1**(1): p. 71-82.

106. Lacelle, P.L. and Rothstei.A, *Passive Permeability of Red Blood Cell to Cations.* Journal of General Physiology, 1966. **50**(1): p. 171-&.

107. Valeri, C.R., *Simplification of Methods for Adding and Removing Glycerol during Freeze-Preservation of Human Red Blood-Cells with High or Low Glycerol Methods - Biochemical Modification Prior to Freezing.* Transfusion, 1975. **15**(3): p. 195-218.

108. Meryman, H.T. and M. Hornblower, *A simplified procedure for deglycerolizing red blood cells frozen in a high glycerol concentration.* Transfusion, 1977. **17**(5): p. 438-42.

109. Han, V., K. Serrano, and D.V. Devine, *A comparative study of common techniques used to measure haemolysis in stored red cell concentrates.* Vox Sanguinis, 2010. **98**(2): p. 116-23.

110. Lovelock, J.E., *The haemolysis of human red blood-cells by freezing and thawing.* Biochim Biophys Acta, 1953. **10**(3): p. 414-26.

111. Toon, M.R. and A.K. Solomon, *Transport parameters in the human red cell membrane: solute-membrane interactions of hydrophilic alcohols and their effect on permeation.* Biochim Biophys Acta, 1990. **1022**(1): p. 57-71.

112. Williams, R.J. and S.K. Shaw, *The relationship between cell injury and osmotic volume reduction: II. Red cell lysis correlates with cell volume rather than intracellular salt concentration.* Cryobiology, 1980. **17**(6): p. 530-9.

113. Farrant, J. and A.E. Woolgar, *Human red cells under hypertonic conditions; a model system for investigating freezing damage. 2. Sucrose.* Cryobiology, 1972. **9**(1): p. 16-21.

114. Farrant, J., *Human red cells under hypertonic conditions; a model system for investigating freezing damage. 3. Dimethylsulfoxide.* Cryobiology, 1972. **9**(2): p. 131-6.

115. Meryman, H.T., *Osmotic Stress as a Mechanism of Freezing Injury.* Cryobiology, 1971. **8**(5): p. 489-&.

116. Liley, H.G., *Immune Hemolytic Disease, in : D.G. Nathan, S.H. Orkin, D. Ginsberg, A.T. Look, (Eds.), Hematology of Infancy and Childhood*. 6th ed. 2003, pp. 56-85: Saunders.

117. Brugnara, C. and O.S. Platt, *The neonatal erythrocyte and its disorders, in : D.G. Nathan, S.H. Orkin, D. Ginsberg, A.T. Look, (Eds.), Hematology of Infancy and Childhood*. 2003, pp.19-55, Saunders.

118. Luban, N.L.C., *Neonatal red blood cell transfusions.* Vox Sanguinis, 2004. **87**: p. 184-188.

119. Hume, H., *Red blood cell transfusions for preterm infants: The role of evidence-based medicine.* Seminars in Perinatology, 1997. **21**(1): p. 8-19.

120. Tooley, W.H., *Neonatal anemia, in: W.H.Tooley, (Ed), Intensive Care Nursery House Staff Manual*. 8th ed. 2004, pp.108-110: UCSF Children's Hospital at UCSF Medical Center.

121. Sloan, S.R., et al., *Transfusion medicine, in : D.G. Nathan, S.H. Orkin, D. Ginsberg, A.T. Look, (Eds.), Hematology of Infancy and Childhood*. 6th ed. 2003, pp. 1709-1756: Saunders.

122. Moise, K.J., Jr., *Intrauterine transfusion with red cells and platelets.* West J Med, 1993. **159**(3): p. 318-24.

123. Matovcik, L.M. and W.C. Mentzer, *The membrane of the human neonatal red cell.* Clin Haematol, 1985. **14**(1): p. 203-21.

124. Oski, F.A., *The unique fetal red cell and its function. E. Mead Johnson Award address.* Pediatrics, 1973. **51**(3): p. 494-500.
125. Jain, S.K., *The neonatal erythrocyte and its oxidative susceptibility.* Semin Hematol, 1989. **26**(4): p. 286-300.
126. Oski, F.A., *Fetal hemoglobin, the neonatal red cell, and 2,3-diphosphoglycerate.* Pediatr Clin North Am, 1972. **19**(4): p. 907-17.
127. Nagel, R.L., *Hemoglobins: normal and abnormal, in : D.G. Nathan, S.H. Orkin, D. Ginsberg, A.T. Look, (Eds.), Hematology of Infancy and Childhood*. 6th ed. 2003, pp.745-789: Saunders.
128. Ludvigsen, B.F., *Hemoglobin synthesis and function, in : E.A. Stiene-Martin, C.A. Lotspeich-Steininger, J.A. Koepke, (Eds.), Clinical Hematology: Principles, Procedures, Correlations*. 2nd ed. 1997, pp. 73-86: Lippincott.
129. Clark, C., et al., *Blood transfusion: a possible risk factor in retrolental fibroplasia.* Acta Paediatr Scand, 1981. **70**(4): p. 537-9.
130. Hepner, W.R., Jr. and A.C. Krause, *Retrolental fibroplasia: clinical observations.* Pediatrics, 1952. **10**(4): p. 433-43.
131. Mallek, H. and P. Spohn, *Retrolental fibroplasia.* Can Med Assoc J, 1950. **63**(6): p. 586-8.
132. Collard, K.J., S. Godeck, and J.E. Holley, *Blood transfusion and pulmonary lipid peroxidation in ventilated premature babies.* Pediatr Pulmonol, 2005. **39**(3): p. 257-61.
133. Cooke, R.W., et al., *Blood transfusion and chronic lung disease in preterm infants.* Eur J Pediatr, 1997. **156**(1): p. 47-50.
134. Korhonen, P., et al., *Very low birthweight, bronchopulmonary dysplasia and health in early childhood.* Acta Paediatr, 1999. **88**(12): p. 1385-91.
135. Brune, T., et al., *Efficacy, recovery, and safety of RBCs from autologous placental blood: clinical experience in 52 newborns.* Transfusion, 2003. **43**(9): p. 1210-6.
136. Brune, T., et al., *Autologous placental blood transfusion for the therapy of anaemic neonates.* Biol Neonate, 2002. **81**(4): p. 236-43.

137. Eichler, H., et al., *Cord blood as a source of autologous RBCs for transfusion to preterm infants.* Transfusion, 2000. **40**(9): p. 1111-7.
138. Imura, K., et al., *Usefulness of cord-blood harvesting for autologous transfusion in surgical newborns with antenatal diagnosis of congenital anomalies.* J Pediatr Surg, 2001. **36**(6): p. 851-4.
139. Ballin, A., et al., *Autologous umbilical cord blood transfusion.* Arch Dis Child Fetal Neonatal Ed, 1995. **73**(3): p. F181-3.
140. Surbek, D.V., et al., *Can cord blood be used for autologous transfusion in preterm neonates?* Eur J Pediatr, 2000. **159**(10): p. 790-1.
141. Bertolini, F., et al., *A new method for placental/cord blood processing in the collection bag. I. Analysis of factors involved in red blood cell removal.* Bone Marrow Transplant, 1996. **18**(4): p. 783-6.
142. Perutelli, P., et al., *Processing of human cord blood by three different procedures for red blood cell depletion and mononuclear cell recovery.* Vox Sang, 1999. **76**(4): p. 237-40.
143. Sousa, T., et al., *Umbilical cord blood processing: volume reduction and recovery of CD34+ cells.* Bone Marrow Transplant, 1997. **19**(4): p. 311-3.
144. Appalup, M. and T. Fedorova, *The Effectiveness and Safety of Autologous Umbilical Blood Derived Red Blood Cells in a Treatment of Postoperative Anaemia in Newborns with a Surgical Pathology.* Vox Sanguinis, 2010. **99**: p. 408-408.
145. Strauss, R.G., *Autologous Transfusions for Neonates Using Placental Blood - a Cautionary Note.* American Journal of Diseases of Children, 1992. **146**(1): p. 21-22.
146. Zhurova, M., J. Akabutu, and J. Acker, *Quality of red blood cells isolated from umbilical cord blood stored at room temperature.* J Blood Transfus, 2012. **2012**: p. 102809.
147. Valeri, C.R., *Simplification of the methods for adding and removing glycerol during freeze-preservation of human red blood cells with the high or low glycerol*

methods: biochemical modification prior to freezing. Transfusion, 1975. **15**(3): p. 195-218.

148. Zhurova, M., *Cryobiological characteristics of red blood cells from human umbilical cord blood*, in *Medical Sciences- Laboratory Medicine and Pathology*. 2013, University of Alberta.
149. Bautista, M.L.G., et al., *Cord blood red cell osmotic fragility: a comparison between preterm and full-term newborn infants.* Early Human Development, 2003. **72**(1): p. 37-46.
150. Luzzatto, L., G.J.F. Esan, and Ogiemudi.Se, *Osmotic Fragility of Red Cells in Newborns and Infants.* Acta Haematologica, 1970. **43**(4): p. 248-&.
151. Matovcik, L.M., et al., *The Aging Process of Human Neonatal Erythrocytes.* Pediatric Research, 1986. **20**(11): p. 1091-1096.
152. Valeri, C.R., et al., *Automation of the glycerolization of red blood cells with the high-separation bowl in the Haemonetics ACP 215 instrument.* Transfusion, 2005. **45**(10): p. 1621-1627.
153. Mazur, P. and U. Schneider, *Osmotic Responses of Preimplantation Mouse and Bovine Embryos and Their Cryobiological Implications.* Cell Biophysics, 1986. **8**(4): p. 259-285.
154. Lusianti, R.E., et al., *Rapid removal of glycerol from frozen-thawed red blood cells.* Biotechnology Progress, 2013. **29**(3): p. 609-620.
155. Preston, G.M., et al., *Appearance of water channels in Xenopus oocytes expressing red cell CHIP28 protein.* Science, 1992. **256**(5055): p. 385-7.
156. Verkman, A.S., et al., *Water transport across mammalian cell membranes.* American Journal of Physiology-Cell Physiology, 1996. **39**(1): p. C12-C30.
157. Echevarria, M., E.E. Windhager, and G. Frindt, *Selectivity of the renal collecting duct water channel aquaporin-3.* Journal of Biological Chemistry, 1996. **271**(41): p. 25079-82.

158. Yang, B. and A.S. Verkman, *Water and glycerol permeabilities of aquaporins 1-5 and MIP determined quantitatively by expression of epitope-tagged constructs in Xenopus oocytes.* Journal of Biological Chemistry, 1997. **272**(26): p. 16140-6.

159. Waniewski, J., *Linear-Approximations for the Description of Solute Flux through Permselective Membranes.* Journal of Membrane Science, 1994. **95**(2): p. 179-184.

160. Villarroel, F., E. Klein, and F. Holland, *Solute Flux in Hemodialysis and Hemofiltration Membranes.* Transactions American Society for Artificial Internal Organs, 1977. **23**: p. 225-233.

161. Bahrami, M., M.M. Yovanovich, and J.R. Culham, *Pressure drop of fully-developed laminar flow in microchannels of arbitrary cross-section.* Journal of Fluids Engineering-Transactions of the Asme, 2006. **128**(5): p. 1036-1044.

162. Collins, M.C. and W.F. Ramirez, *Mass-Transport through Polymeric Membranes.* Journal of Physical Chemistry, 1979. **83**(17): p. 2294-2301.

163. Flick, E.W., *Industrial solvents handbook*. 5th ed. 1998, Westwood, N.J.: Noyes Data Corp. xxxi, 963 p.

164. Karlsson, J.O.M., E.G. Cravalho, and M. Toner, *A model of diffusion-limited ice growth inside biological cells during freezing.* Journal of Applied Physics, 1994. **75**(9): p. 4442-4455.

165. D'Errico, G., et al., *Diffusion coefficients for the binary system glycerol plus water at 25 degrees C. A velocity correlation study.* Journal of Chemical and Engineering Data, 2004. **49**(6): p. 1665-1670.

166. Robinson, R.A. and R.H. Stokes, *Electrolyte solutions; the measurement and interpretation of conductance, chemical potential, and diffusion in solutions of simple electrolytes*. 2d ed. 1959, London,: Butterworths. xv, 571 p.

167. Davidson, M., S. Bastian, and F. Markley, *Measurement of the Elastic Modulus of Kapton Perpendicular to the Plane of the Film at Room and Cryogenic Temperatures*, in *Fourth Annual IISCC Conference*, F.N.A. Laboratory, Editor. 1992: New Orleans, LA.

168. *Catalog of Hemodialysis Membrane Date.* Artificial Organs, 1977. **1**(2): p. 74-77.
169. Chapra, S.C., *Applied numerical methods with MATLAB for engineers and scientists*. 2nd ed. 2008, Boston: McGraw-Hill Higher Education. xx, 588 p.
170. Derevich, I.V. and E.G. Smirnova, *Calculating the parameters of heat transfer between countercurrent flows with variable thermophysical properties.* Theoretical Foundations of Chemical Engineering, 2002. **36**(4): p. 341-345.
171. Valberg, L.S., et al., *Spectrochemical Analysis of Sodium Potassium Calcium Magnesium Copper and Zinc in Normal Human Erythrocytes.* Journal of Clinical Investigation, 1965. **44**(3): p. 379-&.
172. Son, Y., *Determination of shear viscosity and shear rate from pressure drop and flow rate relationship in a rectangular channel.* Polymer, 2007. **48**(2): p. 632-637.
173. Hatch, A.C., et al., *Passive droplet sorting using viscoelastic flow focusing.* Lab on a Chip, 2013. **13**(7): p. 1308-1315.
174. Leverett, L.B., et al., *Red Blood-Cell Damage by Shear-Stress.* Biophysical Journal, 1972. **12**(3): p. 257-&.
175. Polaschegg, H.D., *Red blood cell damage from extracorporeal circulation in hemodialysis.* Semin Dial, 2009. **22**(5): p. 524-31.
176. Liao, Z.J., et al., *Measurement of hollow fiber membrane transport properties in hemodialyzers.* Journal of Membrane Science, 2005. **256**(1-2): p. 176-183.
177. Ding, W.P., et al., *Simulation of removing permeable cryoprotective agents from cryopreserved blood with hollow fiber modules.* Journal of Membrane Science, 2007. **288**(1-2): p. 85-93.
178. Valeri, C.R., et al., *In vitro and in vivo measurements of human RBCs frozen with glycerol and subjected to various storage temperatures before deglycerolization and storage at 4 degrees C for 3 days.* Transfusion, 2001. **41**(3): p. 401-405.
179. Valeri, C.R., et al., *The in vitro quality of red blood cells frozen with 40 percent (wt/vol) glycerol at -80 degrees C for 14 years, deglycerolized with the haemonetics ACP 215, and stored at 4 degrees C in additive solution-1 or additive solution-3 for up to 3 weeks.* Transfusion, 2004. **44**(7): p. 990-995.

180. Vamvakas, E.C. and A.A. Pineda, *Allergic and Anaphylactic Reactions* Transfusion Reactions, ed. M.A. Popovsky. 2001, Bethesda, MD: AABB Press.
181. *Isopore Membrane, polycarbonate, Hydriphilic, 0.4 mm, 90 mm, white, plain*. [cited 2014 February 12]; Available from: https://www.millipore.com/catalogue/item/HTTP09030.
182. Lusianti, R.E., G.N. Jovanovic, and A.Z. Higgins, *Cryoprotectant removal using a microscale dialysis device.* Cryobiology, 2010. **61**(3): p. 372.
183. Davis, J.A., et al., *Deterministic hydrodynamics: taking blood apart.* Proc Natl Acad Sci U S A, 2006. **103**(40): p. 14779-84.
184. *SU-8 2000 Permanent Epoxy Negative Photoresist Processing Guidelines for: SU-8 2025, SU-8 2050 and SU-8 2075*. [cited 2014 February 12]; Available from: http://microchem.com/pdf/SU-82000DataSheet2025thru2075Ver4.pdf.
185. Sakai, H., et al., *Removal of Cellular-Type Hemoglobin-Based Oxygen Carrier (Hemoglobin-Vesicles) From Blood Using Centrifugation and Ultrafiltration.* Artificial Organs, 2012. **36**(2): p. 202-209.
186. Levine, J.A., *Extracorporeal removal of plasma hemoglobin in sepsis*.
187. Benson, J.D., C.C. Chicone, and J.K. Critser, *Exact solutions of a two parameter flux model and cryobiological applications.* Cryobiology, 2005. **50**(3): p. 308-16.
188. Burden, R.L. and J.D. Faires, *Numerical Analysis, Eighth Edition*. 2005, Belmont, CA: Thompson Brooks/Cole.